BIOCOMPATIBILITY AND BIOMECHANICAL PROPERTIES OF NEW POLYCAPROLACTONE-BIOGLASS BASED BONE IMPLANT MATERIALS

A THESIS SUBMITTED TO
THE GRADUATE SCHOOL OF NATURAL AND APPLIED SCIENCES
OF
MIDDLE EAST TECHNICAL UNIVERSITY

BY

ÖZGE ERDEMLİ

IN PARTIAL FULFILLMENT OF THE REQUIREMENTS
FOR
THE DEGREE OF MASTER OF SCIENCE
IN
ENGINEERING SCIENCES

SEPTEMBER 2007

Approval of the thesis:

BIOCOMPATIBILITY AND BIOMECHANICAL PROPERTIES OF NEW POLYCAPROLACTONE-BIOGLASS BASED BONE IMPLANT MATERIALS

submitted by **ÖZGE ERDEMLİ** in partial fulfillment of the requirements for the degree of **Master of Science in Engineering Sciences Department, Middle East Technical University** by,

Prof. Dr. Canan Özgen
Dean, Graduate School of **Natural and Applied Sciences** _____

Prof. Dr. Turgut Tokdemir
Head of Department, **Engineering Sciences** _____

Assist. Prof. Dr. Ayşen Tezcaner
Supervisor, **Engineering Sciences Dept., METU** _____

Assist. Prof. Dr. Dilek Keskin
Co- Supervisor, **Engineering Sciences Dept., METU** _____

Examining Committee Members

Prof. Dr. M. Ruşen Geçit _____
Engineering Sciences Dept., METU

Assist. Prof. Dr. Ayşen Tezcaner _____
Engineering Sciences Dept., METU

Assoc. Prof. Dr. Serhat Akın _____
Petroleum and Natural Gas Engineering Dept., METU

Assist. Prof. Dr. Zafer Evis _____
Engineering Sciences Dept., METU

Assist. Prof. Dr. Dilek Keskin _____
Engineering Sciences Dept., METU

Date: 06.09.2007

I hereby declare that all information in this document has been obtained and presented in accordance with academic rules and ethical conduct. I also declare that, as required by these rules and conduct, I have fully cited and referenced all material and results that are not original to this work.

Name, Last name:

Signature :

ABSTRACT

BIOCOMPATIBILITY AND BIOMECHANICAL PROPERTIES OF NEW POLYCAPROLACTONE-BIOGLASS BASED BONE IMPLANT MATERIALS

Erdemli, Özge
M.S., Department of Engineering Sciences
Supervisor : Assist. Prof. Dr. Ayşen Tezcaner
Co-Supervisor: Assist. Prof. Dr. Dilek Keskin

September 2007, pages 133

Researches on bone defects are focused on the use of composites due to the composite and well-organized hierarchical structure of the bone. In this study, it is aimed to develop Polycaprolactone based implants with different organic – DBM, HYA- and/or inorganic –bioglass, calcium sulfate- compositions for augmenting bone healing.

Bioactivity of the discs was evaluated by scanning electron microscopy and EDS analysis after incubation in SBF for 1, 7 and 14 days. All bioglass containing groups showed apatite molecules at different incubation times. Degradation studies demonstrated that only PCL/BG/HYA discs had fast degradation upon incubations in PBS (4 and 6 weeks). Initial mechanical properties of composites were found to be directly related to the composition. However, decreases in disc mechanical properties were also obtained in the same order with the amount of water uptake at composite groups.

According to biocompatibility studies investigated with cytotoxicity tests on Saos-2 cells, all groups, except the HYA involving one were found as biocompatible.

After in vivo application of discs to critical size defects on rabbit humeri (for 7 weeks), their efficacy on healing was studied with computerized tomography, SEM and biomechanical tests. The results revealed that bone-implant interface formation has started for all groups with high bone densities at the interface of implant groups compared to empty defect sites of negative controls. Also the healing was suggested to be gradual from bone to implant site as microhardness values increased at regions closer to bone. However, regeneration was found to not reach to healthy bone levels.

Keywords: Polycaprolactone, DBM, Bioglass, Hyaluronan, Calcium Sulfate

ÖZ

DEĞİŞİK KOMPOZİSYONLARDA POLİKAPROLAKTON/BİYOCAM TEMELLİ KOMPOZİT MALZEMELERİN GELİŞTİRİLMESİ, MEKANİK VE BİYOETKİNLİK ÖZELLİKLERİNİN İNCELENMESİ

Erdemli, Özge
Yüksek Lisans, Mühendislik Bilimleri Bölümü
Tez Yöneticisi : Y. Doç. Dr. Ayşen Tezcaner
Ortak Tez Yôneticisi: Y. Doç. Dr. Dilek Keskin

Eylül 2007, sayfa 133

Kemiğin kompozit ve iyi organize olmuş yapısından dolayı, kemik hasarı üzerine araştırmalar biyokompozit kullanımı üzerine odaklanmıştır. Bu çalışmada, kemik iyileşmesini arttırmak için farklı organik –DKM, HYA- ve/veya inorganik –biyocam, kalsiyum sülfat- kompozisyonlarda polikaprolakton temelli implantların geliştirilmesi amaçlanmıştır.

Disklerin biyoaktiviteleri, SBF içinde 1, 7 ve 14 gün inkübasyon sonrasında SEM ve EDS analizleri ile değerlendirilmiştir. Bütün biyocam içeren gruplarda farklı inkübasyon zamanlarında yüzeyde apatit molekülleri gözlenmiştir. PBS içerisinde inkübasyonla (4 ve 6 hafta) yapılan bozunma çalışmaları, sadece PCL/BG/HYA disklerinin hızlı bozunmaya sahip olduğunu göstermiştir. Kompozitlerin başlangıçtaki mekanik özellikleri içerikleriyle doğrudan ilintili

bulunmuştur. Ancak kompozit gruplarda, su tutma miktarındaki artışla ile aynı yönde disk mekanik özelliklerinde azalmalar olduğu da görülmüştür.

Saos-2 hücreleri üzerine sitotoksite testleri ile incelenmiş biyouyumluluk çalışmalarına göre, HYA içeren grup dışındaki bütün gruplar biyouyumlu bulunmuştur.

Disklerin tavşan ön bacağındaki kritik boyutta hasarlara in vivo uygulanmasından (7 haftalık) sonra, iyileşme üzerindeki etkinlikleri bilgisayarlı tomografi, taramalı elektron mikroskopisi ve biyomekanik testler ile çalışılmıştır. İmplant gruplarının arayüzeyinde negatif kontrolün boş hasar bölgesine oranla yüksek kemik yoğunluklarına sahip olduğu ve kemik-implant arayüzey oluşumunun bütün gruplarda başladığı sonuçlarla açıklanmıştır. Ayrıca, mikrosertlik değerlerinin kemiğe yakın bölgelerde artması ile iyileşmenin kemikten implanta doğru kademeli olduğu önerilmiştir. Ancak, implant gruplarındaki iyileşmenin sağlıklı kemik düzeyine ulaşmadığı bulunmuştur.

Anahtar Sözcükler: Polikaprolakton, DKM, Biyocam, Hiyaluronan, Kalsiyum Sülfat

To My Father,

Mehmet Erdemli

ACKNOWLEDGMENTS

I would like to express my gratitude to my advisor Assist. Prof. Dr. Ayşen Tezcaner and co-advisor Assist. Prof. Dr. Dilek Keskin for their guidance, encouragement and patience at every stage of this thesis.

Many people guided me throughout this study and I would especially like to mention, Prof. Dr. Doğan Turhan, Prof. Dr. M. Ruşen Geçit and Assist. Prof. Dr. Senih Gürses for sharing their valuable knowledge with me about mechanical testing.

I wish to extend my sincere thank to Prof. Dr Hasan Bilgili and his assistant Özge Çaptuğ, Ankara University, Faculty of Veterinary Medicine for performing the animal operations. I also want to thank to Assoc. Prof. Dr. Serhat Akın for t carrying out QCT analysis and his guidance in calculation of the measurements.

Further, I must extend thanks to Ayşegül Kavas for her encouragement, assistance at in vitro experiments and emotional support. Many thanks to my friends, Burçin Başar, E. Emre Çalık, Erkan Doğan, Ömer Aktürk, Özlem Aydın, Parisa Sharafi, Seylan Aygün and Volkan İşbuğa to their supports.

Special thanks to my mother, Zuhal Erdemli and my brother, Önder Erdemli for their encouragement and emotional support.

I would like to thank to TÜBİTAK for the support to the study via project number: 104M172.

TABLE OF CONTENTS

LIST OF TABLES

LIST OF FIGURES

LIST OF ABBREVIATIONS

BG : Bioglass
BMPs : Bone Morphogenic Proteins
CaS : Calcium Sulfate
DBM : Demineralized Bone Matrix
DMEM : Dulbecco's Modified Eagle's Medium
DMSO : Dimethyl Sulfoxide
EDS : Energy Dispersive X-Ray Spectroscopy
FCS : Fetal Calf Serum
GAG : Glycosaminoglycan
HA : Hydroxyapatite
HCA : Hydroxyl Carbonate Apatite
HYA : Hyaluronic Acid
MSCs : Mesenchymal Stem Cells
MTT : 3-(4, 5-Dimethylthiazol-2-yl)-2,5-Diphenyl Tetrazolium
PBS : Phosphate Buffered Saline
PCL : Poly(ε-caprolactone)
SBF : Simulated Body Fluid
SEM : Scanning Electron Microscopy
β-TCP : β-Tricalcium Phosphate
QCT : Quantitative Computerized Tomography

CHAPTER 1

INTRODUCTION

1.1. Bone Physiology

Bone is the primary load bearing structure in the human body. It provides internal support to the body and sites of attachment to tendons and muscles essential for locomotion. Other functions of bone involve protection to the vital organs of the body, production of the blood cells and deposition of important elements, particularly calcium and phosphorus. Bones have different gross anatomical shapes related with their position in the body. The classification of bones according to the shape is given in Table 1.1. Beyond their general structure, in order to fulfill their functions, bones have complex internal and external architecture (Currey, 2002).

1.1.1. Bone Composition and Structure

Bone is a natural composite material which contains about 43 % mineral, 32 % organic matrix, and 25 % water by volume (Nyman et al., 2005). The organic matrix is approximately 90 % type I collagen. The remaining 10 % contains various non-collagenous proteins, including most abundantly osteocalcin, osteonectin, osteopontin, and bone sialoprotein. The mineral phase consists of hydroxyapatite, (HA), which has a molecular formula of $Ca_{10}(PO_4)_6(OH)_2$. HA is in the form of small crystals located within and between collagen fibers of the bone matrix (Jee, 2001). The mineral components are mainly responsible for compressive strength and stiffness, while organic components

provide some flexibility (Nigg and Herzog, 2007) and tensile strength in the direction of their alignment in the bone structure. Water is found in various forms in the bone tissue: freely mobile in vascular-lacunar-canalicular space and attached to the mineral phase, and to the collagen network (Nyman et al., 2005).

Table 1.1. Classification of bone according to their shape

Shape	**Some Examples**	**Function**
LONG	Femur Tibia	- provide support - act as levers to allow movement - transmit longitudinal force
SHORT	Carpal bone Tarsal bone	- allow movement - provide elasticity, flexibility, and shock absorption
FLAT	Ribs Skull bones	- protect internal organs (heart, lungs, brain, etc.) and provide attachment sites for muscles
IRREGULAR	Ischium Vertebrae	- various functions (movement, protection, etc.)
SESAMOID	Patella	- alters the muscle orientation at a joint

To perform the mechanical, biological and chemical functions accurately, bone is composed of several materials that are at many length scales and in various arrangements. Scale is important in discussing the bone architecture as the structure is hierarchical and complex. For example, bone structure can be divided into hierarchical levels as shown in Figure 1.1 and Table 1.2.

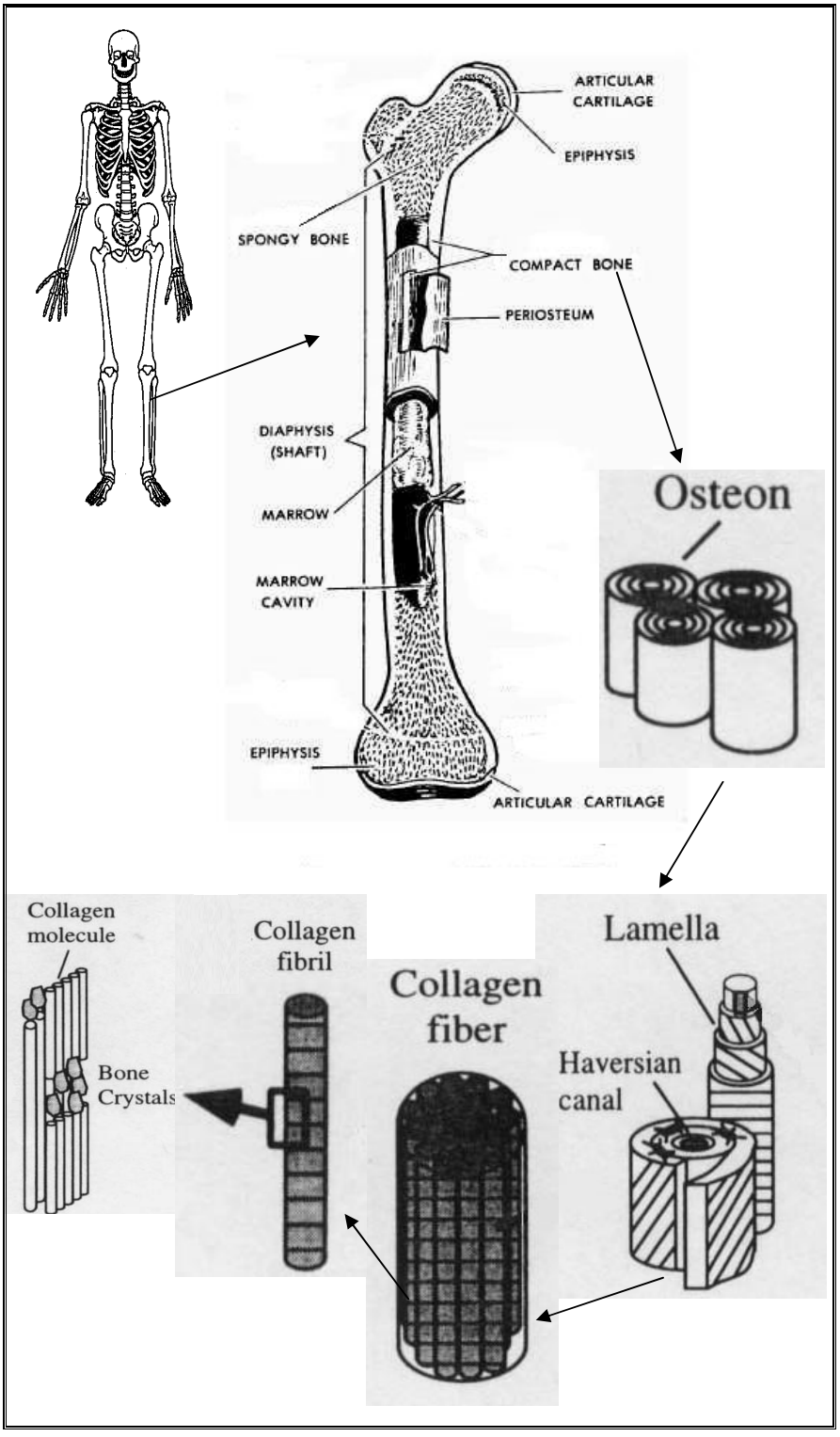

Figure 1.1. Structures and hierarchical levels of bone structure (Rho et al., 1998, Cull, 1989, and Heiserman, 2002)

Table 1.2. Hierarchical levels of bone structure (Rho et al., 1998)

Hierarchical Levels	Size Range	Structure
Macrostructural Level	whole bone	Cortical and cancellous bone
Microstructural Level	10-500 μm	Haversian systems, osteons or trabeculae
Sub-microstructural Level	1-10 μm	Lamellae
Nanostructural Level	from a few hundred nanometers to 1 μm	Collagen fibrils and mineral matrix
Sub-nanostructural Level	below a few hundred nanometers	Collagen, mineral and water molecules

For the macroscopic structure of bone, long bones serve as the classical model. A typical adult long bone consists of a cylindrical central shaft and two wider and rounded ends called diaphysis and epiphyses (Figure 1.1). The diaphysis and epiphyses are connected via the region called metaphysis. Outer surface of the bone is covered by a membrane called periosteum which has the potential to form bone during growth and fracture healing. The inner surfaces of bone, marrow cavity of diaphysis and the cavities of cortical and cancellous bone are covered by endosteum. Although periosteum is a sheet of fibrous connective tissue and an inner cellular layer of undifferentiated cells, endosteum is the membrane of bone surface cells, such as osteoblasts, osteoclasts and bone lining cells. In the hollow interior of bone, there is bone marrow, which produces blood cells (Jee, 2001).

Bone is also classified as cortical (compact) and cancellous (trabecular) types as shown in Figure 1.2. While the epiphysis and metaphysis mostly contain cancellous bone with a thin shell of cortical bone, the diaphysis is mainly composed of cortical bone. Although both types of bones contain the same inorganic and organic constituents, they differ in both proportion and

organization of organic and inorganic constituents and in degree of porosity (Table 1.3). The main structural unit of cortical bone is the osteon (Figure 1.1). Osteons are concentric cylindrical elements, consisting of lamellae, or layers of bone, surrounding a long hollow passageway, the Haversian canal. The Haversian canal contains small blood vessels responsible for the blood supply to bone cells. In cancellous or trabecular bone the structural unit is the trabecula that is formed by organization of plate- and rod-like struts. Unlike osteons, trabeculae do not have a central canal with blood vessels.

There are three types of bone cells: osteoblasts, osteoclasts and osteocytes (bone lining cells)**.** Osteoblasts are responsible for bone formation. They secrete unmineralized bone matrix and serve to calcification besides regulating the flux of calcium and phosphate in and out of the bone. Osteoclasts, multinucleated giant cells, have the role in resorbing bone. Osteocytes are the most abundant cell type in the mature bone. They serve as sensors of mechanical stimuli and communicate with osteoblasts and osteocytes according to these stimuli. During bone formation some osteoblasts are trapped in the matrix and become osteocytes. Bone lining cells are in fact, inactive osteoblasts.

Both types of bone are formed by two different tissues: lamellar and woven bone. Lamellar bone is highly organized, slowly formed bone that consists of parallel layers of osteons. Woven bone, however, is a quickly formed weak tissue which involves a less organized matrix of coarse fibers. It is formed without a preexisting structure during periods of repair and growth. Woven bone is replaced by lamellar bone during growth and healing (Jee, 2001).

Compact bone may be subcategorized as primary or secondary bone according to their formation. Primary bone is formed without a pre-existing bone by mineralization of cartilage. Secondary bone results from the resorption of existing bone and replacement by new, lamellar bone.

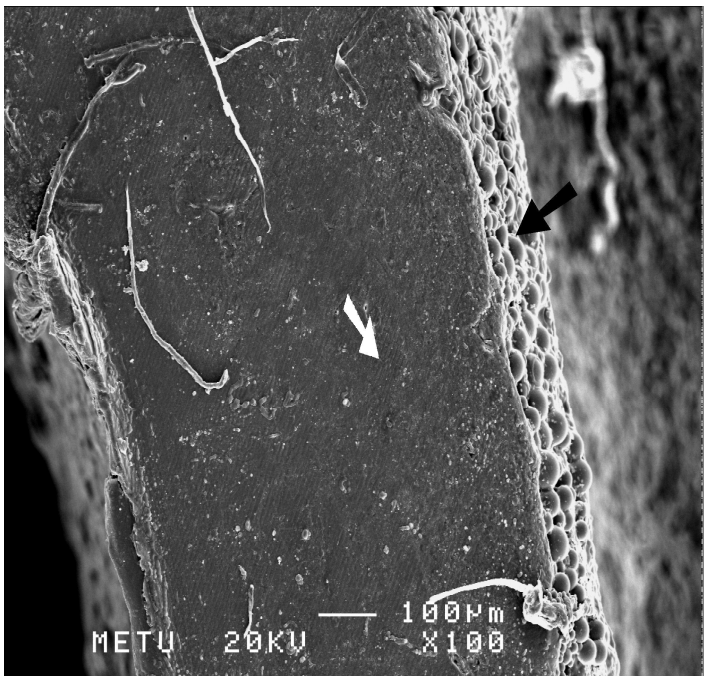

Figure 1.2. Scanning electron micrograph of the rabbit cortical (white arrow) and cancellous bone (black arrow)

Table 1.3. Comparison of cortical and cancellous bone (Jee, 2001)

Cortical Bone	Cancellous Bone
- 80 % of the skeletal mass - dense (5 % -10 % porosity) - outer wall of all bones - supportive and protective function - main structure in cortical bone is osteon	- 20 % of the skeletal mass - less dense -porous (75 % -95 % porosity) - inner walls of bones - support articular surfaces; transfer joint and muscle loads to long bones - main structure in cancellous bone is trabeculae

1.1.2. Biomechanical Properties of Bone

The composition of bone and organization of its constituents determine the physical properties of bone. The physical properties of bone provide insight into its mechanical function. The biomechanical properties of bone are established in response to the normally subjected load. Since it is a dynamic tissue, its structure can change in response to new loading patterns. As Wolff's Law states; increased loading leads to an increase in bone mass and decreased loading leads to a reduction in bone mass (Nigg and Herzog, 2007). Thus, the information at normal physiological loading provides an insight for understanding the functional changes at disease state.

Because of having both the osteonic and trabecular structures, bone is an anisotropic material. Hence, mechanical properties differ depending on the direction considered. Bone is a viscoelastic material because of its water and type I collagen content (Yamashita et al., 2001 and Fratzl et al., 2004). When bone is loaded, water flows through the structure viscously and a small amount of energy is lost. In order to avoid complicated analysis, bone is assumed to be an isotropic homogeneous elastic tissue which obeys the Newton's laws and Hooke's law of mechanics (Turner and Burr, 1993). Hooke's law states that the amount by which a material body is deformed is linearly related to the force causing the deformation.

Biomechanical properties of bone can be determined by various testing methods, such as tensile test, bending test, compression test, torsion test, pure shear test, ultrasonic test and acoustic microscopy test. Usually tensile tests and three-point bending tests are applied to analyze the mechanical properties of long bones.

In most measurements of bone mechanical properties, the relation between the applied force and the deflection is used to generate a load-deflection curve. This curve gives the ultimate load (force at failure), extrinsic stiffness or rigidity, work to failure (area under the load-displacement curve), and ultimate

displacement. Ultimate load is a measure of the general integrity of bone structure and stiffness is related to bone mineralization. Work to failure is the amount of energy necessary to break the bone, and ultimate displacement is inversely related to brittleness of the bone.

When force and deformation are normalized as stress and strain, the load-displacement curve is transformed to stress-strain curve (Figure 1.3). The slope of the stress-strain curve at linear region is called the elastic modulus or Young's modulus and it is a measure of the intrinsic stiffness. Stress is obtained by dividing load to the cross-sectional area and strain is obtained by dividing change in length to the original length of specimen. This curve also presents yield strength, ultimate stress and toughness (work of fracture) and ultimate strength. The elastic region and plastic region of stress-strain curve are separated by the yield point and the stress at this point is called yield strength. After this point stresses begin to cause permanent damage to the bone. The maximum stress and strain is called ultimate strength and ultimate strain, respectively. These strength values are intrinsic properties of bone. Thus, they are independent of the size and shape of bone. The area under the stress-strain curve represents the energy absorbed when the object is loaded (Turner and Burr, 2001).

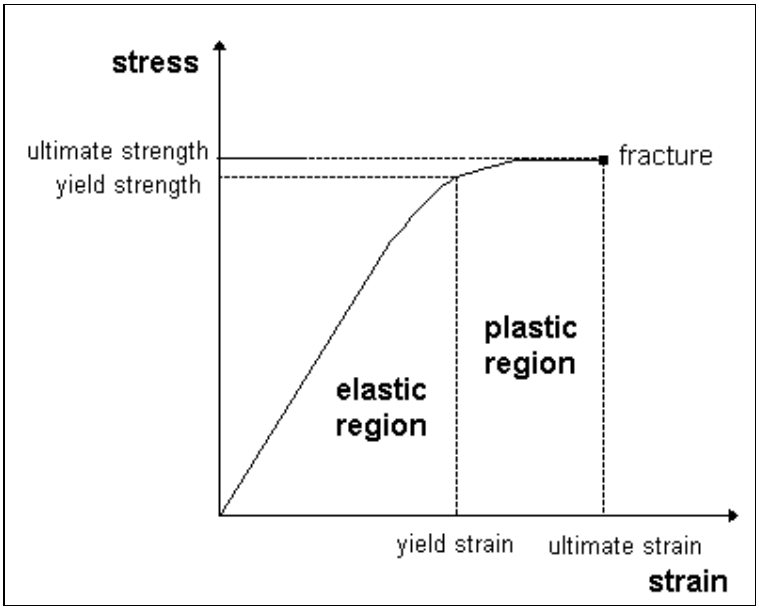

Figure 1.3. A typical stress-strain curve of bone loaded in a single pull to fracture (Rooney, 2007)

1.1.3. Bone Healing and Treatments of Bone Defects

Bone is a dynamic tissue that can self-regenerate and self-model under normal situations. Bone repair occurs by different mechanisms at micro and macro-structural levels. At the microstructural level, the remodeling process is responsible for repairing microdamages. In remodeling process, osteoclasts first resorb a section of bone in a tunnel called a cutting cone. Following this step, osteoblasts form bone to fill up the tunnel. Through remodeling, bone adapts its structure to mechanical stimuli and repairs microstructural damage.

At the macroscopic level fractures, formation of woven bone (callus) is required to repair the damage. At the first step of healing, blood from the ruptured vessels quickly fill the fracture gap and the macrophages remove the dead cells. Additionally, the periosteum ruptured during fracture formation

stimulates the rapid formation of the callus or woven bone. The periosteum also provides temporary strength and support for the fractured bone. These initial events are followed by differentiation of mesenchymal stem cells from bone marrow and periosteum into chondrocytes, osteocytes, osteoblasts or fibroblasts depending on the biological and mechanical conditions. Osteoblasts that are currently present in the damaged tissue produce the woven bone and at the same time, at the center of callus cartilage is formed by chondrocytes. When the callus is filled, bone formation will begin and cartilage is replaced by bone. After all the gap has been ossified, remodeling of the fracture begins gradually resulting in restoration of original bone structure and shape (Doblaré et al., 2004).

In some circumstances, such as large bone defects resulting from trauma, infection or tumor, bone defect cannot heal itself spontaneously. Hence, different treatment strategies need to be applied for such bone repair problems. These strategies can be divided into three main groups: bone grafts, tissue engineered composite grafts and gene therapy strategies (Lieberman and Gamradt, 2006). In all of these approaches the main aim is to provide time and space for the formation of new bone at the defect site and restore the integrity throughout the bone. Otherwise, the surrounding soft tissue will grow into the defect site faster than the growth of bone tissue. Currently used bone grafting treatments are based on autograft, allograft or synthetic material implantation. These bone grafting applications will be discussed in detail in the following section.

In cell-based therapy, cell-seeding to a substrate is done to prepare an implantable graft. The substrate enhances bone regeneration by providing a space to support cell migration, proliferation and differentiation. In recent years, differentiated osteoblasts and undifferentiated bone marrow stem cells, such as mesenchymal stem cells (MSCs) are used with scaffolds in bone tissue engineering. Trojani et al. (2005) examined silated hydroxypropylmethyl- cellulose (Si-HPMC) -based hydrogel as a scaffold for 3D culture of osteogenic cells by using mineralization assays and gene expression analysis of osteoblastic markers. *In vitro* analysis showed that

these cells were at more mature and differentiation status than the cells cultured in monolayer. It was concluded that osteoblastic survival, proliferation and differentiation were supported by the scaffold (Trojani et al., 2005). In another study, Wu and his coworkers (2006) seeded autologous marrow stromal cells into porous beta-tricalcium phosphate carriers after differentiation to osteoblasts. They then implanted these cell/scaffold composites into the canines' mandibula defects. Although incomplete bone repair was examined in pure beta-tricalcium phosphate group, new bone formation was observed histologically on the surface and in the pores of beta-tricalcium phosphate of cell/scaffold composite group (Wu et al., 2006).

Mesenchymal stem cells can be directly derived from bone marrow. They serve as a readily available source of undifferentiated cells that can be differentiated to bone, cartilage, adipose tissue or other tissues of mesenchymal origin. In a recent *in vitro* study, MSCs were introduced into a nano-hydroxyapatite/polyamide (n-HA/PA) composite scaffold and it was shown that n-HA/PA scaffold supported osteoblastic differentiation of MSCs (Wang et al., 2007). Another group cultured bone marrow derived MSCs on gelatin microcarrier beads in spin culture and studied their potential for bone formation in rat femur defects (Yang et al, 2007). They observed a significant induction of trabecular bone formation in comparison to empty defects and defects with only gelatin microcarrier beads (Yang et al., 2007).

In gene therapy, genes are inserted into an individual's cells to generate a desired protein product that is originally absent or defective in that individual. Gene therapy may involve an *in vivo* or an ex vivo approach. *In vivo* studies, a vector, which provides the entry of the genetic material into the cells, is delivered via injection or direct local implantation. In ex vivo studies, a specific type of cell is harvested and modified under *in vitro* conditions and then implanted into the site of injury (Phillips et al., 2007). The bone tissue engineering applications of gene therapy are given in Table 1.4.

Table 1.4. Some examples of gene therapy studies in bone tissue engineering

Type	Viral Vector	Target Gene	Target Tissue or Cell	In Vivo Application	Reference
in vivo	retroviral vector	BMP-2/4	Bone marrow stromal cells	rat femoral fracture	Rundle et al., 2003
	lentiviral vector	BMP-2	bone marrow cells	critical sized rat femoral defect	Hsu et al., 2007
	adenoviral vector	BMP-2	bone marrow cells	(NOD/ SCID) mice limb	Gugala et al., 2007
ex vivo	retroviral vector	BMP4	muscle-derived stem cells	critical-sized mice skull bone defect	Shen et al., 2004
	retroviral vector	*β*-Galactosidase	bone marrow stromal cells	mice femoral bone marrow cavity	Zhang et al., 2004

1.2. Bone Grafts

Bone grafting procedures have been developed to repair bone defects or improve reconstruction in the damaged bone tissue. These grafts are developed to provide mechanical or structural support to the bone, and to improve bone tissue formation.

There are mainly three processes involved in bone regeneration: osteoinduction, osteoconduction, and the recruitment of osteogenic cells. Osteoinduction can be defined as the process in which the host cells are stimulated to synthesize new bone. Osteoconduction is a process that provides an interconnected structure through which new cells can migrate into the graft and new vessels can form (Goldberg and Akhavan, 2006; Murugan and Ramakrishna, 2005). The process of bone formation (osteogenesis) occurs in two ways: intramembranous ossification or endochondral ossification. Intramembranous ossification involves the replacement of sheet-like connective tissue membranes with bony tissue by differentiation of mesenchymal cells into osteoblasts without cartilage formation. Flat bones of the skull and some of the irregular bones are formed in this way. Endochondral ossification forms bone by replacing a cartilaginous model, or precursor, that appeared earlier in embryonic development. Most of the bones of the skeleton are formed in this manner (Jee, 2001). Hence in selection of materials and preparation of bone grafts these processes have to be considered for the success of the implant.

1.2.1. Types of Bone Grafts

There are several bone grafting methodologies available, which include autografting, allografting, xenografting, and alloplastic or synthetic bone grafting. Each of these grafting methods has some advantages and disadvantages as listed in Table 1.5.

Table 1.5. Advantages and disadvantages of different bone grafting methods (Jenis and Erulkar, 2006, Moore et al., 2001, Vogt, 1999, Artico et al., 2003, and Abjornson and Lane, 2006)

	Advantages	**Disadvantages**
Autografting	- current gold standard - histocompatible - has all three process at bone regeneration - no risk of disease transmission - does not require vascular tissue bed	- need of second operation - harvesting causes additional trauma and infection risk - limited availability - variable quality - cosmetic disability at the donor site
Allografting	- available in substantial amounts - provides a good, natural, bony scaffold - no additional trauma - can be stored, bone bank	- risk of transmitting HIV and hepatitis, needs donor screening - rejection risk - requires vascular tissue bed (avascular grafts) -poor mechanical properties
Xenografting	- available in substantial amounts - no additional trauma - potential genetic therapies in the donor animal	- rejection risk - ethical issues - risk of disease transmission - physiological incompatibility
Synthetic Bone Grafting	- availability - no additional trauma and infection risk - no risk of disease transmission - biocompatible - provide a platform for the delivery of bioactive materials, antibiotics - be able to be designed to fit defect - controlled quality - easy stored	- inflammatory risk - need manipulation of material - need adaptation to the bone defect - complications related with mechanical, thermal and electrical stresses

Autografting can be defined as tissue transplantation from one site to another on the same individual. Allografting involves tissue transplantation between individuals of the same species with non-identical genetic composition. Xenografting is a process of transplanting tissue from one species to another (e.g., from animal to human). As an alternative to these three types of bone grafts, alloplastic or synthetic bone grafts have been developed. In this type of grafting the synthetic biomaterials (polymers, ceramics etc.) are used to repair or regenerate defective bone tissue.

Demineralized bone matrix (DBM) is a form of allograft that is used in filling cranial defects and many orthopedic applications (Chesmel et al., 1998, Cook et al., 2002, and Chakkalakal et al., 1999). It is produced after a mild acid extraction of cadaveric bone. In this extraction process, the mineral phase of the bone is removed and organic phase -collagen (93 %), growth factors (5%), and non-collagenous proteins (2%) - is retained. The bone morphogenic proteins (BMPs) are the osteoinductive component and collagen is the osteoconductive component in the DBM (Abjorson and Lane, 2006, and Lee et al., 2005). The advantages and disadvantages of use of DBM in bone grafting are given in Table 1.6.

DBM has been widely used in bone tissue engineering. Chesmel et al. (1998) compared the bone repair abilities of a bone autograft and four distinct forms of human DBM in cranial defects created in athymic rats. They observed that DBM could support bone healing as equivalent to an autograft. In another study, the osteoinductive properties of two distinct human DBM bone grafts were compared in an athymic rat model and the results showed that the preparation methods of DBM, carrier and dose of DBM per volume affected the osteoinductive properties of DBM bone grafts (Takikawa et al., 2003). DBM can be used as a composite component, as in the study of Yee et al. (2003). In this study, the potential of DBM-hyaluronan putty as a bone graft enhancer was studied by spinal fusion process in rabbit models. After 9 weeks, lumbar spines were examined by radiography and computed tomographic analysis. According to the results, DBM-hyaluronan addition improves the fusion rate and bone volume (Yee et al., 2003). Besides the

experimental studies, DBM has also been used in clinical applications. There are commercially available DBM bone grafts, such as DBX, Grafton, Orthoblast, Osteoset 2 DBM graft. In the study of Cheung et al. (2003), two of these DBM bone grafts, Grafton and Orthoblast, were used in treatment of periarticular fractures. They observed that DBM allografts had a favorable success rate comparable to autografts in periarticular fractures and other osseous defects.

Table 1.6. Advantages and disadvantages of the use of DBM in bone grafting (Abjorson and Lane, 2006, Burg et al., 2000, Marsh, 2006, Glowacki, 1992, and Pietrzak et al., 2005)

Advantages	Disadvantages
- osteoconductive - osteoinductive - does not need harvesting cells - unlimited supply according to autogenous cells	- risk of disease transmission - antigenicity - need for sterilization step - can not provide structural support (non-weight bearing) - batch variability - expensive - require solvent for handling

1.3. Bone Substitutes

Bone graft substitute is a general term to describe any biomaterial used to aid in the regeneration or promotion of bone.

1.3.1. Ceramics

Ceramics are usually solid inorganic compounds with various combinations of ionic or covalent bonding. They are widely used in dentistry and skeletal hard tissue repair and replacement applications. The type of tissue response to biomaterials is directly related with the tissue-implant attachment. Bioceramics can be classified according to their tissue attachment property as shown in Table 1.7.

Table 1.7. Types of bioceramics according to the tissue attachment type (Hench and Best, 2004)

Type of attachment	Example
Dense, nonporous, nearly inert ceramics	- alumina (Al_2O_3), - zirconia (ZrO_2), - titania (TiO_2)
Porous inert implants	- alumina (Al_2O_3), - porous metals
Dense, nonporous surface reactive ceramics	- bioactive glasses - hydroxyapatite
Dense, nonporous (or porous) resorbable ceramics	- calcium sulfate - calcium phosphate ceramics

1.3.1.1. Resorbable Ceramics

Resorbable ceramics are ceramics which can be broken down into smallest units and can be absorbed by the body over a period of time. Osteogenesis occurs after resorption of this type of ceramics. The rate of resorption of the graft depends on its chemical composition, shape and architecture (Carson and Bostrom, 2007). Calcium sulfates and calcium phosphates can be given as examples of such resorbable ceramics.

Calcium sulfates function as bone void fillers and as osteoconductive carriers for antibiotics, DBM powder, bone morphogenetic proteins (BMPs) or any other biologic molecule (Abjorson and Lane, 2006). Plaster of Paris is a hemihydrate of calcium sulfate based resorbable ceramic and has been used in maxillofacial osseous defects (Su-Gwan et al., 2001). Calcium sulfate bone grafts have some advantages and disadvantages as listed in Table 1.8.

Calcium sulfates are used widely in bone tissue engineering. In a study, the *in vivo* response of calcium sulfate alone and as a carrier for coralline hydroxyapatite was examined in a corticocancellous defect model in rabbits (Stubbs et al., 2004). They observed that although calcium sulfate supported the new bone formation alone, bone defects could not be filled completely. When calcium sulfate was used with coralline hydroxyapatite, it provided an easy surgical handling scaffold and enabled the defect to be completely filled. In another *in vivo* study, the effect of chitosan bead encapsulation of calcium sulfate on the defects at mandibular bone of dogs was studied. At the end of radiographic, mechanical and histological analyses it was observed that chitosan bead encapsulation of calcium sulfate stimulated early bone formation (Cho et al. 2005). Intini and his co-workers (2007) recently used a combination of calcium sulfate and platelet-rich plasma for the dental and craniofacial clinical cases for bone regeneration. They observed that the combination induced the bone formation at critical size bone defects.

Table 1.8. Advantages and disadvantages of use of calcium sulfates in bone grafting (Peltier and Speer, 1992, Carson and Bostrom, 2007, Pecora et al., 1997, Cho et al., 2005, and Abjorson and Lane, 2006)

Advantages	Disadvantages
- osteoconductive - inexpensive - readily available in a variety of sizes and volumes - moldable - easily prepared and sterilized - indefinite shelf life - well tolerated - absorbable - can be used as carrier for biological molecules	- no internal strength or support - dissolve before new bone formation - only used to fill small bone defects - quite random pore structure - lack of connectivity

The ceramics made of calcium phosphate salts are resorbable and can also be used for replacing bone tissue. They are osteoconductive and in some cases, osteoinductive. The most widely used calcium phosphates are HA and β-tricalcium phosphate (β-TCP). Both of them have Ca/P ratios within the range of 1.50-1.67 which has shown to promote bone ingrowth (Temenoff and Mikos, 2000).

HA is the most widely used calcium phosphate ceramic because of the chemical and structural homology with natural bone mineral. Bone mineral is a HA that is calcium deficient and contains carbonate in its structure. The HA is derived either from natural sources like coralline HA, or by chemical synthesis. There are different techniques for the synthesis of HA: solid-state reactions, solution precipitation and co-precipitation, hydrolysis and other solution-mediated reactions, hydrothermal reactions, emulsion and micro-emulsion techniques, and sol-gel techniques (Thamaraiselvi and Rajeswari, 2004). HA

is widely applied as bone substitutes, coatings for bone-dental implants and carrier for some biologic materials, such as bone morphogenic proteins (BMPs), bone marrow–derived autogenous stem cells (Sopyan et al., 2007, Chambers et al., 2007, Ono et al., 1995, and Chistolini et al., 1999).

TCPs have basically two forms: α-TCP and β-TCP. Beta-TCP and alpha-TCP have the same macrostructure and microstructure, but they have different crystalline structures. The solubility of α-TCP is much higher than that of β-TCP. Therefore, the dissolution of α-TCP is at a greater rate than bone repair *in vivo* (Kitamura et al., 2004). β-TCP is mostly used as an osteoconductive scaffold and is resorbed by osteoclastic activity. It, therefore, will not disappear until new bone formation occurs (Abjorson and Lane, 2006). HA has slower dissolution rate than β-TCP in bone tissue. Studies have been mainly focused on ceramic composites of HA and TCP to obtain an optimum resorbability of the implant (Kwon and Jenis, 2005).

1.3.1.2. Bioactive Ceramics

Bioactive ceramics can form an interfacial attachment to the host bone and enhance bone tissue formation. Bioactive ceramics are intermediate between resorbable and bioinert ceramics.

As the well known example of the bioactive ceramics, bioglasses which are silica glasses with a specific composition are used in maxillofacial reconstruction, dental applications, in coating of orthopedic prostheses and as fillers for bony defects (Hattar et al., 2005, Oliva et al., 1998, and Vogel et al., 2001). They contain less than 60 mole % SiO_2 while having high NaO_2 and CaO contents. The CaO/P_2O_5 ratio in bioglass is similar to that found in native bone. These types of glasses have highly reactive surfaces. A hydroxyl carbonate apatite (HCA) layer that has similar crystallinity as the bone apatite is formed on their surfaces in an aqueous medium (Hench, 1992). Bone

bonding in bioglass is based on the formation of this layer. The advantages and disadvantages of bioglass bone grafts are given in Table 1.9.

There are many experimental and clinical studies related to the applications of bioglass in bone tissue engineering. Silver et al. (2001) studied the effects of different bioactive glasses, such as 45S5 Bioglass®, bioactive glasses 58S and 77S on metabolism and cell viability with osteoblasts *in vitro*. Their results showed that 45S5 Bioglass® caused intra- and extracellular alkalinization and stimulated cellular energy production. In another study, a bioglass/dextran composite as a bone graft substitute was used to fill bony defects in rabbit models. The group observed 100 % bony ingrowth within 6 weeks (Chan et al., 2002). There are also clinical applications of bioglass. In the case study of Shapoff et al. (1997), four severe osseous defect cases were treated by using PerioGlass® bone graft material. The defects were greatly reduced and filled with a hard, vascularized material that resembles bone.

Table 1.9. Advantages and disadvantages of use of bioglass in bone grafting (Hench, 1992, Vogel et al., 2001, and Thamaraiselvi and Rajeswari, 2004)

Advantages	Disadvantages
- excellent bioactivity, bone-bonding through biologically active HCA layer - excellent biocompatibility (no inflammation, toxicity etc.) - bioresorbable - easy adaptation to the defect shape - good handling qualities	- poor mechanical strength without ceramic additives and cannot be used in stress-bearing sites - low fracture toughness

1.3.1.3. Bioinert Ceramics

Bioinert ceramics do not appear to have any reactivity because of their extremely slow dissolution rate within the living tissue. A fibrous protective cell membrane, therefore, occurs at the implant surface upon implantation to protect neighboring cells from mechanical damage. These types of ceramics are often composed of metal oxides such as alumina (Al_2O_3), zirconia (ZrO_2), and titania (TiO_2). They are widely used for long bone defects because of their excellent compressive strength. In total hip replacements, these ceramics are applied as coating materials to improve biocompatibility and bone ingrowth through the implant and to minimize wear, friction and corrosion (Carson and Bostrom, 2007).

1.3.2. Polymers

Polymers are high molecular weight molecules that are composed of repeating structural units, monomers, connected by covalent bonds. Many polymers that are potential candidates for bone graft substitutes represent different physical, mechanical and chemical properties. Polymers may also be important potential carriers for bioactive substances such as antibiotics and osteoinductive agents. Polymers can be obtained from natural products, (natural polymers) or by chemical synthesis (synthetic polymers). The comparison of the properties of natural and synthetic polymers is given in Table 1.10. Synthetic polymers can be subdivided into degradable and nondegradable types. The former ones are degraded and resorbed by the body like the natural polymers. The benefit of having the implant resorbed by the body is that it enables the body to heal completely without foreign bodies remaining from the implant.

Table 1.10. Comparison of the properties of natural and synthetic polymers (Lee and Shin, 2007)

Polymers	Advantages	Disadvantages
Natural	- biocompatible - degradable - readily solubilized in physiological fluid	- poor chemical and mechanical properties - immunogenecity - difficulty in processing - risk transmission of pathogens
Synthetic	- excellent chemical and mechanical properties - less immunogenic - no risk transmission of pathogens - easy processing - can be modified easily -controlled molecular weight, functional properties	- inflammation risk - harmful degradation products - limited biological function

1.3.2.1. Natural Polymers

The most widely used natural polymers in bone tissue engineering are collagen, fibrin, hyaluronic acid, alginate, chondroitin sulfate and chitosan (Lee et al., 2007, Patel et al., 2006, Kim et al., 2007, Li et al., 2005, and Rammelt et al., 2006).

Hyaluronic acid (HYA), also known as hyaluronan, is a naturally derived high molecular weight, linear polysaccharide found in all connective tissues of mammalians. It is composed of N-acetyl-D-glucosamine and D-glucuronic acid units. HYA is a component of extracellular matrix (ECM) in long bones

constituting about 3 % of the total glycosaminoglycan (GAG). It has a positive effect in bone mineralization (Zou et al., 2004).

Because of its excellent lubrication property and interaction with chondrocytes, HYA is also widely used in cartilage tissue engineering studies. HYA is also a viscoelastic material and this property is important for the ocular surgery and cartilage repair applications (i.e. defects in osteoarthritis). Besides these, its antioxidant property (ability of serving as a free radical scavenger) enhances its role in osteoarthritis treatment. HYA also takes role in morphogenesis of cells, cell migration, differentiation and adhesion in developmental stages. With all of these properties, it is important in wound healing. HYA has, therefore, also been used as a wound dressing material (Cho et al., 2002, Xu et al., 2007 and Park et al., 2004). Since native hyaluronan can be rapidly metabolized *in vivo* by free radicals, covalent crosslinking and chemical modifications are necessary for their applications. Because of its hydrophilic properties cells adhesion to the unmodified HYA is restricted (Varghese and Elisseeff, 2006).

Hyaluronic acid is a preferred biomaterial for scaffold fabrication in bone tissue engineering applications. Kim et al. (2007) studied an acrylated hyaluronic acid scaffold as carriers for bone morphogenic protein-2 (BMP-2) and human mesenchymal stem cells (hMSCs) for regeneration in rat calvarial defects. According to the histological and immunohistological examinations, HYA scaffolds with MSCs and BMP-2 showed higher osteocalcin expression and mature bone formation than empty defects. The MSC-BMP-2 implant area was filled with thicker new bone than the implant area loaded with BMP-2 only (Kim et al., 2007). In another study, the defects at the tibia of rabbits were filled with a HYA and spongiosal bone graft together and spongiosal bone graft alone. At different time points, the implants were analyzed histopathologically and the defects filled with HYA and bone graft showed better healing than only bone graft filled groups at every time points (Aslan et al., 2006). Lisignoli et al. (2002) studied the treatment of the large segmental radius defects in a rat model by implanting a biodegradable non-woven hyaluronic acid-based polymer scaffold (Hyaffs11) alone or in combination

with bone marrow stromal cells (BMSCs). They examined the healing at different time periods by using radiographical and histological analyses. They found that HYA-based scaffold with BMSCs can be used as an appropriate carrier vehicle for delivery of osteoinductive factors in the repair of bone fractures (Lisignoli et al., 2002).

1.3.2.2. Synthetic Polymers

Synthetic polymers have also been used for bone tissue engineering for decades. For example, polymethylmethacrylate (PMMA) is used widely as a bone substitute to fill defects and as a fixation agent in orthopedic surgery (Yamamuro et al., 1998, Walsh et al., 2004, and Tsukeoka et al., 2006).

In recent years, resorbable synthetic polymers (i.e. poly(glycolic acid) (PGA), poly(L-lactide) (PLLA), poly(DL-lactide) (PDLLA), poly(lactic-glycolic) acid (PLGA) and poly(ε-caprolactone) (PCL)) are introduced into bone grafting area. These types of polymers are preferred mainly as bone grafts since they allow new bone ingrowth in time. All of these polymers are derived from synthetic aliphatic polyesters. These polyesters are widely used biomaterials in surgical practices. Polylactic acid screws were used in hip osteotomy surgery as fixation materials (Ito et al., 2002). PLLA-PGA bone fixation devices were applied clinically in maxillary and mandibular bone site surgeries (Edwards et al., 2001). In hand surgery, PLLA and PLGA fixation devices were used clinically (Waris et al., 2004).

Poly (ε-caprolactone) is a semicrystalline linear, resorbable polymer with a low glass-transition temperature (-60℃) and a low melting point (60℃). Because of its low glass transition temperature, the amorphous phase of PCL shows higher molecular mobility at body temperature (Tay et al., 2007). PCL has high degree of crystallinity and hydrophobicity thus it has long degradation time, nearly 2 years *in vivo* (Prabhakar et al., 2005). The degradation of PCL involves random hydrolytic chain scission of the ester linkages and occurs via

both surface and bulk erosion under normal physiological conditions (Ang et al., 2007).

PCL is a highly biocompatible polymer as its non-toxic degradation products are totally eliminated by the body (Hao et al., 2002). PCL had been approved by the Food and Drug Administration for human clinical use *in vivo* and has been used widely as suture material, in long-term drug delivery systems and bone tissue engineering (Taddei et al., 2005 and Pitt, 1990). Although PCL is highly compatible with osteoblasts, pure PCL has poor cell adhesion and proliferation on its surface (Mano et al., 2004). To provide good adhesion and growth of osteoblast like cells and mature osteoblasts, it has been blended with bioceramics, such as HA and silica (Ciapetti et al., 2003 and Rhee, 2004). In bone repair applications, reinforcement of PCL is also necessary to improve its poor mechanical properties (Coombes et al., 2004). To improve mechanical properties, PCL has been either blended with other polymers, such as PLA and PLGA (Mano et al., 2004 and Pitt, 1990), or reinforced with bioceramics, such as HA (Ang et al., 2007, Azevedo et al., 2003).

PCL is used for both *in vitro* and *in vivo* bone repair applications. In an *in vitro* study, a PCL/ tricalcium phosphate (4:1) scaffold seeded with osteoblasts was used to examine the effects of distinct concentrations of human recombinant bone morphogenetic protein- 2 (rhBMP-2) on the osteoblasts. Histological staining results showed that cells from PCL/TCP with or without rhBMP-2 maintained their osteogenic phenotype throughout the experiment (Rai et al., 2004). In another study, the pore size effect on cell and tissue interactions of PCL cylindrical scaffolds with gradually increasing pore size along the longitudinal direction was investigated (Oh et al., 2007). PCL scaffolds were seeded with different types of cells namely, chondrocytes, osteoblasts, and fibroblasts. The group also applied only PCL implants into skull bone defects in a rabbit model. They observed that pore size ranges of 380–405 mm were effective for chondrocyte and osteoblast growth and that of 186–200 mm for fibroblast growth. They also showed that 290–310 mm pore size range was suitable for new bone formation (Oh et al., 2007). In another study, a hybrid scaffold system was implanted to rabbit femoral condyle to examine its

potential for large- and high-load-bearing osteochondral defect repair. In this system, medical-grade PCL (mPCL) was used for bone part and fibrin glue for the cartilage part. Both matrices were seeded with allogenic bone marrow-derived mesenchymal cells prior to implantation. *In vivo* cell tracing, histological and micro-CT analyses revealed that the scaffold/cell system promoted structural and functional repair of osteochondral defects in 3 months (Shao et al., 2006).

1.3.3. Metals

Metals are substances with high thermal and electrical conductivity, luster, and malleability, which readily lose electrons to form positive ions. Because of their strong mechanical properties, they are widely used for load-bearing applications such as total joint replacement and fracture fixation (Katti, 2004). There are mainly three types of biomedical metals: 316L stainless steel, cobalt-chromium-molybdenum alloys and pure titanium /titanium alloys. However, their low biocompatibility which mainly arises from their chemical degradation (corrosion) in physiological environment is a problem for their clinical applications. To avoid corrosion, some bioactive materials can be applied as coatings (Ravaglio and Krajewski, 1992). Their other disadvantages involve difficult fabrication and mechanical mismatch with the bone (Dee et al., 2002). The porous metallic materials have recently been developed to minimize the mechanical mismatch between the implant and the host tissue. Spoerke and his coworkers (2005) coated titanium foam with an organically-modified apatite layer (organoapatite) and examined its effectiveness in bone healing by *in vitro* and finite element analyses. The results of finite element analyses showed that there was a reduction of stress-concentration in the titanium matrix. Besides, *in vitro* analysis indicated cellular ingrowth occurred through the organoapatite-coated titanium (Spoerke et al., 2005). Similarly, Sevilla et al. (2007) compared tantalum and nickel–titanium porous materials according to their pore sizes and mechanical properties. Both metallic foams with an open and interconnected porosity showed

Young's modulus values very similar to that of cancellous bone (Sevilla et al., 2007). In another study, the mechanical properties of porous nickel-titanium materials were examined and the results indicated that the material provided structural support during the bone ingrowth (Barrabés et al., 2007).

1.3.4. Composites

Composites can be defined as materials consisting of two or more chemically distinct constituents, having a distinct interface separating them on a scale larger than the atomic scale. Biocomposites are nonviable composite materials that can be used in medical applications to interact with biological systems. These are composites that consist of one or more discontinuous phases embedded within a continuous phase. The discontinuous phase is usually harder and stronger than the continuous phase matrix. Some reinforcement materials like fibers (composed of glass, carbon or polymer), calcium salts, and polymers are used as matrix materials. According to the reinforcement forms, synthetic biocomposites can be divided into three general groups: continuous fiber composites, particulate composites and short fiber composites (whisker and blade reinforcement composites) (Ramakrishna and Huang, 2007).

Because of the composite nature of the bone, single phase materials do not provide all the properties necessary for a successive bone grafting. The combination of two or more materials with different properties can be applied for graft composites. Therefore, the disadvantages of one material are eliminated by the properties of other material. For example, Kong et al. (2006) prepared chitosan/nano-HA composite scaffolds to increase the biocompatibility and bioactivity of chitosan. They incubated these scaffolds in simulated body fluid to study their bioactivity properties and observed that their bioactivity was higher than pure chitosan. They have also investigated their biocompatibility with cell culture studies (Kong et al., 2006). In another study, coating of poly(DL-lactic-co-glycolic acid) with natural biomaterial solutions of

collagen, chitosan, or N-succinyl-chitosan was used to increase the cell attachment on PLGA (Wu et al., 2006). Degradation studies in PBS and *in vitro* analysis of composite (such as cell attachment, cell viability and alkaline phosphatase (ALP) assay revealed that chitosan and collagen treatment significantly improved the surface hydrophilic characteristics than N-succinyl-chitosan and collagen. This, in turn, affected the cell attachment, proliferation and differentiation more significantly than the others.

Besides the biological improvements, the mechanical properties were also enhanced by composite approaches in bone tissue engineering. Juhasz et al. (2004) characterized the glass-ceramic apatite–wollastonite (A–W) particulate reinforced polyethylene (PE) composite by three-point bending test. They observed that as the filler content increased, the mechanical properties of the composite were improved.

Although synthetic biocomposites showed good performance in bone tissue engineering, some of them failed to stimulate the osteogenic functions. Tissue engineered-biocomposite approach has been developed since only living bone cells ultimately generate new bone tissue. Zhou et al. (2007) developed a scaffold/cell construct consisting of sheets of bone marrow stromal cells and a fully interconnected medical-grade polycaprolactone–calcium phosphate scaffold. After *in vitro* characterization, they implanted these constructs into the dorsal pockets of rats either with or without pre-culturing in osteogenic medium for 8 weeks. Histological examination showed that healthy bone formation without fibrous tissue capsule formation was observed in 8 weeks *pre*-cultured constructs. On the other hand, dense fibrous tissue was formed around the noncultured constructs (Zhou et al., 2007).

In another study, the ectopic *in vivo* bone formation was examined by implanting a new resorbable ceramic, calcium deficient hydroxyapatite (CDHA), with and without human MSCs into the subcutaneous pocket of mice. The study compared CDHA with β-tricalcium phosphate, hydroxyapatite ceramics and demineralized bone matrix. According to the alkaline ALP activity results and morphological analysis, bone formation occurred after 8

weeks in 4 of 16 MSC/CDHA and 2 of 16 MSC/X-TCP samples and no bone formation occurred in constructs without MSCs (Kasten et al., 2005).

1.4. Aim of the Study

An ideal bone graft should both augment bone regeneration and support the bone mechanically during healing process. However, there is yet no one ideal biomaterial that fulfills the requirements of an ideal implant for healing large bone defects. In this study, development of poly(ε-caprolactone) based composite implants with different organic –DBM, HYA- and/or inorganic –bioglass, calcium sulfate- compositions have been aimed for augmenting bone formation.

For this purpose, PCL, PCL/BG, PCL/BG/DBM, PCL/BG/CaS, and PCL/BG/HYA discs were prepared by compression molding. Discs were characterized with *in situ*, *in vitro* and *in vivo* methods. For *in situ* analysis, mass loss, water uptake, maintenance of structural integrity and changes in mechanical strength were studied after incubation in phosphate buffered saline (PBS) for 4 and 6 weeks. In order to evaluate the bioactivity of the discs in relation to their composition, they were incubated in Simulated Body Fluid (SBF) for 1, 7 and 14 days and surface morphology, and surface crystal formation was studied with scanning electron microscopy. Biocompatibility of the discs was investigated by cytotoxicity tests using osteosarcoma cell line (Saos-2).

The *in vivo* behavior of all discs was studied by implanting them to the critical size defects created on humeri of the rabbits. The animals were terminated 50 days after the operations and the bones were harvested and analyzed with scanning electron microscopy, and computerized tomography. The biomechanical properties of the humeri were measured at both macro and micro-levels by three point bending and microhardness tests.

CHAPTER 2

MATERIALS AND METHODS

2.1. Materials

For disc preparation: The bioactive agents, calcium sulfate (min. 99 %), hyaluronic acid sodium salt (from human umbilical cord), and poly(ε-caprolactone) (M_w=14,000 g/mol) were obtained from Sigma-Aldrich Chemie GmbH, Germany. Perioglass® (bioglass) was obtained from US Biomaterials Corp., USA; Demineralized bone matrix® (DBM) was purchased from LifeNet, USA.

For *in situ* analysis: Trizma hydrochloride (TRIS-HCl reagent grade, min. 99 % redox titration), sodium azide (NaN_3), potassium phosphate monobasic (KH_2PO_4), potassium chloride (KCl, max. 0.0001 % Al, puriss.), sodium chloride (NaCl, max. 0.00002 % Al, puriss.), sodium hydrogen carbonate ($NaHCO_3$); hydrochloric acid (HCl) and calcium chloride-2-hydrate ($CaCl_2 \cdot 2H_2O$) were obtained from Sigma-Aldrich Chemie GmbH, Germany. Magnesium sulfate heptahydrate ($MgSO_4 \cdot 7H_2O$) was purchased from Merck, Germany. Di-potassium hydrogen phosphate anhydrous and formaldehyde solution were the products of Fluka, Switzerland.

For *in vitro* testing: Sodium pyruvate solution, foetal calf serum (FCS), DMEM low glucose (1 g/l) with L-glutamine, DMEM high glucose (4.5 g/l) with L-glutamine, trypsin EDTA and penicillin/streptomycin were purchased from PAA Laboratories, Austria. 3-(4, 5-dimethylthiazol-2-yl)-2,5-diphenyl tetrazolium bromide (MTT bromide) was obtained from Gerbu Biotechnik GmbH,

Germany; Dimethyl sulfoxide (DMSO) (molecular biology grade) was obtained from AppliChem, Germany. Trypan blue solution (0.4 %) was purchased from Sigma-Aldrich Chemie GmbH, Germany. Ethanol (absolute extra pure) was purchased from Merck, Germany.

For *in vivo* analysis: Xylazine hydrochloride (Alfazyne 2%) and ketamine hydrochloride (Alfamine 10%) were obtained from Egevet, Turkey. Vicryl (3/0) was obtained from Ethicon, UK; Propylene (3/0) was purchased from Doğuş Ltd.,Turkey; Pentotal (Thipentotal) was the product of Abbott, Italy, Neo-terramycin was obtained from Pfizer, Turkey and AcryFix Kit was obtained from Struers, Denmark.

2.2. Methods

2.2.1. Development of PCL Based Discs

2.2.1.1. Particle Size Reduction of the Composite Components

In order to obtain a homogenous composite, the particles of bioactive agents that were going to be used in disc preparation -bioglass, calcium sulfate (CaS), hyaluronic acid (HYA) and demineralized bone matrix (DBM)- were ground to the micron level using a Ceramic Ball Mill (Retsch MM200, Germany). Due to high water solubility of the last three, bioglass was used as the reference material in particle size determination and optimization studies that require aqueous dispersion of the agent. Before grinding, the particle size distribution of unground bioglass was measured using Mastersizer 2000 Particle Size Analyzer (Malvern Instruments Ltd., UK) at Central Laboratory, METU.

To compare the effects of different grinding conditions, 300 mg bioglass was ground at the following settings:

1) Dry grinding for 30 minutes at 25 Hz frequency;
2) Dry grinding for 2 hours at 25 Hz frequency;
3) Wet grinding for 2 hours at 25 Hz frequency (within absolute ethanol)

Particle size distribution of the ground powders was analyzed by the same particle size analyzer in the Central Laboratory.

2.2.1.2. Preparation of PCL Based Discs

Five different groups of discs were prepared with the following compositions:

1. PCL discs,
2. PCL/Bioglass discs (2.5:1, w/w),
3. PCL/Bioglass/Calcium sulfate discs (2.5:1:1, w/w),
4. PCL/Bioglass/DBM discs (2.5:1:1, w/w)
5. PCL/Bioglass/HYA discs (2.5:1:1, w/w/w).

After melting PCL on a Teflon sheet at around 40°C, other ground disc components were added and mixed via a Teflon rod. The mixture was then poured to a special metal mould (5 mm Die, Specac, Britain) and a 1000 N load was applied for 5 minutes with Lloyd LS 500 mechanical test device (Lloyd Instruments, UK) (Figures 2.1 and 2.2) for compaction. Each disc was approximately 5 mm in diameter, 2 mm in height and 60 mg in weight (Figure 2.3). They were stored in a desiccator at 4 °C until use.

Figure 2.1. The metal mould used in disc preparation

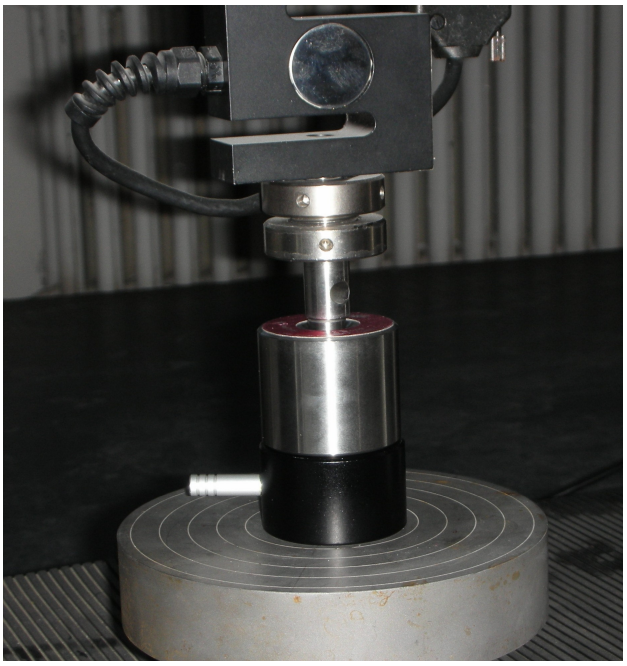

Figure 2.2. Preparation of discs by compression molding

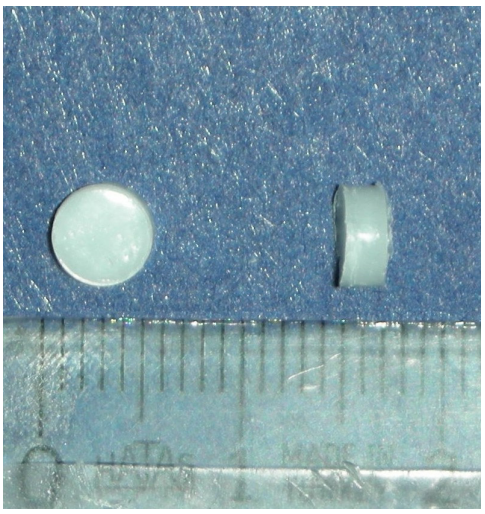

Figure 2.3. The dimensions of discs

2.2.2. *In situ* Characterization of the PCL Based Discs

The bioactivity, mechanical and degradation properties of discs were examined by mechanical, microscopic, and gravimetric tests.

2.2.2.1. Bioactivity Analysis

2.2.2.1.1. SBF Testing

Surface mineralization property of the discs was evaluated by incubation in simulated body fluid (SBF) for different periods of time. For preparing SBF solution, the following materials were dissolved in 700 ml of deionized H_2O: KCl (0.298 g), NaCl (7.013 g), $NaHCO_3$ (0.454 g), $MgSO_4 \cdot 7H_2O$ (0.247 g), $CaCl_2 \cdot 2H_2O$ (0.368 g), TRIS-HCl (6.058 g), NaN_3 (1 g) and KH_2PO_4 (0.136 g).

The pH of solution was then adjusted to 7.75-7.85 at room temperature and the volume was then completed to 1000 ml with distilled water. The final composition of SBF solution was expected to be: $[Na^+]$ = 142 mmol/l; $[K^+]$ = 5 mmol/l; $[Ca^{2+}]$ = 2.5 mmol/l; $[Mg^{2+}]$ = 1 mmol/l; $[Cl^-]$ = 131 mmol/l; $[HCO_3^-]$ = 5 mmol/l; $[SO_4^{2-}]$ = 1 mmol/l and $[HPO_4^{2-}]$ = 1 mmol/l with a pH of 7.75 - 7.85 at room temperature. The pH of SBF depends on temperature and in order to obtain 7.3 and 7.4 at 37 °C, a solution with a pH of 7.75-7.85 at room temperature is required (Müller, 2006).

One disc from each group was incubated in a 20 ml SBF solution within volumetric flasks at 37 °C in a shaking water bath (ST402, Nüve, Turkey) for 3 different incubation periods, 1 day, 7 days and 15 days. Also, one disc from each group was used as zero time control without incubation in SBF solution. At the end of the incubations, the changes in weight and gross structure were examined by the gravimetric measurements and light microscopy, respectively. The changes in dry weight and water uptake properties of SBF incubated discs were calculated according to the equations given in Section 2.2.2.2.1.

Upon drying in an oven at 35°C, the samples were coated with a gold-palladium alloy by Hummle VII Sputter coating device (Anatech, USA) for more detailed structural as well as surface mineralization analysis via scanning electron microscopy (SEM) as will be explained in Section 2.2.4.4.

2.2.2.2. *In Situ* Degradation Analysis

The discs of each group were incubated with 20 ml phosphate buffered saline (PBS) solution (10 mM, pH 7.4) at 37 °C in a shaking water bath for 4 and 6 weeks (ST402, Nüve, Turkey). To evaluate and compare the degradability and stability; structural integrity, water uptake, weight loss, and mechanical properties were studied for each incubation period.

2.2.2.2.1. Structural Integrity, Water Uptake, and Weight Loss Analysis

Five discs of each group were analyzed for the changes in weight and gross structure, as well as water uptake properties after incubations. The structural changes were examined by light microscopy.

Disc weight loss during PBS incubation was measured by the changes in dry weight after incubation for 4 and 6 weeks as shown the Equation 1:

$$\text{Weight loss (\%)} = \frac{W_i - W_t}{W_i} \times 100 \quad (1)$$

where W_i is the initial dry weight and W_t is the final dry weight at time, t.

The water uptake was calculated at each time point by Equation 2:

$$\text{Water uptake (\%)} = \frac{W_{wet} - W_i}{W_i} \times 100 \quad (2)$$

where W_{wet} is the wet weight at time, t.

2.2.2.2.2. Mechanical Testing

The changes in the mechanical strength of the discs upon *in situ* incubations in PBS were evaluated by compression tests using a Universal testing

machine (LR50K Lloyd Instruments, UK) with Nexygen MT Software Version 4.5 (Ametek Inc., UK). Three discs from each group were tested for each time point. Also, three discs from each group without incubation were used as zero time controls. The discs were tested by unconfined compression method with a crosshead speed of 1 mm/min using a 2.5 kN load cell. The elastic modulus (Young's modulus) and yield strength of the discs were calculated from the initial elastic region of the stress-strain curves obtained from the compression tests. The compression experiments were done according to the ASTM D 695M standards with small modification on the dimensions of the sample, i.e. with sample diameter/height ratio of 2.5:1 instead of 1:2. Modification in terms of increasing the ratio was also suggested as acceptable for these types of studies in literature (Dalgarno and Goodridge, 2004).

2.2.3. *In Vitro* Cytotoxicity Studies

The biocompatibility of implants was evaluated according to the standards of ISO 10993-5.

2.2.3.1. Saos-2 Cell Line Culture

For *in vitro* studies, the human osteosarcoma cell line (Saos-2) was used and routinely cultured in Dulbecco's modified Eagle's medium (DMEM, high glucose) supplemented with 10 % (v/v) fetal calf serum (FCS), 1 % (v/v) sodium pyruvate solution and 10U/ml penicillin/streptomycin at 37 $^{\circ}$C under humidified atmosphere of 5 % CO_2-95 % air. The medium was refreshed every third day. When the cells reached 80 % confluency, they were trypsinized using 0.05 % trypsin-EDTA and passaged in 1:3 ratios.

For cytotoxicity studies, Saos-2 cells were seeded at an initial seeding density of 7.5 x10^4 cells/well and incubated overnight before adding extracts from discs as will be described in Section 2.2.3.2.

2.2.3.2. Extraction from PCL Based Discs

The discs were sterilized with 70 % alcohol containing 150 U/ml penicillin/streptomycin for 2 hours and then exposed to UV-irradiation for 30 minutes. After sterilization, each disc was incubated for 24 hours in DMEM (0.2 g disc/ml) (ISO 10993-5) at 37 $^{\circ}$C in humidified environment of 5 % CO_2 in CO_2 incubator (5215, Shel Lab., USA). At the end of the incubation period, the extracts were collected for cytotoxicity assay. All experiments were carried out in triplicates.

2.2.3.3. Cytotoxicity Assay

2.2.3.3.1. Microscopic Examination

Extracts of the discs (150 µl) and FCS (7.5 µl) were added to the wells seeded previously with Saos-2 cells at a concentration of 7.5 x10^4 cells/well and incubated for 24 hours at 37 $^{\circ}$C in humidified environment of in carbon dioxide incubator (5215, Shel Lab., USA). After the incubation period; cells were evaluated in terms of morphological changes, degree of detachment from the surface, presence of floating and vacuole formation within the cells by microscopic examination (Nikon Eclipse TS100, China).

2.2.3.3.2. MTT Assay

The biocompatibility of the discs was also measured by using MTT [3-(4,5-dimethylthiazol-2-yl)-2,5-diphenyl tetrazolium bromide] assay. This method is based on reduction of a tetrazolium salt by mitochondrial dehydrogenases to a dark blue formazan product (Mosmann, 1983). The extent to which MTT is reduced to a formazan product has been correlated with the cell viability.

At the end of 24 h incubation with extracts, the number of viable cells in the wells was determined using a modified MTT assay protocol (Martinez et al., 2006). Briefly, the medium was removed and 100 µl DMEM low glucose medium and 100 µl MTT (5 mg/ml in PBS solution) were added to each well. The cells were incubated for 4 hours at 37 $^{\circ}$C in incubator in dark. After removal of the medium and washing with PBS, the insoluble formazan crystals formed inside the cells were dissolved by adding 100 µl dimethyl sulfoxide (DMSO) and shaking the wells for 10 minutes. The absorbance was measured at 550 nm using a µQuant^{TM} Microplate Spectrophotometer (Biotek Instruments Inc., USA). The number of viable cells were determined from the calibration curve constructed (Figure A.1 in Appendix A).

2.2.4. *In Vivo* Applications of PCL Based Discs

2.2.4.1. Animals and Surgery

For *in vivo* applications, 35 white male, 8 months old 2-2.5 kg rabbits were used. All the studies on animals were performed in accordance with ethical guide lines for animal care and the approval of studying on these animals was obtained from the Animal Care and Ethics Committee of the Ankara University, Faculty of Veterinary Medicine (No: 2004/19). Rabbits were anesthetized using an intramuscular injection of the combination of 2 mg/kg

body weight Xylazine hydrochloride (Alfazyne 2%) and 10 mg/kg body weight ketamine hydrochloride (Alfamine 10%) before surgery. The lateral regions of left and right humerus were shaved, disinfected and operated by the standard surgery techniques. Single unicortical bone defect with 5 mm diameter was created at the 1/3 diaphyseal proximal region of the humerus of all rabbits. The bone defects were either filled with prepared discs or left without filling (as the negative control). For each group 10 implants were applied to the defects at left and right humerus at equal numbers. 10 defects were left empty as negative control. The muscles and subcutaneous tissues were closed by resorbable (Vicryl, 3/0) and the skin was sieved by unresorbable suture (Propylene, 3/0). 30 rabbits undergone a surgical operation and 5 rabbits were left as positive control group without doing any operation. After surgery, the rabbits were kept caged freely in standard rabbit cages and given their usual regime of food and water. At postoperative period, powder Neo-terramycin was mixed with their water and given to the rabbits for 4 weeks.

At the end of 50 days, the rabbits were sacrificed by using the general anesthesia protocol (overdosage thipentotal-Pentotal application). The humeri were then removed, placed in separate tubes as wrapped in saline soaked gauze sponge and stored at -20℃ until QCT analysis and biomechanical testing.

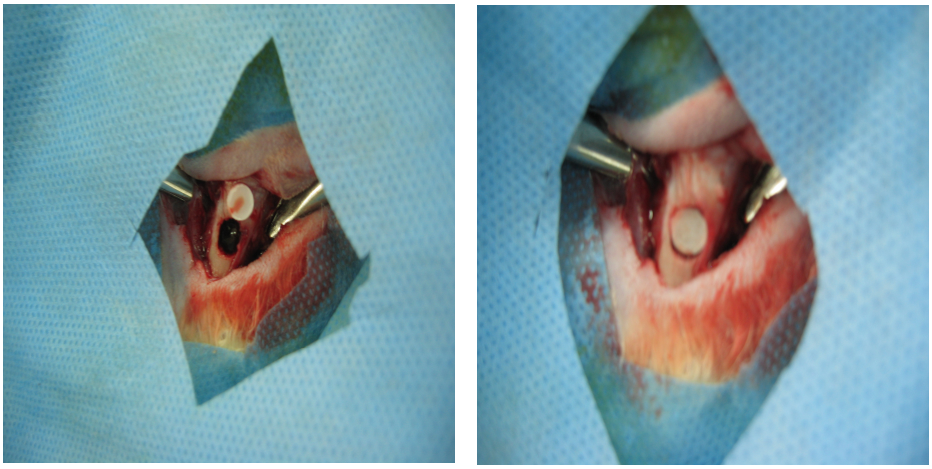

(a) **(b)**

Figure 2.4. *In vivo* application of the disc implants **(a)** defect formation on humeri, **(b)** implantation of disc to the defect

2.2.4.2. Quantitative Computed Tomography (QCT)

The humeri were kept until the experiment day as wrapped with serum wetted gauze in deep-freeze (-20°C). On the experiment day; after the samples were thawed, the densities of bone, implant and implant/bone interfaces were measured by quantitative computed tomography (QCT) using a Phillips Tomoscan 60/TX third generation scanner (Phillips, USA) in Department of Petroleum and Natural Gas Engineering, METU.

The bone densities of rabbit humeri after *in vivo* applications were calculated by using the calibration curve in Figure B.1 (Appendix B). For that, different materials with known densities were measured by using the same device and their CT numbers were recorded. The calibration curve was constructed by plotting CT numbers vs. densities. The measured CT numbers and densities of materials were given in Table B.1 in Appendix B.

2.2.4.3. Biomechanical Testing

2.2.4.3.1. Three Point Bending Test

After QCT analysis, soft tissues and periosteum of humeri were completely removed and cross-sectional dimensions were measured with a micrometer (Mitutoyo, Japan). The three point bending tests of the whole bone specimens were done using the Lloyd LS500 testing machine (Lloyd Instruments, UK) with a 2,5 kN load cell under displacement control (0,5 mm/min). The test was carried with a constant span length of 50 mm. The press head as well as the two support points were rounded to avoid shear load and crash (Ostim, Turkey). During preparation and testing, the specimens were kept in moisture with isotonic saline. Load versus deflection data were collected and from these data the stress-strain curves were constructed by using Equations 3-7 (Akkas et al., 1997).

$$M = \frac{FL}{4} \tag{3}$$

$$\sigma = \frac{FLc}{4I} \tag{4}$$

$$I = \frac{\pi\left[ab^3 - (a-2t)(b-2t)^3\right]}{64} \tag{5}$$

$$\sigma = E\varepsilon \tag{6}$$

$$E = \frac{FL^3}{48dI} \tag{7}$$

M: Bending moment

F: Applied force

L: Span length

σ: Stress

a,b: Major and minor diameters of cross-section at break point

c: Distance from the neutral axis

E: Young's modulus

I: Moment of inertia

D: Deflection

ε: Strain

t: Bone-wall thickness

The Young's moduli of the bone samples were calculated from the stress-strain curves constructed. In these calculations, the bone-wall thickness and the diameters of the cross-section at the break point were used.

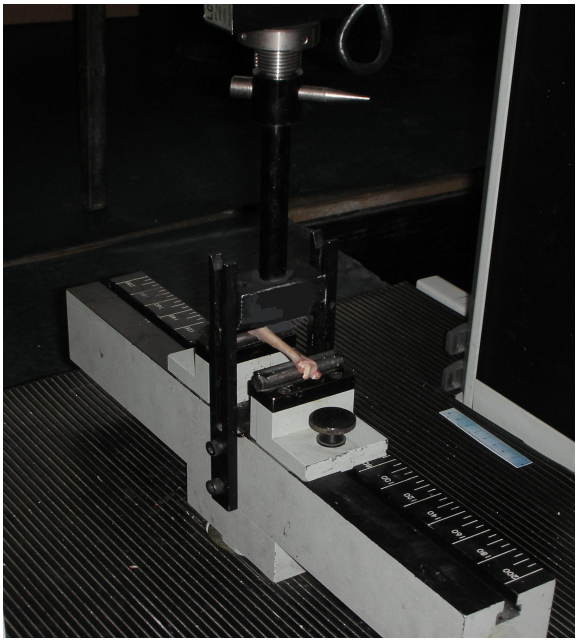

Figure 2.5. Three point bending of rabbit humerus

2.2.4.3.2. Microhardness Test

All samples were stored at -20℃ until the microhardness test. On the experiment day, after thawing, the humeri were embedded into acrylic polymer by using AcryFix Kit for molding. The molded humeri were then cut into small discs through the implant region using a low speed Isomet diamond saw (Buehler, USA). The values of bone microhardness were measured by a microhardness tester (Wilson Tukon Series A240 RHT, England). The measurements were done at the implant region, at the intact bone and at the bone-implant interface. The indentations were done via a Vickers indenter: a square based four sided pyramid that has 136° apex angle between opposite sides. A load of 50 g was applied with a 5 s dwell time in the tangential direction to the examined area (Fini et al., 2002).

The Vickers hardness value (HV) was computed from Equation 8:

$$HV = \frac{2P\sin\beta}{d^2} = \frac{1.8544P}{d^2} \quad \text{.....(8)}$$

where P is the applied load in kg, β is half of the pyramid angle and d is the mean diagonal of indentation, mm.

The indentation was applied to 12 points at the positive and negative control (empty defect) groups (6 at intact bone, 6 at defect region in the later). 18 points (6 at intact bone, 3-4 at implant region, 6-8 at bone/implant interface) were used for implant groups.

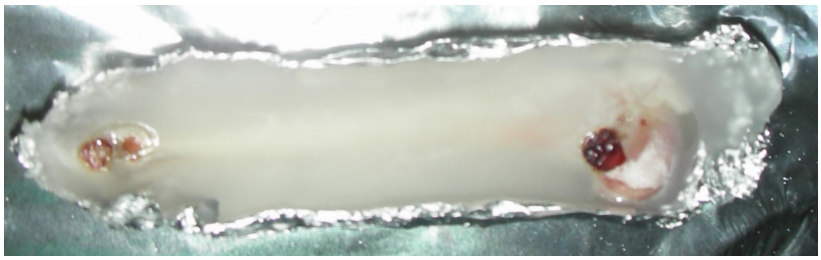

(a)

(b) **(c)**

Figure 2.6. Sample preparation for microhardness test **(a)** AcryFix molding of the bone **(b)** Preparation of Bone cross-sections at the implant site with Isomet diamond saw **(c)** Cross-sectional view of the sample to be used in the test

(a)

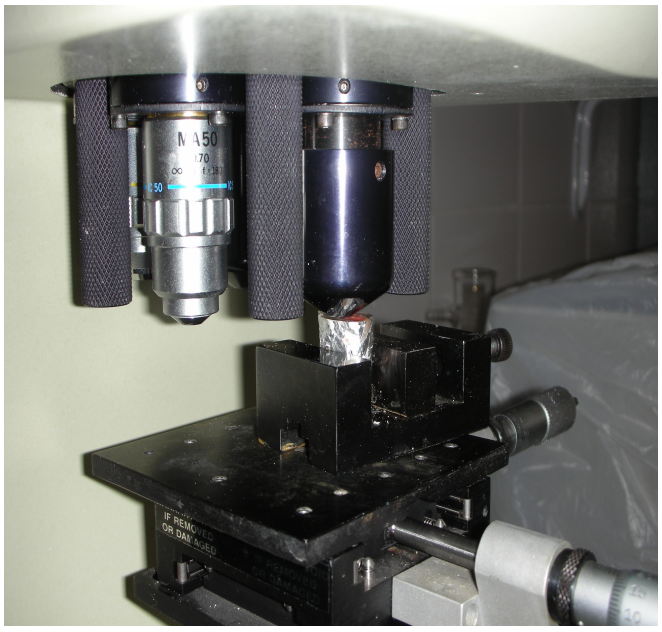

(b)

Figure 2.7. (a) Microhardness testing of bone **(b)** Closer view

2.2.4.4. Scanning Electron Microscopy (SEM) Analysis

The ability of apatite formation on discs' surfaces was analyzed by Scanning electron microscope (SEM) which is an electron microscope capable of producing high-resolution images of a sample surface. After being coated with gold, *in situ* samples and humerus cross-sections at the implant site of each group were analyzed by JSM-6400 Electron Microscope, equipped with NORAN System 6 X-ray Microanalysis System & Semafore Digitizer (JEOL Ltd., Japan) at Scanning Electron Microscopy Laboratory of Metallurgical & Materials Engineering Department, METU.

2.2.5. Statistical Analysis

Statistical analysis was applied to the mechanical test results of *in situ* and *in vivo* samples as well as to QCT results. In comparing the treatment groups and controls for a single parameter (Young's modulus, bone density, etc) One-way ANOVA test was done with Tukey's Multiple Comparison Test for the post-hoc pairwise comparisons using SPSS-9 Software (SPSS Inc., USA). Differences were considered significant for $p \leq 0.05$.

CHAPTER 3

RESULTS AND DISCUSSION

3.1. Particle Size of the Composite Components

Prior to the composite processing, the particle sizes of the disc components, except polymer (PCL) were reduced by grinding. After testing different grinding conditions on bioglass particles, the best grinding procedure was found. Firstly, the commercial form of bioglass without any grinding was analyzed as the initial point and particle size distribution curve was obtained as given in Figure 3.1. Then, bioglass grinding either for 30 minutes or 2 hours in dry and wet conditions were applied to compare the results of different grinding conditions on particle diameters (Figures 3.2, 3.3, and 3.4, respectively). The particle size distribution tables of each curve are given in Appendix C.

Particle size analysis of the original bioglass showed that mean size of the particles (50 %) was around 500 μm and 90 % of the particles were below 1000 μm in diameter. Upon grinding for even a short period of time (30 minutes), the overall size distribution curve has shifted to left with the mean size of particles being about 7.5 μm and 90 % of the particle diameters being reduced to below 27 μm (data read from related tables of particle size distributions in Appendix C). However, 2 hours of dry grinding results did not change this outcome significantly as the mean of the particle size and 90 % of the particle size distribution were almost the same with the short term grinding (about 7 and 28 μm respectively).

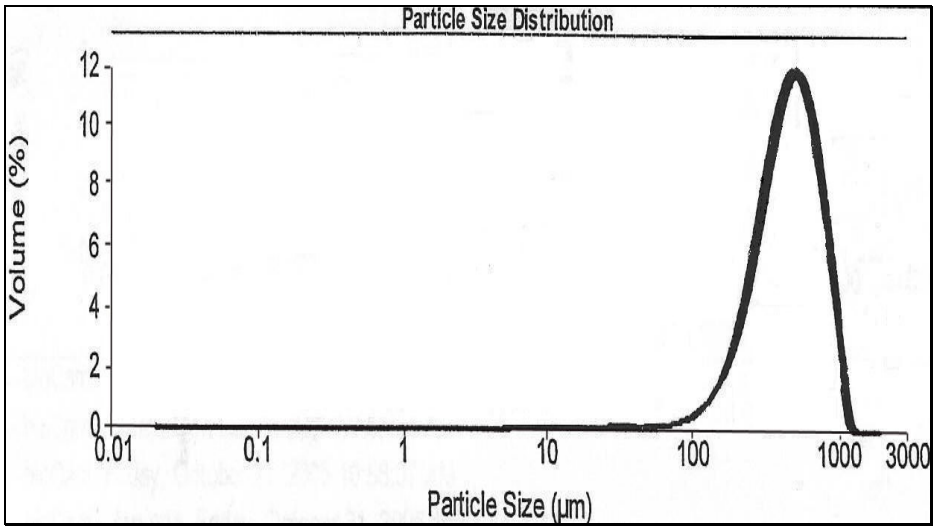

Figure 3.1. The particle size distribution curve of original commercial bioglass

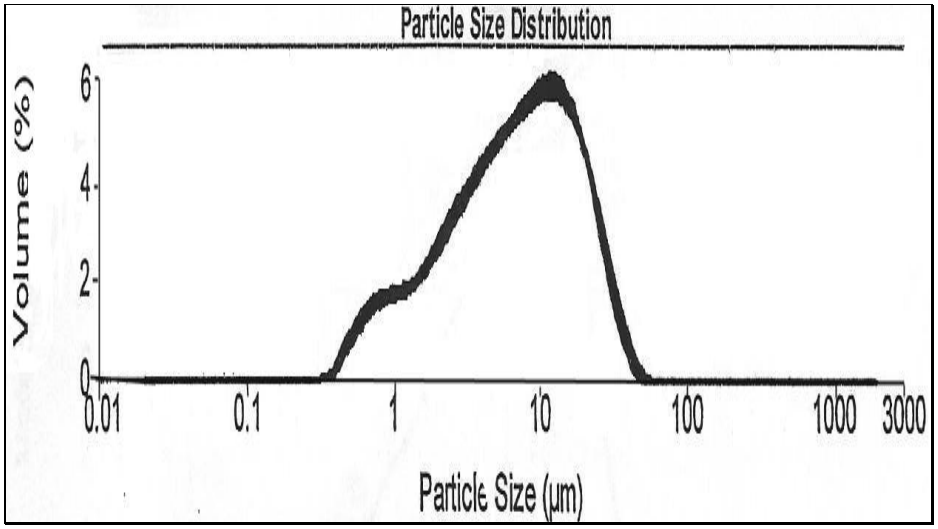

Figure 3.2. The particle size distribution curve of bioglass after 30 minutes-dry grinding

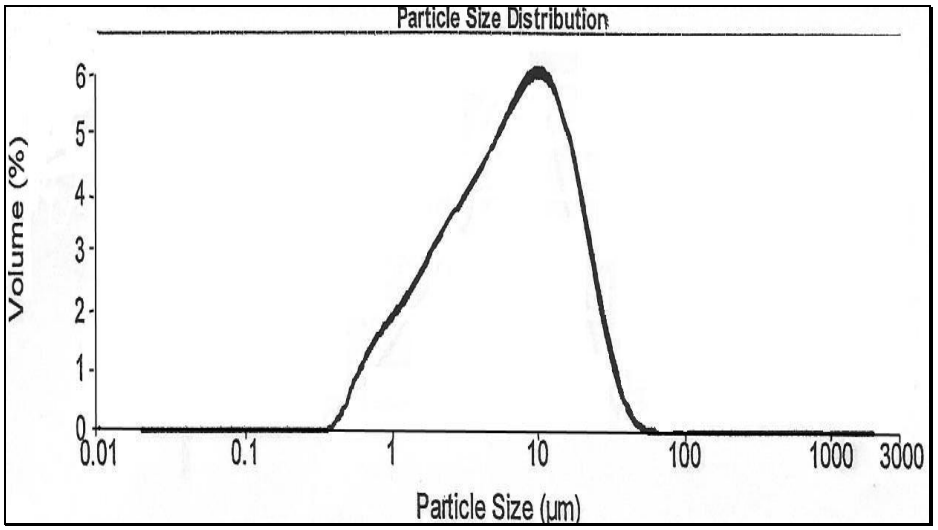

Figure 3.3. The particle size distribution curve of bioglass after 2 hours-dry grinding

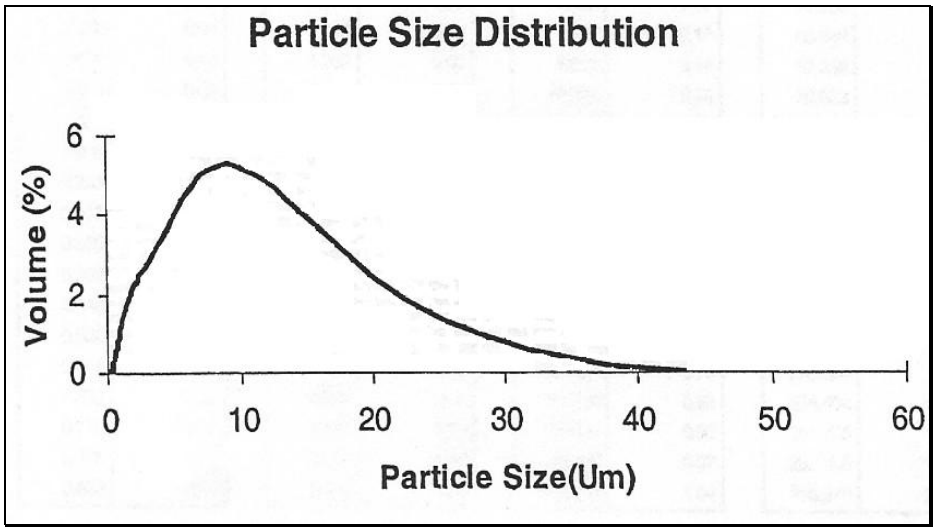

Figure 3.4. The particle size distribution curve of bioglass after 2 hours- wet grinding

Wet grinding was then applied to further reduce the particle sizes. When bioglass was ground within absolute ethanol for 2 hours, the mean of the particle size distribution has been reduced to 6 μm and 90 % of the particle sizes were reduced to less than 20 μm. Thus, smaller particle sizes could be obtained by wet grinding. Yet, this was not a big difference and considering the solubility of other components (DBM and HYA) in water or alcohol made this method unfavorable for the future studies.

According to these results, reducing the particle size of the disc components by dry grinding for 2 hours at 25 Hz frequency was chosen as the most suitable method to obtain homogeneous composites.

As can be seen in previous studies, the composite properties are affected by the particle size of components. Chen and Sun (2005) compared hydroxyapatite (HA) reinforced PCL composites with different particle sizes and molecular weight distributions. After the composites were prepared by melt processing, the interfacial interactions between PCL and HA were analyzed by differential scanning calorimetry (DSC) and the mechanical properties of composites were tested by tensile testing and by dynamic mechanical thermal analysis (DMTA). Their results showed that 3-8 μm of HA particles provided greater specific surface and interfacial areas within the PCL matrix than 20-80 μm particles. Because of the stronger interaction, composites containing smaller particle sized HA showed better processing and mechanical properties (Chen and Sun, 2005). In this study the mean particle size has the same value as HA particle size of the better group in that study and 90 % of the particles sizes are below the unfavoured groups' particle size of that study. This comparison has supported the selection of the second method as the most suitable one for particle size reduction.

3.2. *In situ* Characterization of PCL Based Discs

3.2.1. Bioactivity Analysis

The ability of bonding between bone and material is one of the most important criteria for the success of a filler type implant material. By forming an apatite layer on its surface a material is able to bond to living bone through this apatite layer (Granja et al., 2005). Hence, the *in vivo* bioactivity of a biomaterial intended for use in bone is often evaluated by studying its ability of apatite formation on its surface in a simulated body fluid (SBF) that has ion concentrations nearly equal to those of blood plasma.

3.2.1.1. Evaluation of Bioactivity of the Discs by Gravimetric Measurements

The results of gravimetric measurements were used for calculation of weight changes from discs at different time periods as represented in Table 3.1.

Table 3.1. The weight changes after SBF incubations at 37 °C

	Wet Weight Change (%)			Dry Weight Change (%)		
	1 Day	7 Days	15 Days	1 Day	7 Days	15 Days
PCL	15.0	22.2	16.3	-2.5	-2.2	-2.3
PCL/BG	25.5	12.7	22.9	0.0	-2.8	0.0
PCL/BG/CaS	18.8	18.8	18.4	-1.4	-5.8	-1.3
PCL/BG/DBM	27.8	13.4	33.3	0.0	0.0	0.0
PCL/BG/HYA	42.6	51.4	38.5	-19.1	-25.0	-23.1

According to these results, the water uptake percentage of PCL/BG/HYA group was significantly higher than the other discs at each time period. This result was mostly due to HYA being a highly water soluble polysaccharide that holds high amount of water before dissolving. It was also stated as a molecule that reacts rapidly with water (Renier et al., 2005).

Except for seven day incubations, DBM had the second highest water uptake results owing to its water solubility. Under aqueous conditions, the cause of its high water uptake is the swelling of collagen and bone morphogenic proteins (BMPs) present in the structure (Han et al., 2005). However, it is also known that collagens despite their high water holding capacity are quite large proteins with many functional groups on their amino acids' side chains. These groups might have interactions with the polymer or BG component of the composite or they might not be able to leave the compacted structure of polymer matrix owing to their large size.

In spite of its hydrophobic nature, PCL discs had high water uptake especially at the 7^{th} day. This was thought to be due to PCL's hydrophilic C=O groups. The water molecules firstly diffuse into free volume or disperse in the PCL matrix and then react with C=O groups by forming hydrogen bonds (Peng et al., 2003). During melting and molding processes of the discs, the polymer chains are thought to extend making their hydrophilic groups less hindered than the original form.

PCL/BG and PCL/BG/CaS discs had moderate water uptake values. At day 1, PCL/BG had a higher water uptake than discs containing PCL only. This might be due to BG that further reduced the hydrophobicity of PCL. One may suggest that BG, as a hard filler material, creates a less organized structure from highly mobile chains of the PCL by intrusion of solid particles between the polymer chains that modifies their movement ability. It is known that the less organized or more amorphous structures are more prone to the water uptake.

Only PCL/BG/HYA group showed a significant dry weight change throughout the incubation period because of the high solubility of HYA. During macroscopic investigations of the discs, cracks were observed after 4 hours of incubations in SBF. Larger cracks were also seen in PCL/BG/HYA discs at the end of day one. Being a hydrogel, HYA starts swelling in the presence of water. This behavior has been thought to create a pressure to the PCL matrix and form large cracks. Eventually, HYA was easily dissolved and diffused out from these cracks resulting in a large mass change compared to the other discs. When the change in dry weight was converted to gram % of the initial weight after 7 (also for 15) days of incubation, it was recognized that this value exactly matched with the initial weights of PCL and BG in the disc structure. Thus, the HYA component of the discs seemed to leave the structure at an early stage.

The minimal weight loss of other groups indicated that discs normally have a slow degradation rate. Thus, it was thought that the degradation process was still in its early stage.

3.2.1.2. Evaluation of Bioactivity by Surface Analysis Techniques

3.2.1.2.1. Analysis of Apatite Formation on Disc Surfaces by Scanning Electron Microscopy (SEM)

The apatite formation on surfaces at discs was analyzed by SEM and the images of the disc surfaces for different time periods of SBF incubation were given in Figures 3.5-3.11.

SEM observations showed that mostly at day 7, all bioglass containing composites were covered by some crystal structures at some regions. These structures were found to be similar to hydroxyl carbonate apatite (HCA) crystals which are apatite precursor molecules represented by the electron

micrographs in related studies. HCA crystals are similar to bone apatite and have the ability to bond directly with the bone (Maeda, 2007). The HCA layer formation was dependent on the bioglass content. In Figure 3.10 a and b, the crystal formation on the PCL/BG disc had the same general form with the HCA crystal images of previous studies (Xin et al., 2005 and Maeda, 2007). However, there was no apatite formation on the surface of PCL discs, because of lack of the bioactive component, bioglass.

From the scanning electron micrographs taken at lower magnifications it was possible to recognize very small changes on the surface of the discs. It has been observed that long microcracks have occurred at day 1 on the surface of discs other than PCL. These changes were seen for PCL discs after 7 days of SBF incubation. The molecular weight of PCL used in this study was 14,000 Da and the crystallinity at this molecular weight was found to be about 65 % according to the degree of crystallinity-molecular weight relationship curves obtained by Pitt et al. (1990). Other researchers also stated that PCL having some degree of crystallinity and hydrophobicity has a long degradation time of nearly 2 years (Prabhakar et al., 2005). This explains the nonexistence of surface erosions or cracking in PCL discs. When composite discs were considered, however, the other components added to the PCL matrix might have disturbed the homogeneity of the polymer, resulting in its decreased crystallinity. In these discs one also expects to have boundaries between different phases that lower crystallinity and might explain the microcracks observed throughout incubations.

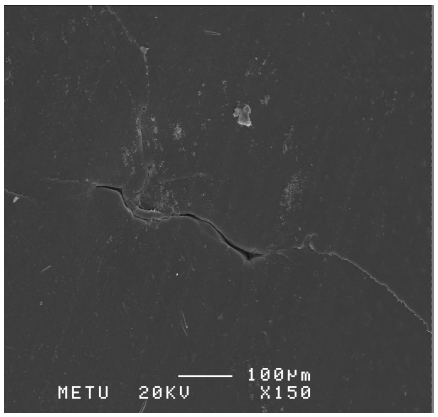

a) PCL Disc Surface (day 0)

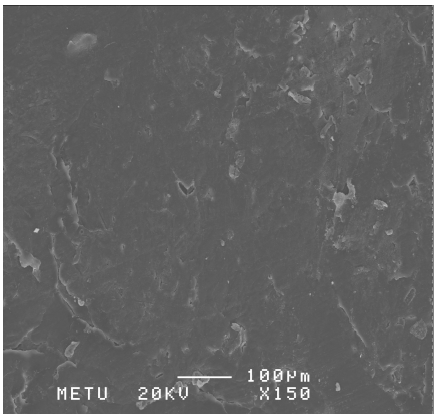

b) PCL Disc Surface (day 1)

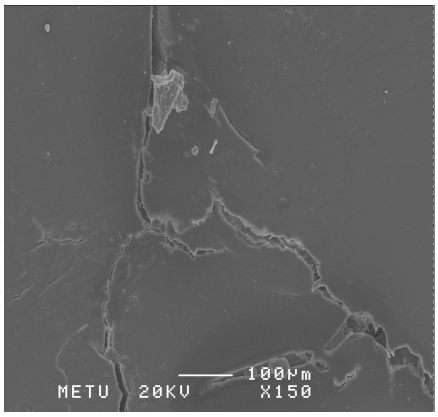

c) PCL Disc Surface (day 7)

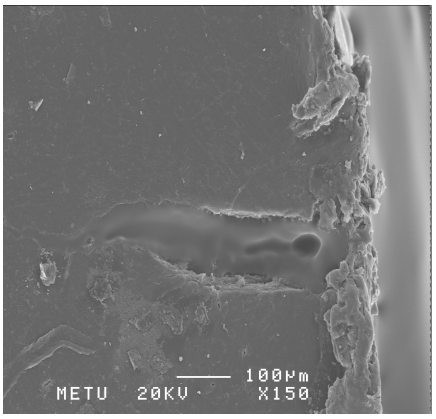

d) PCL Disc Surface (day 15)

Figure 3.5. SEM micrographs of PCL group after different incubation periods in SBF at 37 ˚C

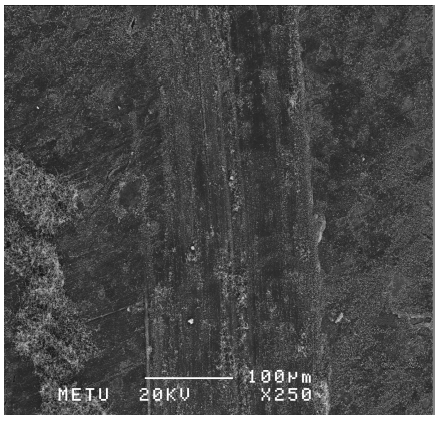

a) PCL/BG Disc Surface (day 0)

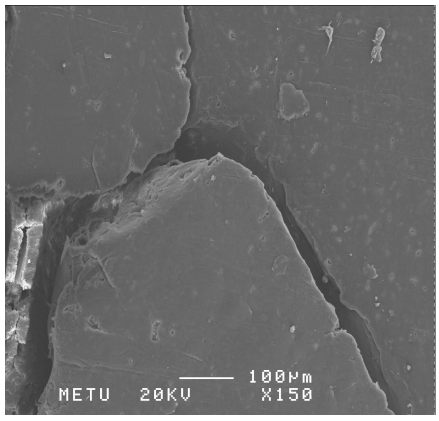

b) PCL/BG Disc Surface (day 1)

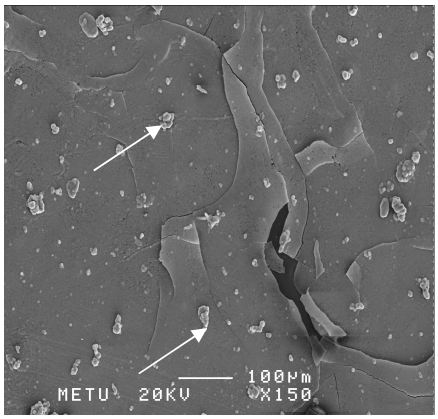

c) PCL/BG Disc Surface (day 7)

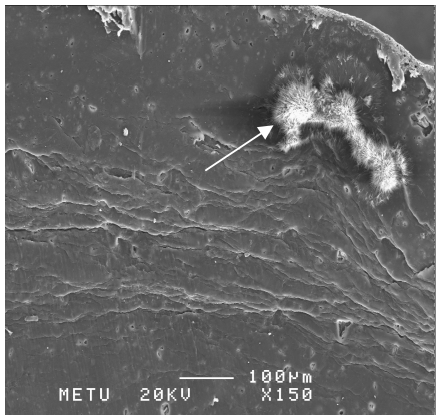

d) PCL/BG Disc Surface (day 15)

Figure 3.6. SEM micrographs of PCL/BG group after different incubation periods in SBF at 37 ˚C

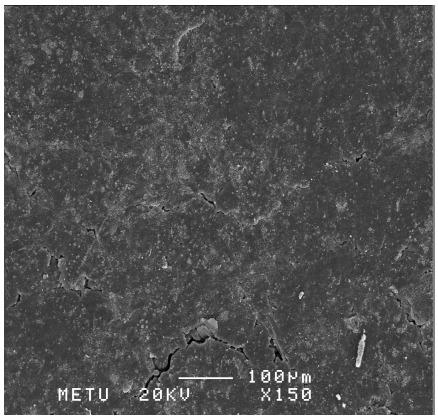

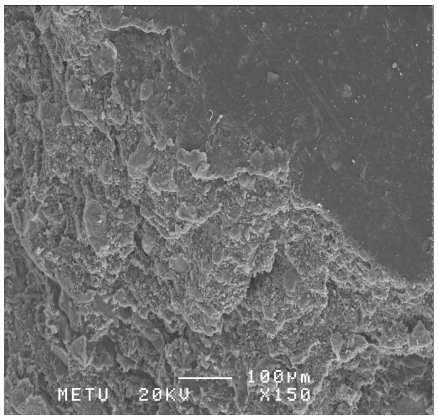

a) PCL/BG/DBM Disc Surface (day 0) **b)** PCL/BG/DBM Disc Surface (day 1)

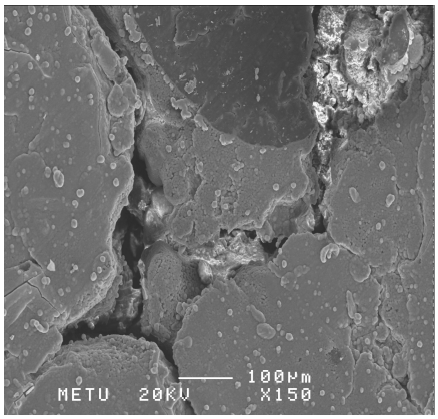

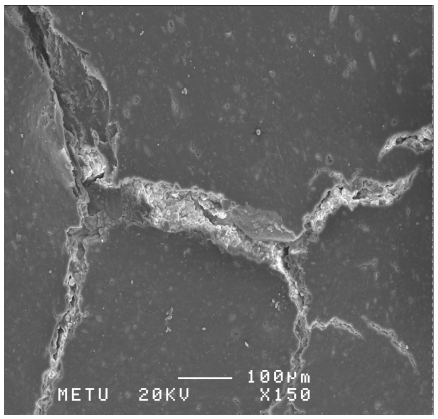

c) PCL/BG/DBM Disc Surface (day 7) **d)** PCL/BG/DBM Disc Surface (day 15)

Figure 3.7. SEM micrographs of PCL/BG/DBM group after different incubation periods in SBF at 37 ˚C

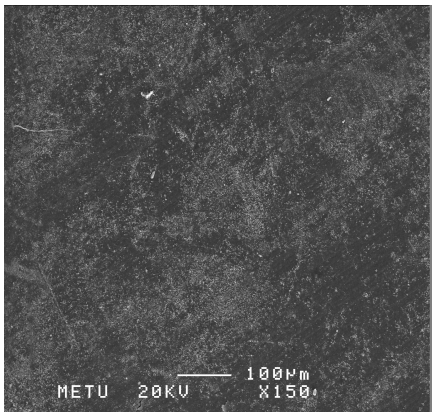

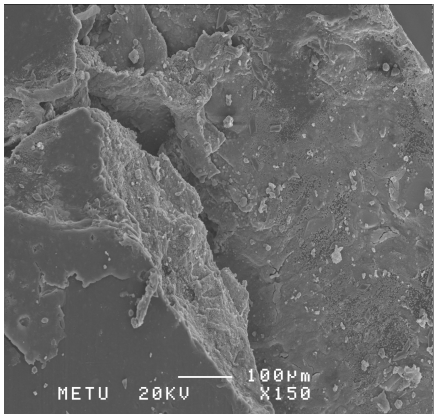

a) PCL/BG/CaS Disc Surface (day 0) **b)** PCL/BG/CaS Disc Surface (day 1)

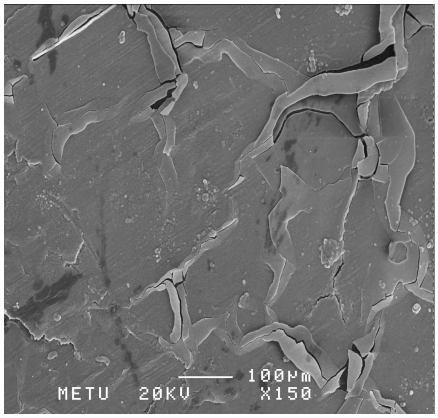

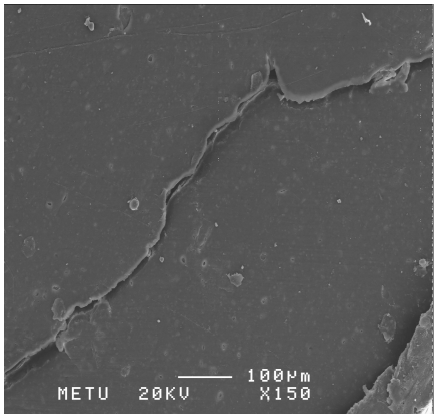

c) PCL/BG/CaS Disc Surface (day 7) **d)** PCL/BG/CaS Disc Surface (day 15)

Figure 3.8. SEM micrographs of PCL/BG/CaS group after different incubation periods in SBF at 37 ˚C

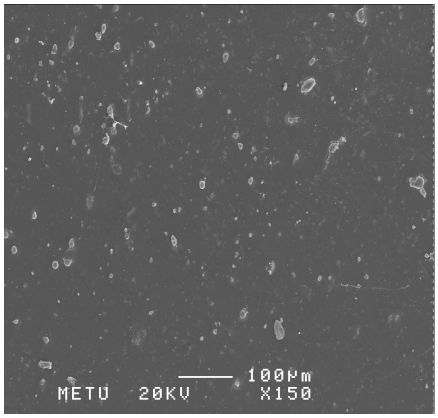

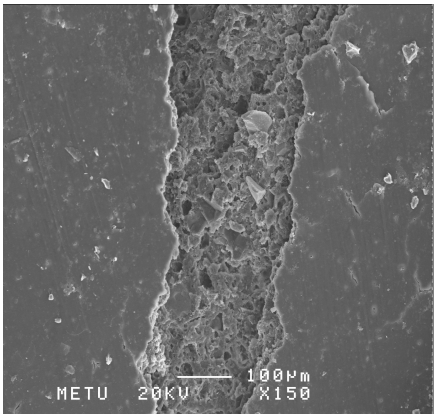

a) PCL/BG/HYA Disc Surface (day 0) **b)** PCL/BG/HYA Disc Surface (day 1)

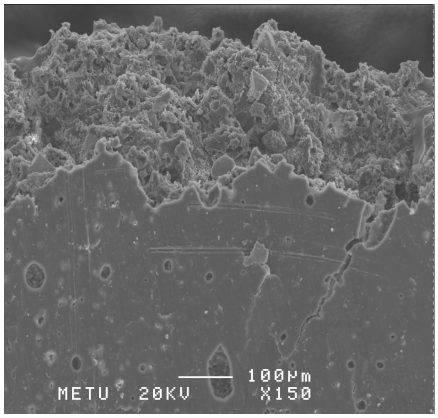

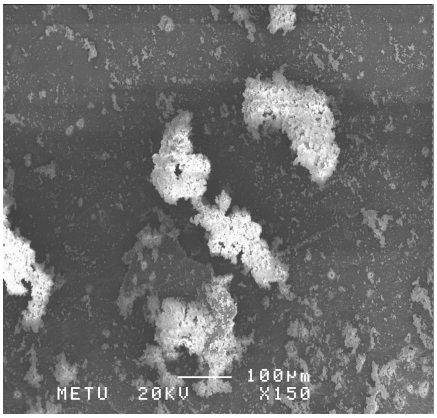

c) PCL/BG/HYA Disc Surface (day 7) **d)** PCL/BG/HYA Disc Surface (day 15)

Figure 3.9. SEM micrographs of PCL/BG/HYA group after different incubation periods in SBF at 37 ˚C

Apatite crystals formed on composite discs were examined at higher magnifications as shown in Figures 3.10 and 3.11.

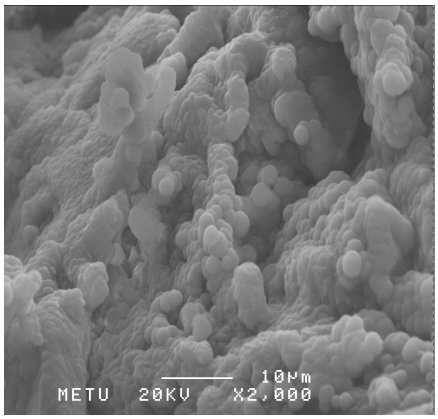

a) PCL/BG Disc Surface (day 1)

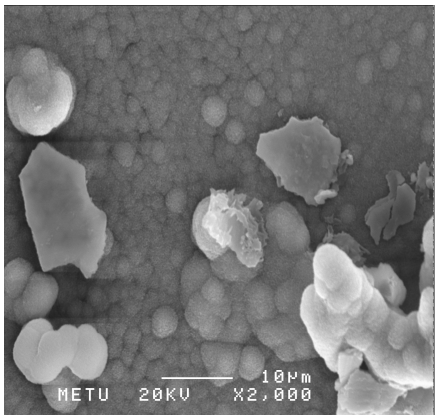

b) PCL/BG Disc Surface (day 7)

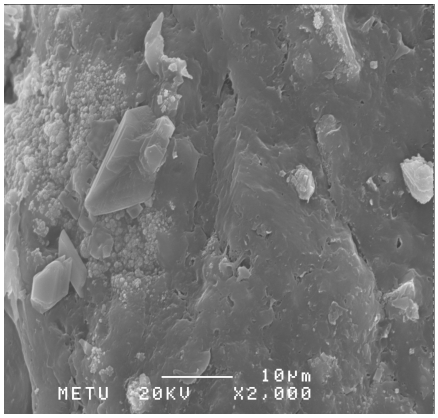

c) PCL/BG/CaS Disc Surface (day 1)

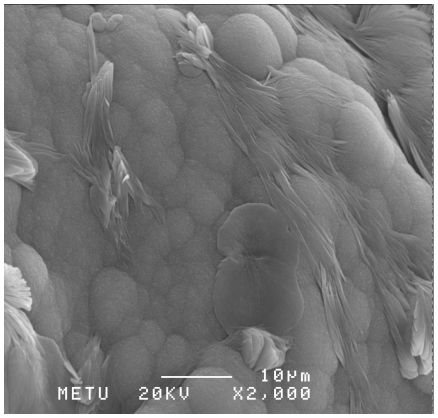

d) PCL/BG/CaS Disc Surface (day 7)

Figure 3.10. SEM micrographs of apatite crystals formed on the surface of PCL/BG and PCL/BG/CaS composite discs

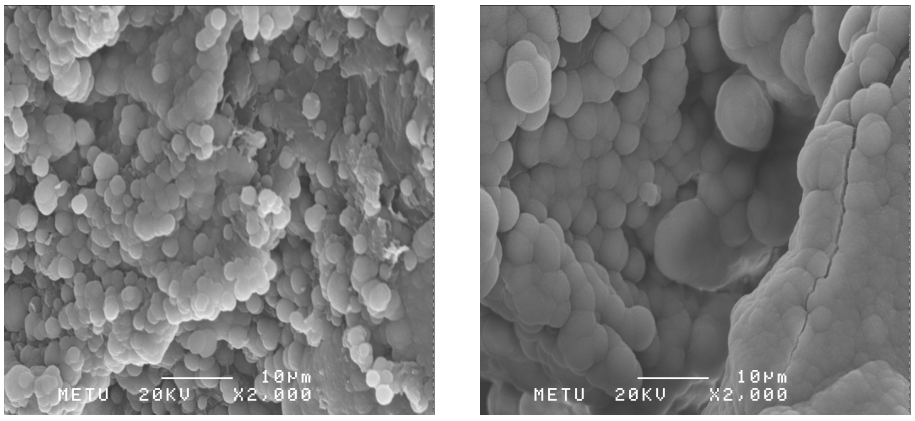

a) PCL/BG/DBM Disc Surface (day 1) **b)** PCL/BG/DBM Disc Surface (day 7)

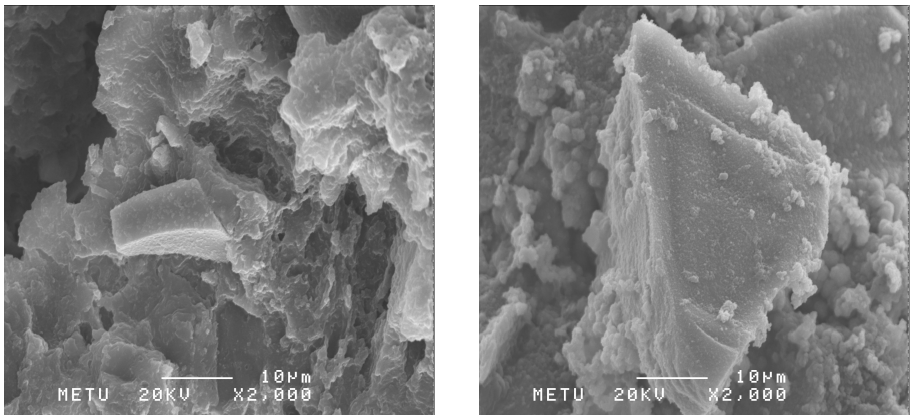

c) PCL/BG/HYA Disc Surface (day 1) **d)** PCL/BG/HYA Disc Surface (day 7)

Figure 3.11. SEM micrographs of PCL/BG/DBM and PCL/BG/HYA groups at 2000x magnification

3.2.1.2.2. Analysis of Surface Apatite Formation by Energy Dispersive X-Ray Spectroscopy (EDS)

The X-Ray elemental analysis of the surface gives the elements on the surface of a material quantitatively in terms of percentage. Hence, if the main elements present in HCA (mainly calcium, phosphorus, hydrogen and oxygen) are observed on the surface of the discs, this could be considered as a good indication of apatite crystal formation. The EDS results are given in Figures 3.12-3.17.

When the surfaces of discs were examined for elemental analysis, the peak of calcium element was observed clearly (Figures 3.12, 3.14, 3.16 and 3.17). In order to suggest the apatite crystal presence on the surface it was also necessary to observe the other critical element's (namely phosphorous, P) peak. However, owing to interference of gold (Au) peak with P peak, as shown in Figure 3.12, it was not possible to make that conclusion at the first sight. That's why the surface of only gold-palladium coated sample holder was also examined as shown in Figure 3.13. Here, the pure Au peak was found to be quite different than the peaks present in the samples at the same point, indicating the overlapping of the two elements' peaks. From these comparisons, the presence of phosphorus element was suggested qualitatively, without considering its amount.

The elemental analysis of PCL/BG disc surface (Figure 3.14) showed the presence of calcium, phosphorus, sodium and silisium peaks, all of which are characteristic elements of the bioglass component (Lu et al., 2005).

When the element composition of PCL/BG/DBM disc surface was analyzed, the carbon peak has emerged (Figure 3.15). This peak, aside from PCL structure, is mostly expected to come from the organic nature of DBM.

Carbon and calcium peaks were observed in the elemental analysis of PCL/BG/CaS disc surface (Figure 3.16). Carbon peak was thought to be the

carbon backbone of PCL matrix and calcium peak from CaS content and the apatite structures on its surface.

Carbon and oxygen peaks observed on the surface of PCL/BG/HYA disc indicated the existence of organic component of HYA and calcium peak showed the apatite formation.

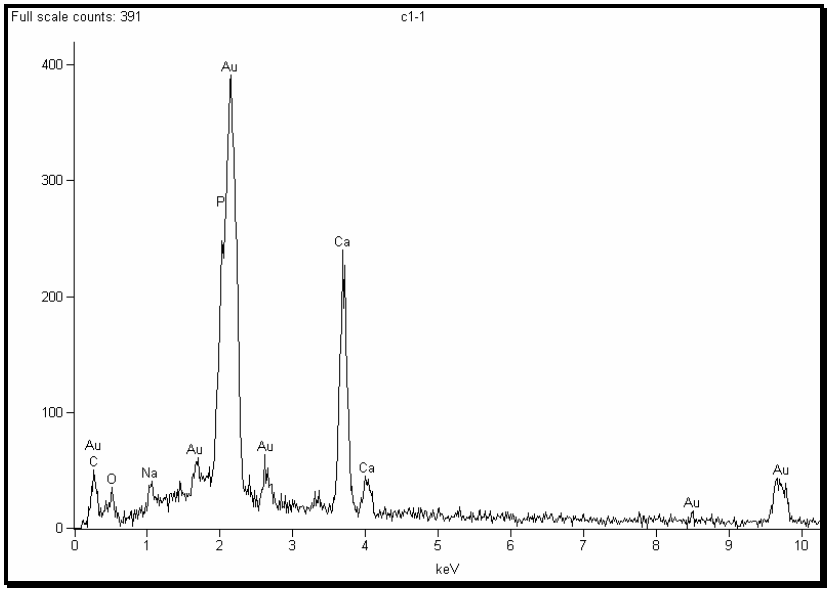

Figure 3.12. Elemental analysis of PCL/BG disc surface after 15 days of incubation in SBF at 37 ˚C

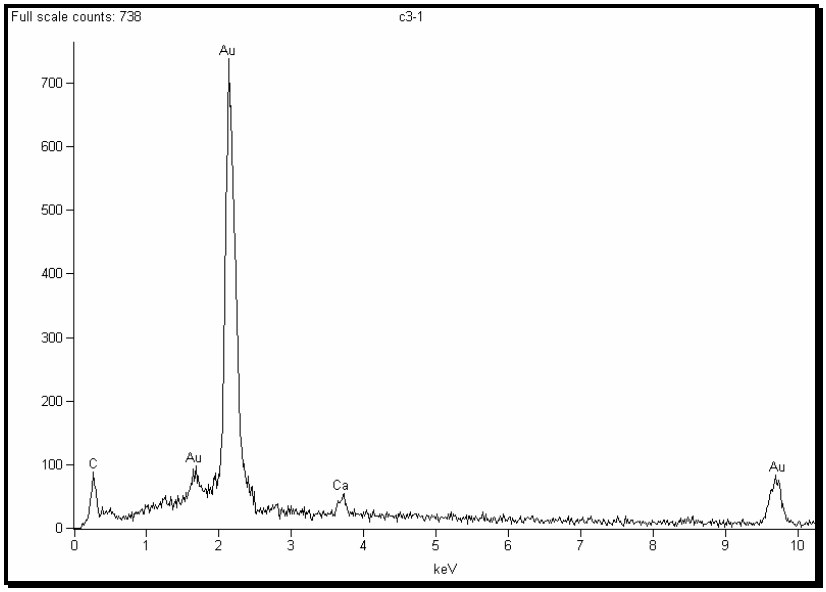

Figure 3.13. Elemental analysis of gold-palladium coated carrier of the samples

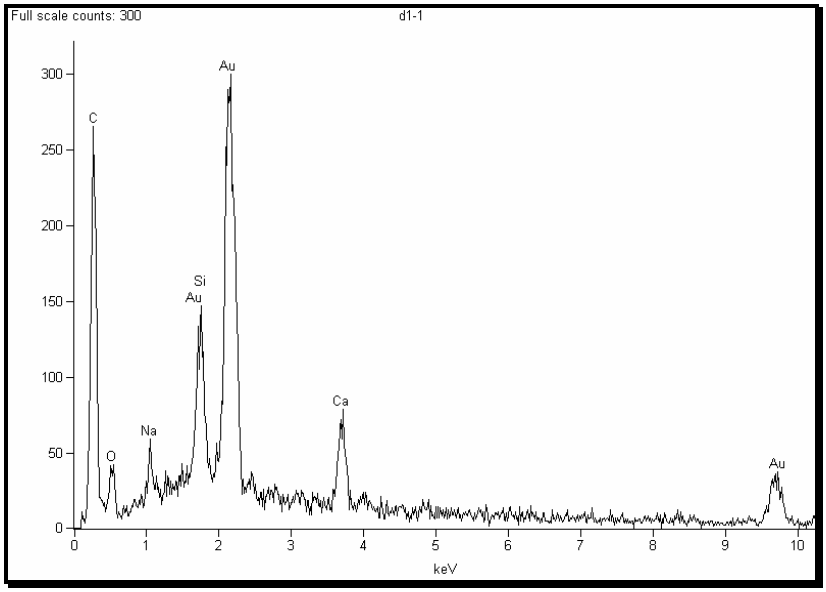

Figure 3.14. Elemental analysis of PCL/BG disc surface after 7 days of incubation in SBF at 37 ˚C

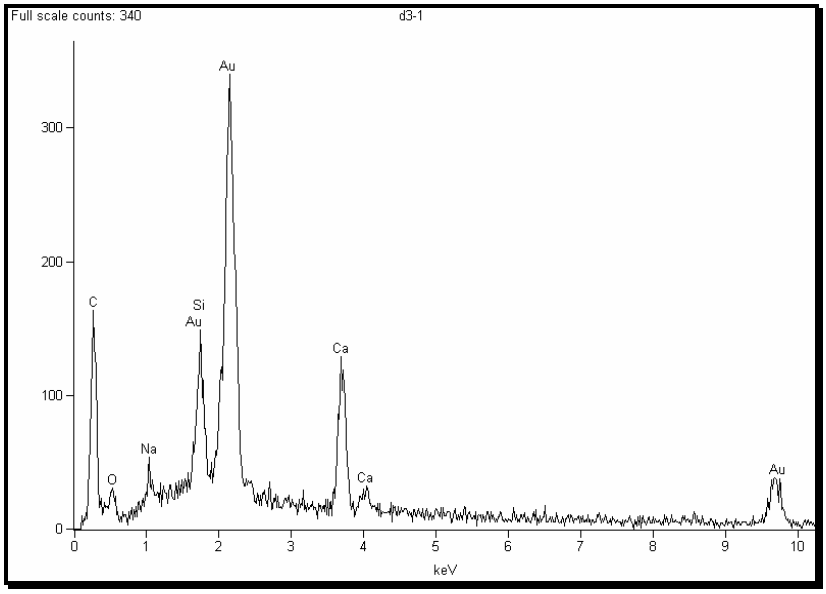

Figure 3.15. Elemental analysis of PCL/BG/DBM disc surface after 7 days of incubation in SBF at 37 ˚C

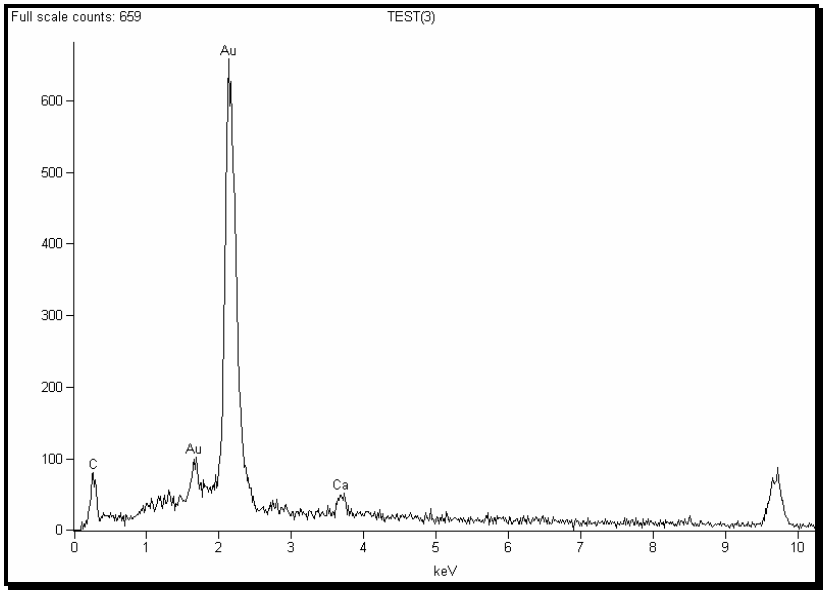

Figure 3.16. Elemental analysis of PCL/BG/CaS disc surface after 7 days of incubation in SBF at 37 ˚C

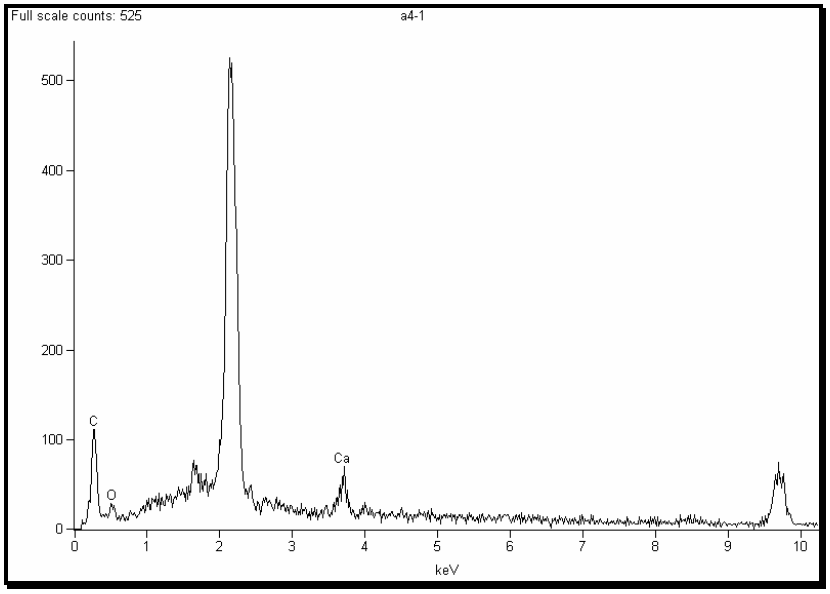

Figure 3.17. Elemental analysis of PCL/BG/HYA disc surface after 15 days of incubation in SBF at 37 ˚C

3.2.2. *In Situ* Degradation Analysis

The *in vivo* degradation behavior of the implant is an important property to be considered for its use in treatment of bone defects. The degradation rate of implant must be adequate to support the bone during the healing period while allowing bone ingrowth. Hence, the discs were characterized for their degradation, structural integrity, water uptake, weight loss, and mechanical properties by *in situ* incubations in PBS at 37 ˚C for 4 and 6 weeks.

3.2.2.1. Evaluation of Degradation, Structural Integrity, Water Uptake and Weight Loss Properties

After implantation, any bone filler material was expected to be in contact with the physiological fluids. The study of the effect of water on the properties of discs and the weight changes caused by leaching of any component thus had a critical importance in predicting the long term *in vivo* performance.

The results of water uptake, structural integrity and weight loss analyses as shown in Tables 3.2 and 3.3 were in accordance with the results of *in situ* analysis. PCL/Bioglass/HYA group showed significantly higher percentages of water uptake and weight loss at each time period than the other discs because of the high water solubility of HYA (Renier et al., 2005).

Macroscopic examinations of the structural integrity also showed macrocracks and even breaking into halves for the HYA involving group at the end of all incubations periods. As previously mentioned all these changes were related with the hydrogel nature of HYA. HYA has been suggested for use in combination with durable, hydrophobic biomaterials because of its extreme hydrophilicity that causes limitations to permanent applications (Zhang and James, 2005). Some researchers decreased the degradation rate and improved mechanical properties of HYA (Leach et al., 2003 and Renier et al., 2005) by crosslinking.

The parallel results with the SBF incubations were also observed in other disc groups. PCL/BG/DBM group had the second highest water uptake value; but the dry weight change has occurred after 6 weeks of incubation. There was no significant weight change at 4 week incubation probably due to the strong attachment of DBM particles by the polymer matrix. The swelling of collagen matrix caused cracks on the composite surfaces as seen in the macroscopic examinations of the structural integrity.

Despite its hydrophobic nature, PCL also showed a higher water uptake at each time period compared to the PCL/BG and PCL/BG/CaS discs. The same reasons with SBF incubations were thought to be valid in this result.

Table 3.2. The weight changes after *in situ* incubations

	Wet Weight Change (%)		**Dry Weight Change (%)**	
	4 Weeks	**6 Weeks**	**4 Weeks**	**6 Weeks**
PCL	13.37	20.21	-0.99	-2.13
PCL/BG	8.50	12.45	-0.81	-1.61
PCL/BG/CaS	14.09	14.09	0.00	-1.03
PCL/BG/DBM	30.00	35.48	-0.01	-7.17
PCL/BG/HYA	45.76	50.00	-27.63	-28.36

Table 3.3. Results of macroscopic observations on the structural integrity

	Structural Integrity	
	4 Weeks	**6 Weeks**
PCL	No visible change	No visible change
PCL/BG	No visible change	No visible change
PCL/BG/CaS	No visible change	No visible change
PCL/BG/DBM	visible cracking	visible cracking
PCL/BG/HYA	near to breaking	crack to two pieces

Only PCL/BG/HYA group showed significant dry weight changes at each time period. The minimal weight loss of other groups indicated that the discs were degrading slowly. Slower degradation rate than the bone formation is an

advantage in tissue engineering. Consequently the bone regeneration is thought to be supported more by mechanical means when the degradation is slow (Lei et al., 2007).

Despite moderate water uptake of PCL/BG/CaS group, no weight change was observed upon incubations. This unexpected result was thought to occur by a different series of events discussed for other disc groups. After the penetration of water into the matrix, the CaS particles might have dissolved due to their high solubility. The dissolved CaS molecules were thought to be kept by the reactive bioglass particles and were not allowed to leave the matrix. Hence, for PCL/BG/CaS groups rather than releasing highly soluble component, holding it inside to form apatite precursors within the structure, might have changed the weight in an unexpected way.

3.2.2.2. Evaluation of the Mechanical Properties of PCL Based Discs

For the mechanical evaluation of the discs, compression tests were done and load-displacement curves were obtained for each sample. A typical compression test result of a composite disc is given in Figure 3.18. After an elastic region, the failure of the material occurs at yield point and the permanent deformation starts. Because of the rubbery nature of PCL, the discs showed a flow behavior when the applied load was further increased. Finally, the disc forms a thin, sheet-like structure that spreads onto the surface of the metal test platform. Hence after the yield point a sharp increase in load was observed corresponding to this flow behavior of crashed discs.

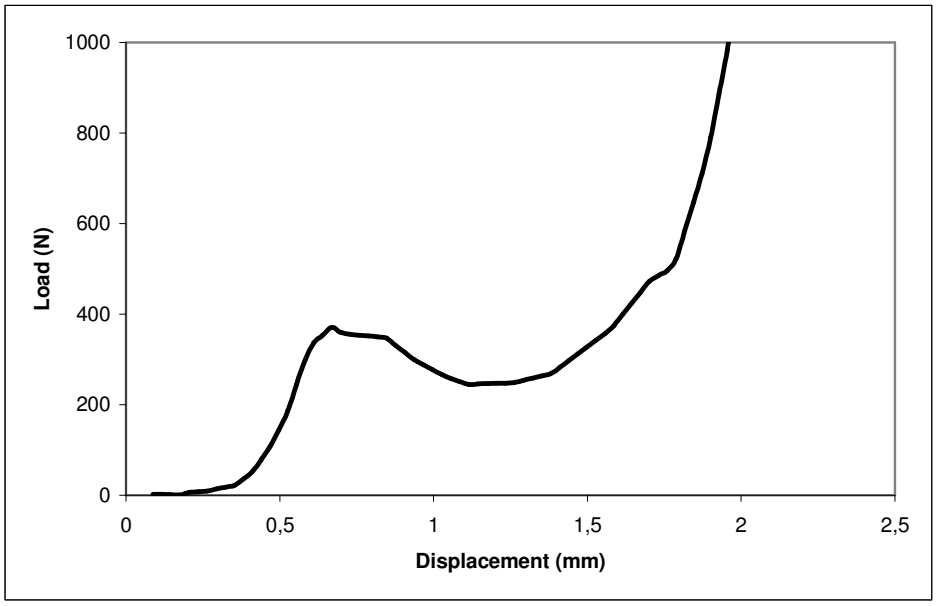

Figure 3.18. A typical load-displacement curve of the composite disc

The load-displacement curves of discs were converted to the stress-strain curves by normalizations with area and initial dimensions. The Young's moduli were calculated from the slopes of linear regions of these graphs for different time periods: zero time, 4 weeks and 6 weeks (Figure 3.19).

At zero time, PCL/BG/HYA group showed significantly high elastic moduli compared to the other groups. The comparison of Young moduli of HYA containing discs with that of other groups showed that the addition of HYA component provided higher resistance and better elastic modulus than the other components at zero time. This result was significant when the role of HYA in natural tissues was considered. In connective tissues HYA has been found at high concentrations and was suggested to have a mechanical role as space filler besides serving to keep tissue swollen (Heatly and Scott, 1988). Hence, its space filling property was better than the other components.

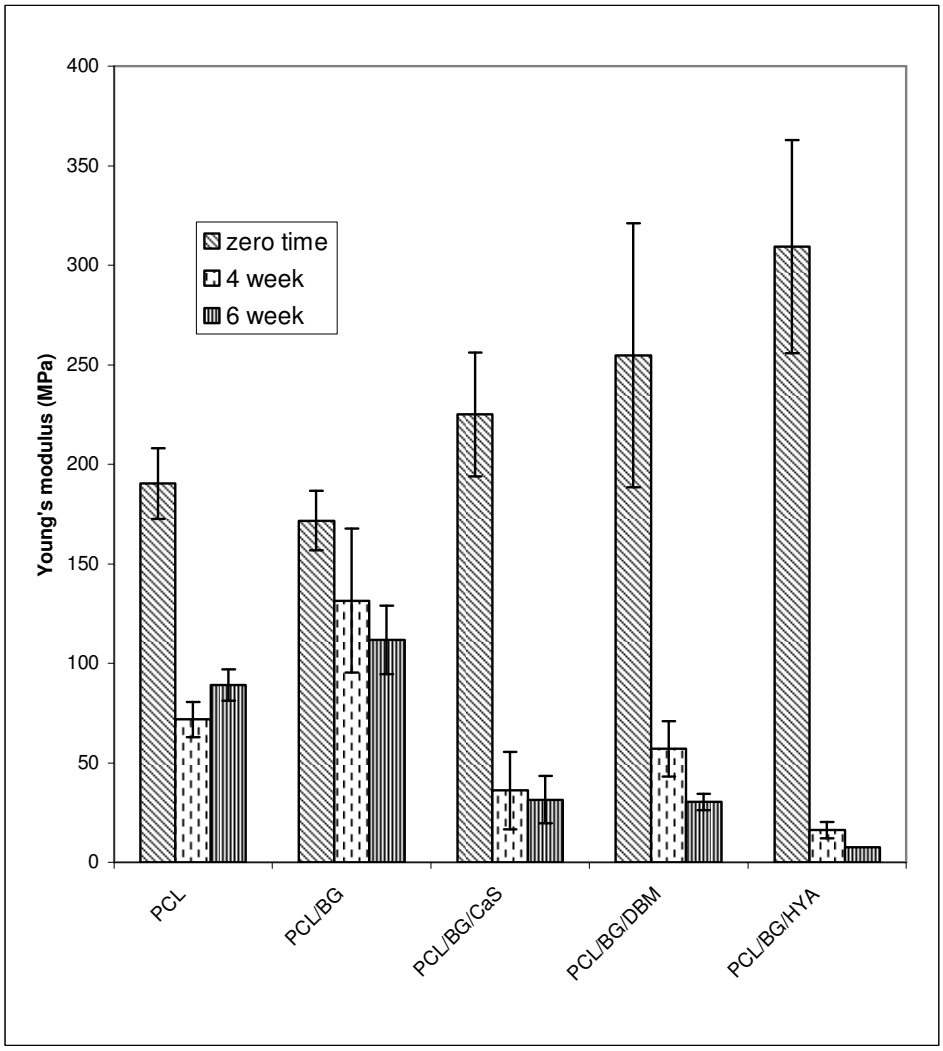

Figure 3.19. Young's moduli of discs incubated for different time periods

PCL/BG/DBM group had the second highest elastic modulus most probably due to its organic component DBM. DBM is prepared by removing mineral portion of bone and the resulting matrix is mainly composed of collagen (Summitt and Reisinger, 2003). Collagen being the natural component of the organic phase of bone is known to contribute to the mechanical properties of the bone tissue. It is known that collagen fibers have the ability to align towards the direction of the load. This property, although more applicable

under tension type of stress, is also present under compression. The collagen fibers constitute an important portion of the spongy bones that are mostly under compression type of load.

PCL and PCL/BG groups showed lower elastic modulus values than the other groups' zero time measurements. PCL has poor mechanical properties owing to its semicrystalline structure and low glass transition temperature (Tg) value. The mechanical property is even lower in the PCL type used in the current research due to its low molecular weight. Because of its poor mechanical properties, mostly PCL implants have been reinforced with a ceramic phase in bone repair applications (Coombes et al., 2004). In contrary to this; when bioglass was added to PCL matrix, lower elastic modulus was observed for PCL/BG group. Initially, this was thought to be due to bioglass' having poor mechanical properties (bending strength and fracture toughness) for the bone application (Guo et al., 2004). But when compared with the other components of the composite discs (CaS, DBM or HYA) BG itself would have better mechanical properties. Thus, the reason for mechanical properties with BG being lower than others was thought to be purely as a result of bioglass' not being a sufficient space filler and hence its ineffectiveness as a reinforcing agent. Initially, before disc formation, to enhance the fillers' efficacy and increase disc homogeneity particle sizes of components other than polymer have been reduced. Although this attempt seemed successful for that purpose, yet, the final structure was found to be not providing what was needed in terms of mechanical properties. In some previous studies it was shown that smaller particle sized components provide an improvement in the mechanical properties of composites (Chen and Sun, 2005). So, the mechanical properties of the final structure seem to be related with the particle size of the reinforcing component.

In another study, the mechanical properties and osteoconductivity of four different bone cements prepared with different sized glass beads (4, 5, 9 and 13 μm) were examined to investigate the effect of the size of the bioactive glass bead fillers in poly(methyl methacrylate) (PMMA) matrix. The mechanical properties were analyzed by three point bending test. Cements

that contained the smallest sized glass beads were found to have the highest bending strength. The osteoconductivity properties of cements were also evaluated by histological examination and SEM analysis after implantation to cortical bone defects in tibia in a rat model. Again, 4 μm glass beads containing cements showed good direct contact with bone while those with 13 μm glass beads had many gaps at the bone interface (Shinzato et al., 2001). Half of the particle sizes of components used in this study was below the mean size of the components for our study. Hence, if it were possible to decrease the mean particle size or the upper 90 % limit to a smaller value, better mechanical and healing outcomes might have been obtained. This comparison also suggested that the particle size of water soluble components (CaS, DBM, HYA) might have been decreased more than bioglass as these groups had better properties at zero time.

PCL/BG/CaS group showed a moderate elastic modulus at zero time mainly because of the low compressive strength of calcium sulfate, despite its being a good filler material (Huan and Chang, 2007).

Upon incubation in PBS for 4 weeks, elastic moduli were found to decrease in all groups except PCL/BG. The sharpest decreases were observed at PCL/BG/HYA, PCL/BG/DBM, and PCL/BG/CaS groups. The changes in moduli, however, were small between 4 and 6 weeks results.

At the end of both incubation times, DBM group had visible cracks. For HYA group besides these cracks, breakings were also observed. Therefore, it was thought that disruptions of structural integrities gave rise to significant loss in mechanical strength of these groups. The higher water uptake and loss of soluble components (especially HYA) were also thought as important parameters modifying mechanical properties. In general, it may be suggested that as the water uptake into composite increased, the mechanical properties decreased resulting from dissolution of the components.

For PCL/BG/CaS group, there was also a significant decrease in elastic modulus for both 4 and 6 weeks of incubation. The initial elastic modulus of

this group decreased from 225.2 ± 31.16 MPa to 33.9 ± 22.18 MPa and to 25 ± 5.18 MPa after 4 and 6 weeks incubations, respectively. When the water diffused into the composite, the water soluble CaS was dissolved and reacted with bioglass particles as suggested in the PBS degradation results in Section 3.2.2.1. The structural changes of CaS and bioglass and the void formation in the matrix after CaS dissolution were thought to be the main causes of the decline in the elastic modulus of this group.

At the end of 6 weeks incubation, PCL group had a lower elastic modulus (89.1 ± 7.85 MPa) compared with zero time (190.3 ± 17.93 MPa). PCL degradation occurs in two steps in aqueous media. First of all, random hydrolytic scission of the ester groups takes place when water diffuses into the amorphous regions. The cleaved chains cannot leave the matrix and they remain in the interior parts of the polymer. Therefore, molecular weight reduction occurs before mass loss begins (Chouzouri and Xanthos, 2007). This reduction of molecular weight was thought as the main cause of decline in mechanical properties. Even though the Young's modulus of PCL has decreased through incubation period, this group still had higher value of modulus than the other groups except PCL/BG.

PCL/BG group had the highest elastic moduli at the end of both incubation periods. Besides, there was no significant decrease in elastic modulus after 4 and 6 week incubations when compared with zero time. This was a result of lower solubility of BG than other components and also its effect in decreasing the water uptake (least water uptake group) or in turn decreasing the degradation rate of the discs as explained in the previous section. Hence, BG can be considered as protective on the overall structure and thus the mechanical properties. Unfortunately, this property of BG seemed to be eliminated with the addition of high water soluble components into the structure in other groups (Figure 3.19).

At zero time, there were no statistically significant differences between maximum stress and yield stress values of groups as shown in Table 3.4. It was observed that when CaS was added to the disc structure, the maximum

and yield strain values decreased; but when DBM and HYA were added, these values increased. However, these changes were only statistically significant between these groups and not significantly different than the groups involving the basic components of the discs alone (PCL and PCL/BG). Similarly, BG addition caused a decline in the elastic modulus; but addition of any of the organic components caused an increase. Yet, only the increase for PCL/BG/HYA group was significant than PCL/BG and PCL groups.

Table 3.4. The mechanical properties of discs at zero time

	Zero Time				
	Maximum Stress (MPa)	**Maximum Strain**	**Yield Stress (MPa)**	**Yield Strain**	**Young's Modulus (MPa)**
PCL	20.8 ± 2.95	0.6 ± 0.21	23.1 ± 2.85	0.6 ± 0.25	190.3 ± 17.93 β
PCL/ BG	21.0 ± 3.30	0.5 ± 0.05	21.0 ± 0.77	0.5 ± 0.05	171.8±15.03 ν
PCL/BG/ DBM	20.5 ± 3.30	0.8 ± 0.21 *	25.2 ± 3.90	0.9 ± 0.17 $	254.8±66.23
PCL/BG/ CaS	21.4 ± 0.83	0.2 ± 0.10 * #	23.7 ± 1.33	0.3 ± 0.11 $ ^	225.2±31.16
PCL/BG/ HYA	23.4 ± 1.71	0.8 ± 0.17 #	26.2 ± 0.40	0.9 ± 0.17 ^	309.3±52.41 β ν

*, #, $, ^, β, ν indicate the statistically significant differences between groups: $p<0.05$.

Table 3.5. The mechanical properties of discs at the end of 4 weeks incubation

	4 weeks				
	Maximum Stress (MPa)	**Maximum Strain**	**Yield Stress (MPa)**	**Yield Strain**	**Young's Modulus (MPa)**
PCL	7.2 ± 0.28	0.7 ± 0.30	7.4 ± 0.16	0.7 ± 0.29	71.8 ± 9.02 *
PCL/BG	7.3 ± 0.41	0.4 ± 0.08	7.4 ± 0.06	0.5 ± 0.13	131.5 ± 36.06 * # ^ β
PCL/BG/ DBM	5.1 ± 3.36	0.7 ± 0.06	5.8 ± 4.24	0.7 ± 0.07	57.1 ± 13.85 #
PCL/BG/ CaS	3.2 ± 0.18	0.4 ± 0.31	3.7 ± 0.50	0.5 ± 0.35	33.9 ± 22.18 ^
PCL/BG/ HYA	1.4 ± 1.19	0.6 ± 0.31	2.0 ± 1.28	0.6 ± 0.32	18.2 ± 4.48 β

*, #, ^, β indicate the statistically significant differences between groups: $p<0.05$.

Table 3.6. The mechanical properties of discs at the end of 6 weeks incubation

	6 Weeks				
	Maximum Stress (MPa)	**Maximum Strain**	**Yield Stress (MPa)**	**Yield Strain**	**Young's Modulus (MPa)**
PCL	7.9 ± 0.22 *	0.8 ± 0.12	7.9 ± 0.25 #	0.8 ± 0.13	89.1 ± 7.85 ^
PCL/BG	6.1 ± 1.27	0.6 ± 0.34	6.6 ± 1.32	0.7 ± 0.35	111.9 ± 17.17 β
PCL/BG/ DBM	3.1 ± 0.25 *	0.4 ± 0.25	3.1 ± 0.31 #	0.4 ± 0.28	32.8 ± 0.53 ^ β
PCL/BG/ CaS	5.3± 3.69	0.7 ± 0.53	5.3 ± 3.69	0.7 ± 0.53	25.0 ± 5.18 ^ β
PCL/BG/ HYA	1.2	0.9	2.3	0.9	7.4

*, #, ^, β indicate the statistically significant differences between groups: $p<0.05$.

After 4 weeks of incubation, maximum stress and yield stress values decreased significantly compared to zero time values ($p<0.001$). There were numerical changes in strain values; but there wasn't any significant difference from the zero time as shown in Table 3.5. Except for PCL/BG group, the Young's moduli were significantly decreased ($p<0.005$). No significant differences between 4 week and 6 week mechanical properties were observed as shown in Table 3.6. Because HYA containing discs lost their structural integrities, mechanical test for only one disc could be done. Therefore statistical comparison could not be done for this group. However, this group had the weakest mechanical properties with no need for statistical comparison.

3. 3. *In Vitro* Cytotoxicity Studies

The implants for short or long term applications are in contact with body fluids, tissues and organs. Hence, the biocompatibility of materials must be examined under conditions that simulate those of the biological environment after implantation. *In vitro* tests have been used successfully to screen biocompatibility of materials.

3.3.1. Cytotoxicity Assay

To prescreen the biocompatibility, cytotoxicity tests are widely used. There is a good correlation between the results of animal assays and cell culture test methods. In the present work, the cytotoxicity tests of discs were performed using human osteosarcoma cell line (Saos-2).

3.3.1.1. Microscopic Examination

The morphological changes, degree of detachment from the surface, presence of floating cells and vacuole formation within the cells were studied with microscopic examination (Table 3.7). The phase contrast images of cells after 24 hour incubation in the extracts are given in Figures 3.20, 3.21, and 3.22.

Table 3.7. The effects of disc' extracts on Saos-2 cells after 24 hour incubation

	Floating cells	**Negative changes in cell morphology**	**Monolayer formation**	**Detachment in some areas**	**Vacuole formation**
PCL	absent	absent	continued	absent	absent
PCL/BG	absent	absent	continued	absent	absent
PCL/BG/ CaS	absent	absent	continued	absent	absent
PCL/BG/ HYA	absent	present (shrinking, less spreading, aggregate formation)	continued	absent	absent
PCL/BG/ DBM	absent	absent	continued	absent	absent

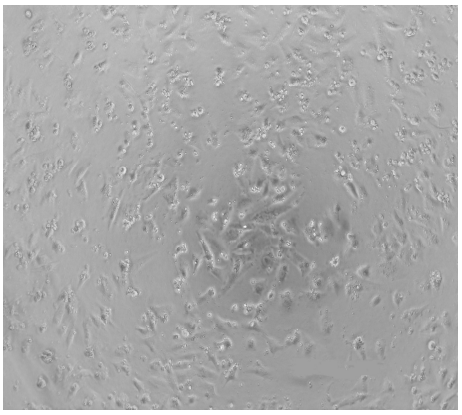

(a) Positive Control (10x)

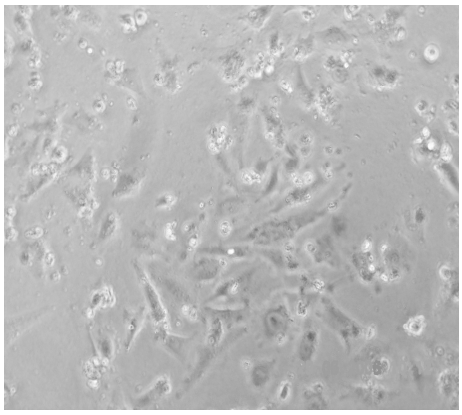

(b) Positive Control (20x)

(a) PCL extract added (10x)

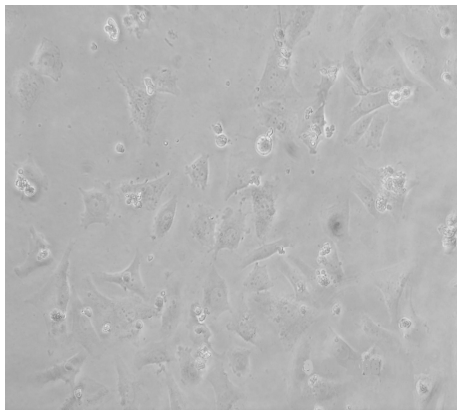

(b) PCL extract added (20x)

Figure 3.20. Phase contrast micrographs of positive control and PCL after 24 hour incubation in the disc derived extracts

(a) PCL/BG extract added (10x)

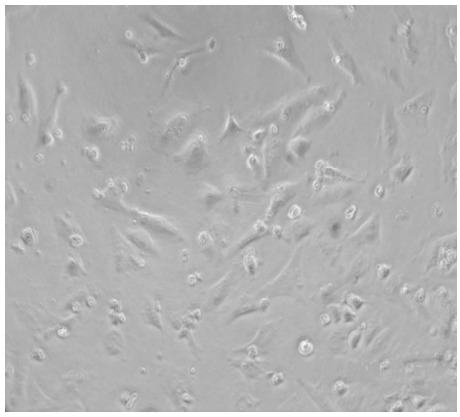

(b) PCL/BG extract added (20x)

(a) PCL/BG/CaS extract added (10x)

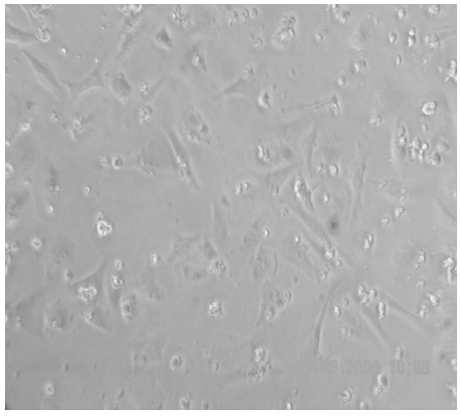

(b) PCL/BG/CaS extract added (20x)

Figure 3.21. Phase contrast micrographs of PCL/BG and PCL/BG/CaS after 24 hour incubation in the composites derived extracts

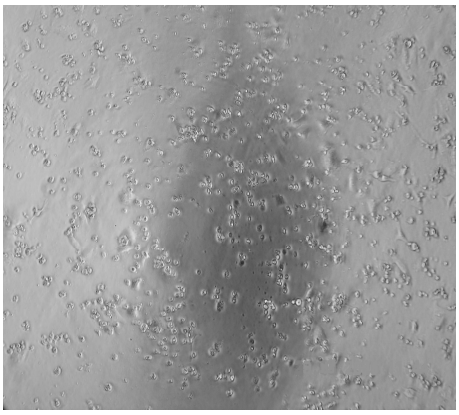

(a) PCL/BG/DBM extract added (10x)

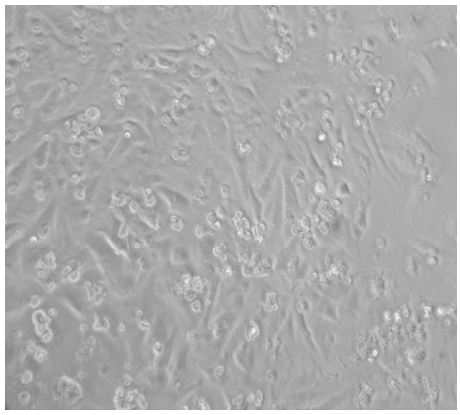

(b) PCL/BG/DBM extract added (20x)

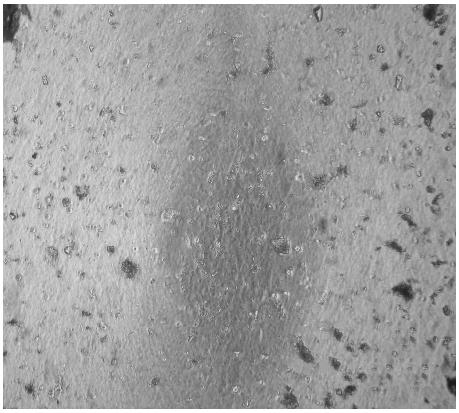

(a) PCL/BG/HYA extract added (10x)

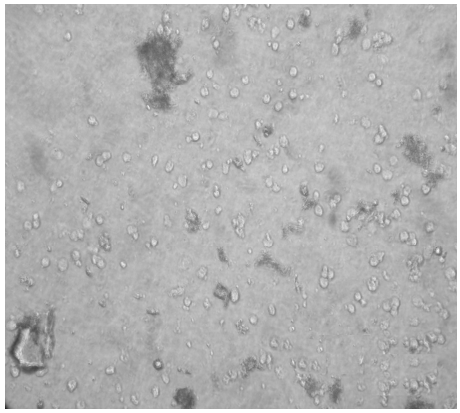

(b) PCL/BG/HYA extract added (20x)

Figure 3.22. Phase contrast micrographs of PCL/BG/DBM and PCL/BG/HYA after 24 hour incubation in the composites derived extracts

According to microscopic examinations, the extracts of all groups other than PCL/BG/HYA group did not induce a cell viability reduction and an inhibition of cell growth. Hence, these groups had no toxic effect to the cells. Cell shrinkage, less cell spreading and aggregate formation were observed in some areas for PCL/BG/HYA group. Due to its high hydrophilicity, HYA was released from the composite into the medium increasing the viscosity of the medium. This viscosity caused the shrinkage of cells and aggregate formation.

3.3.1.2. Cell Viability

MTT [3-(4,5-dimethylthiazol-2-yl)-2,5-diphenyl tetrazolium bromide] assay is a standard colorimetric assay for measuring cell viability. The number of viable cells determined using the calibration curve (Appendix B) is given in Table 3.8 and Figure 3.23.

Table 3.8. The number of viable cells after 24 hour incubation in the disc derived extracts

GROUPS	VIABLE CELL NUMBER
Control	116,167 ± 32,291
PCL	84,489 ± 15,550
PCL/BG	94,584 ± 31,231
PCL/BG/CaS	71,296 ± 14,216
PCL/BG/HYA	168,352 ± 52,979
PCL/BG/DBM	62,755 ± 21,084

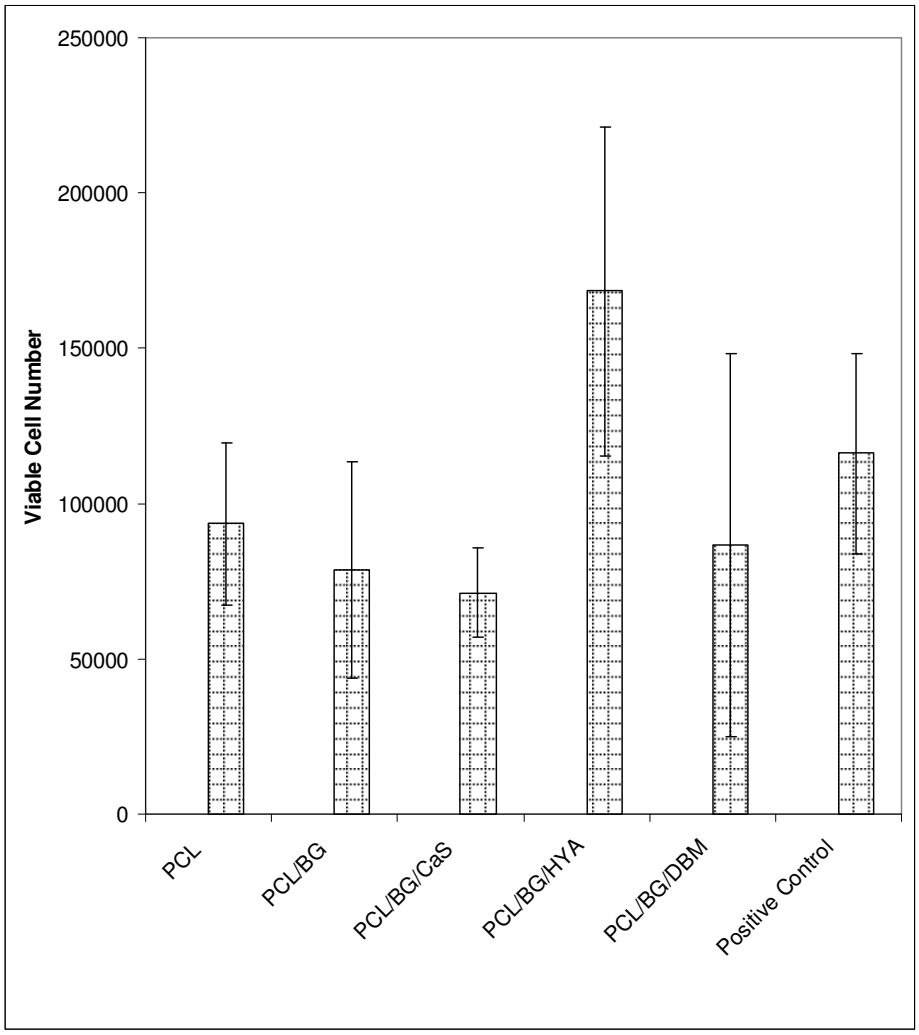

Figure 3.23. The number of viable cells after 24 hours incubation in the disc derived extracts

The MTT assay results showed that there was no significant difference between viable cell numbers of positive control and disc groups except for PCL/BG/HYA. The number of viable cells for PCL/BG/HYA extracts was significantly higher than all groups and positive control. MTT assay result for PCL/BG/HYA group was not in correlation with the microscopic examinations.

The viscous extract medium caused interference in absorbance measurement of this group and the viable cell number determined was overestimated.

The MTT assay results and microscopic examinations showed that there was no toxic material release from the discs and the cell viability and proliferation continued. This indicated that the biomaterials used in disc preparation are biocompatible. These results are in agreement with the literature. For example; PCL had been an approved polymer by the Food and Drug Administration for human clinical use *in vivo* (Taddei et al., 2005). Bioglass has been widely used in dental and orthopedic applications (Oliva et al., 1998, and Vogel et al., 2001). Calcium sulfate has been used in maxillofacial osseous defects (Su-Gwan et al., 2001). DBM has been used widely in cranial defects and orthopedic applications (Chesmel et al., 1998, Cook et al., 2002 and Chakkalakal et al., 1999). HYA has applications at ocular surgery and osteoarthritis (Varghese and Elisseeff, 2006). However, crosslinking is required to decrease its solubility.

3.4. *In Vivo* Studies

In order to evaluate the behavior of discs in living systems as an indication of their usability in bone applications, the *in vivo* experiments were done on critical size bone defects. As it is more difficult to evaluate *in vivo* results than *in vitro* or *in situ* cases, several types of analyze (QCT, SEM, mechanical tests) were carried out on the samples. It is possible to compare different phases of healing with *in vivo* analysis by measuring density changes and biomechanical properties of the implanted bones, and by observations of morphological and physical events at the bone-implant regions.

Before starting destructive test methods on *in vivo* samples general appearance of the bone-implant regions were inspected with macroscopic observations. According to these observations the defect regions were found to be covered either by disc itself or more or less with bony tissues.

General appearances of harvested humeri (7 weeks after the operations) are shown in Figure 3.24. In negative control group, the newly formed tissue had different appearance than healthy bone at the defect site. Thus, the presence of previous damage was easily recognized. The defect site was dark colored, non-uniform and softer than the healthy bone. Therefore, these bones were suggested as healed with an unhealthy appearance.

By visual examination it was possible to see that the operation area was covered with fibrous tissue in all implanted bones with different thicknesses. When this fibrous tissue covering the implant region was removed with a scalpel blade, some implant surfaces could be detected without any degradation and any sign of inflammation except for a few cases of HYA involving group.

The implantation sites were not always easily detectable for some bones. The implant surfaces were covered with healthy compact bone and gained a healthy appearance. The most healthy bone appearance was observed for PCL/BG/DBM group while PCL/BG/CaS group and a few of the PCL and PCL/BG groups had moderate healthy bone appearances.

In PCL and PCL/BG groups, there was moderate fibrous tissue formation around the defect sites compared to the negative control.

In PCL/BG/HYA group, the thickness of fibrous tissue around the bone was moderate and there were more soft tissues than PCL/BG and PCL/BG/CaS groups. However, the bone around the implant site was found to be deformed and widened in most cases.

For PCL/BG/CaS, there was less fibrous tissue formation than negative control and no widening was observed at the defect site.

The PCL/BG/DBM implanted bones had the appearance similar to the positive control-healthy bone suggesting a better regeneration in this group.

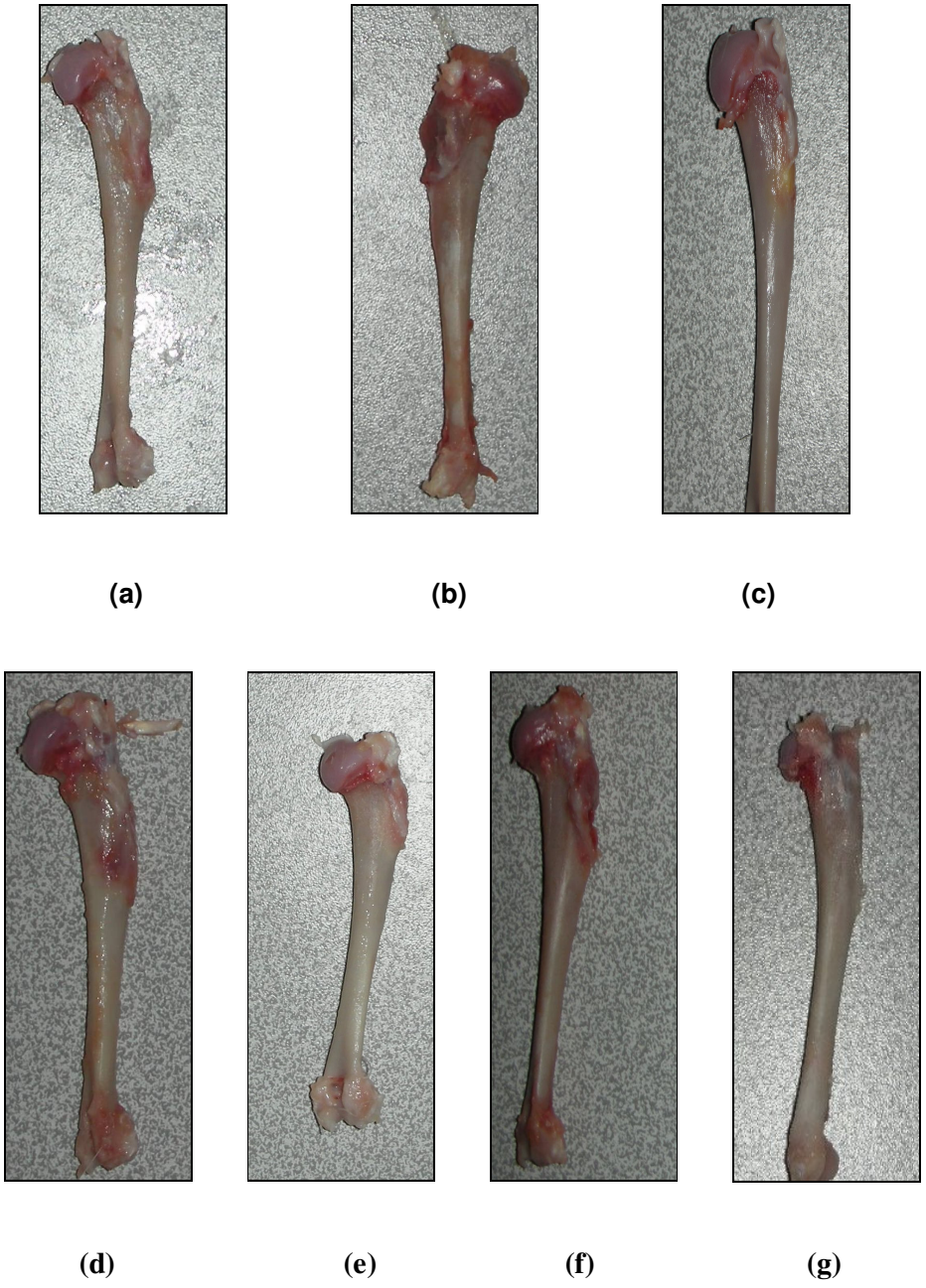

Figure 3.24. General appearance of implanted rabbit humeri 7 weeks after *in vivo* applications: **(a)** PCL Group, **(b)** PCL/BG Group, **(c)** PCL/BG/DBM Group, **(d)** PCL/BG/CaS Group, **(e)** PCL/BG/HYA Group, **(f)** Negative Control Group-empty defect, **(g)** Positive Control Group-unoperated.

3.4.1. Comparison of Bone Densities by Quantitative Computed Tomography (QCT)

Quantitative computed tomography (QCT) has been used for determination of bone densities based on measurements of X-ray attenuation by the sample. QCT results of the bones were obtained by measuring the CT numbers from cross-sectional images of the rabbit humeri (Figure 3.25) and converting them into densities. The comparison of density results for implant regions and bone-implant interfaces is given in Table 3.9.

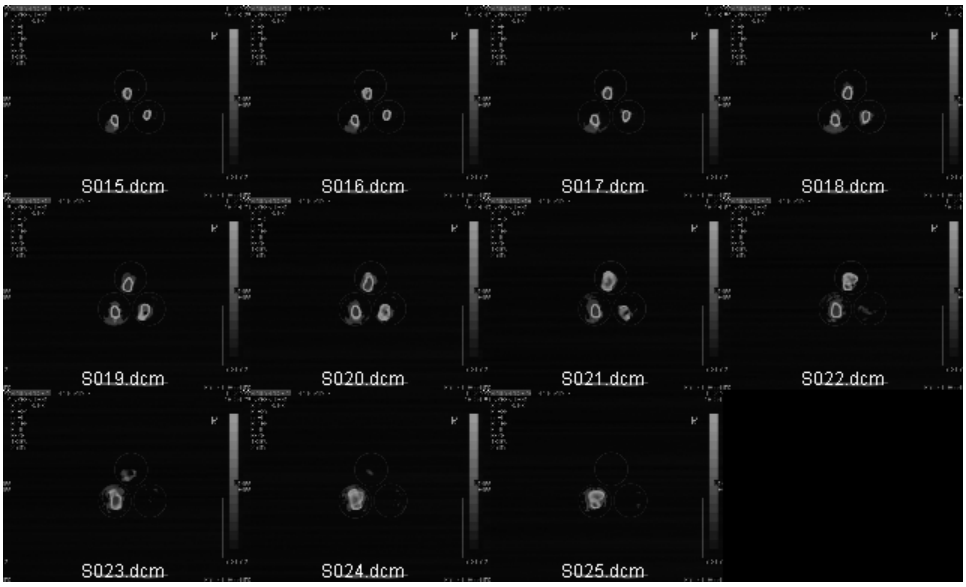

Figure 3.25. Quantitative cross-sectional images of the rabbit humeri from QCT analysis

Table 3.9. Bone mineral density (BMD) of implant regions and bone-implant interfaces

	Bone Mineral Density (g/cm^3)	
Groups	**Implant region**	**Bone-Implant Interface**
PCL	1.596 ± 0.165	1.722 ± 0.141
PCL/BG	1.618 ± 0.053 *	1.709 ± 0.046 *
PCL/BG/DBM	1.585 ± 0.082	1.637 ± 0.074
PCL/BG/CaS	1.635 ± 0.080	1.677 ± 0.094
PCL/BG/HYA	1.628 ± 0.175	1.743 ± 0.094
Negative Control	1.281 ± 0.013	
Positive Control	2.028 ± 0.062	

* indicates the significant difference between interface and implant regions of PCL/BG group ($p=0.002<0.05$)

At both implant regions and implant-bone interfaces, all implant groups had significantly higher BMD values than negative control ($p<0.001$). There were also statistically significant differences between positive control and all other groups ($p<0.001$).

According to these results, it might be concluded that bone-implant interface formation has started in all implant groups, but their BMD values have not reached to that of the positive controls. Only for PCL/BG group, there was a significant density increase from implant region to interface region. This high density result for BG involving group might indirectly indicate the hydroxyl carbonate apatite (HCA) formation that has been suggested previously from *in situ* SEM results. For negative control group, the BMD was low indicating the low density-high porosity- bone formation at the defect site for this group. This result was also in agreement with the SEM results showing the spongy type

bone formation which will be explained in details in Section 3.4.3. Formation of a woven bone structure (callus) was an expected result as stated by other researchers (Doblaré et al., 2004).

Considerable difference between positive and negative control BMDs was due to the differences of the woven bone and compact bone properties. Lamerigts et al. (2000) studied the *in vivo* effects of controlled loading conditions onto a fixed amount of allograft in the goat femurs by using QCT scanning and histomorphometry. After 12 weeks, the loaded grafts turned into a vital trabecular structure and the densities of the loaded grafts were higher than the non-loaded grafts. The average density of the trabecular bone surrounding the defect (0.4878 ± 0.36 g/cm^3) was significantly lower than that of the femoral cortical bone (1.4 ± 0.84 g/cm^3) (Lamerigts et al., 2000).

Martin et al. (2004) studied the effectiveness of peripheral quantitative computed tomography (pQCT) data for computing the bending stiffness of bone accurately. Initially, they obtained the pQCT bone mineral densities of the rabbit humeri and determined the elastic modulus of compact bone as a function of bone mineral densities. When the bending stiffness based on the QCT data and the actual bending stiffness of the bones obtained by four point bending tests were compared, high correlation ($R^2 = 0.96$) was obtained between them. In the same study, they also observed that the apparent densities of bones determined by Archimedes' Principle was higher than the pQCT data. This difference was due to the principles of density determination of the two methods. Although bone mineral mass is measured directly in pQCT, the density of the organic and fluid components, such as bone marrow, blood vessels and interstitial fluid were also measured in the apparent measurement (Martin et al., 2004).

3.4.2. Biomechanical Tests

In biomechanical studies, generally, the mechanical properties of bone at macroscopic level are determined by tension, compression, torsion, bending and shear tests. The most commonly used standard tests are tension and bending tests for whole and segmented bone specimens. Despite high accuracy of tensile testing, bending tests are preferred for measuring the mechanical properties of bones of rodents and other small animals. Three point bending test is a widely used standard method to evaluate the mechanical properties of the implanted bone (Lowry et al., 1997, Yoneda et al., 2005, Emami et al., 2002, and Balçık et al., 2007). Hence, in this study three point bending and microhardness were applied as macro and micro level tests, respectively, in evaluating the biomechanical properties of harvested bones.

3.4.2.1. Three Point Bending Test Results of Rabbit Humeri

The load-deflection curve was obtained from three point bending test for each specimen. From this data, the stress-strain curve was constructed using the equations given in Section 2.2.4.3.1. A typical bending curve for rabbit humeri was shown in Figure 3.26. According to this graph, after an initial linear-elastic region the failure occurred with a rapid decrease in load. The Young's moduli calculated from the slopes of the linear region in stress-strain curves were compared in Figure 3.27.

The elastic modulus of the positive control group (20208 ± 4775 MPa) was correlated with the elastic modulus of compact rabbit bone (22100 MPa) (Cowin, 1989).

Except PCL group, all other groups were found significantly different from positive control group ($p<0.05$) indicating better integration of this implant to

the bone. PCL implants had a stable and continuous structural integrity with bone which will be explained in Section 3.4.3 in more detail. This outcome was also consistent with homogeneous structure and long-degradation half-life of PCL. The combination of these properties was thought to be the main reason for this group to have better mechanical strength than the other groups. Although PCL had a higher Young's modulus, this value was out of the 90 % confidence interval of positive control group.

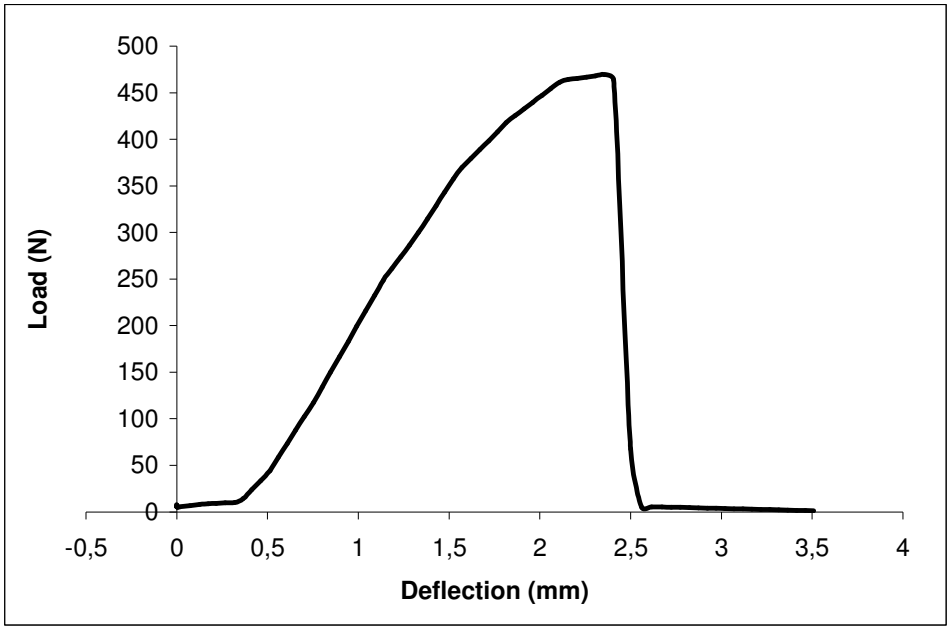

Figure 3.26. A typical load-deflection curve

PCL/BG/CaS and PCL/BG groups showed lower Young's modulus than all other groups. CaS was thought to be released and degraded rapidly before new bone formation. The fast dissolution of CaS *in vivo* was observed in previous studies (Stubb et al., 2004, Huan and Chang, 2007). This behavior of CaS might have caused the decline in the mechanical properties of the composite. For PCL/BG group, it was thought that a smooth interface between

implant and bone was formed initially by crystals of hydroxyl carbonate apatite (HCA) layer as expected from the *in situ* analysis. However, because of less water absorption capacity of these implants compared to PCL implants, these formations were restricted only to the surface or outer regions of the implant, thus destabilizing throughout the time. For both PCL/BG and PCL/BG/CaS implants the least integration with bone was observed as will be explained in results of SEM studies. Hence, PCL/BG group showed a lower elastic modulus than PCL during the three point bending testing as in the case of *in situ* mechanical results. PCL discs had the highest young modulus among all compositions. This was thought to be as a result of its longer degradation time compared to others. However, its Young's modulus did not reach the value of healthy bone. Considering the changes in mechanical properties upon *in situ* incubations, this group had unexpectedly better results than BG involving group. This was found to be related with PCL's providing a smoother and stable surface for the interaction with the bone tissue.

The composite discs with organic component namely, PCL/BG/DBM and PCL/BG/HYA showed higher elastic modulus than the composite discs with inorganic component, PCL/BG and PCL/BG/CaS. The chemical similarity with bone and the larger molecular structure of HYA and DBM provided a more stable interface region. Therefore, they showed higher elastic moduli. This suggests that although it is desired to give some inorganic supply and bioactive precursors to the bone tissue in the long run the favored material is the one that has inductive effect for bone growth. When compared with PCL group, it was concluded that even without inductive components, the results were better when there was no material release from the implant.

In this study, the Young's moduli of all implanted groups were lower than of positive control. Hence, 50 days (nearly 7 weeks) for the termination of the animals seemed not enough for complete healing when the long time needed for the cortical bone regeneration *in vivo* is considered. As seen from the literature, the mechanical properties of implanted bone improved with time. Yoneda et al. (2005) studied bone regeneration capacity of the composites composed of recombinant human bone morphogenetic protein (rhBMP)-2, p-

dioxanone and polyethylene glycol (PLA-DX-PEG) and porous b-tricalcium phosphate (β-TCP) in a critical-sized rabbit femur defect model. After 8 and 24 weeks of implantation, the harvested bones were examined radiologically and biomechanically. According to the three point bending results, implanted groups showed significantly lower stiffness (160 N/m) values than non-operated femurs (400 N/m) at 8^{th} week. Stiffness increased at 24^{th} weeks (370 N/m) and was found to be close to the non-operated healthy femurs (Yoneda et al., 2005). In another study, Komaki et al. (2006) have compared a complex composite composed of β-tricalcium phosphate (β-TCP), collagen, and fibroblast growth factor 2 (FGF-2) with β-TCP/collagen composite by X-Ray, micro-CT scanning and three point test 12 weeks after implantation of the paste like composites to the segmental bone defect created in the tibia of rabbits. The empty defect and healthy tibia were the control groups. The maximum load and stiffness values were calculated from the load-deflection curve obtained by three point bending test. Both radiology and mechanical results indicated healing after 12 weeks in the complex composite implanted bones. They also observed no significant differences between maximum loads for fracturing and stiffness of the complex composite groups and healthy tibia (Komaki et al., 2006).

When the bone densities measured with QCT and Young's modulus from three point bending test were evaluated together, no correlation between these properties was found. This could be explained as bone quality in terms of biomechanical properties was not dependent only on this characteristic of bone. Bone quality means the sum of all characteristics of bone that affect the ability of bone to resist fracture. Other characteristics at different hierarchical scale of bone structure may affect the biomechanical properties of bone. For instance, at macroscopic level, whole bone morphology and bone density spatial distribution influence bone quality. Properties at microscopic level, microarchitecture, porosity, and microstructural constituents determine the bone quality. At nano-scale, mineral and collagen distribution/alignment, micro damage type affects the bone quality (Hernandez and Keaveny, 2006).

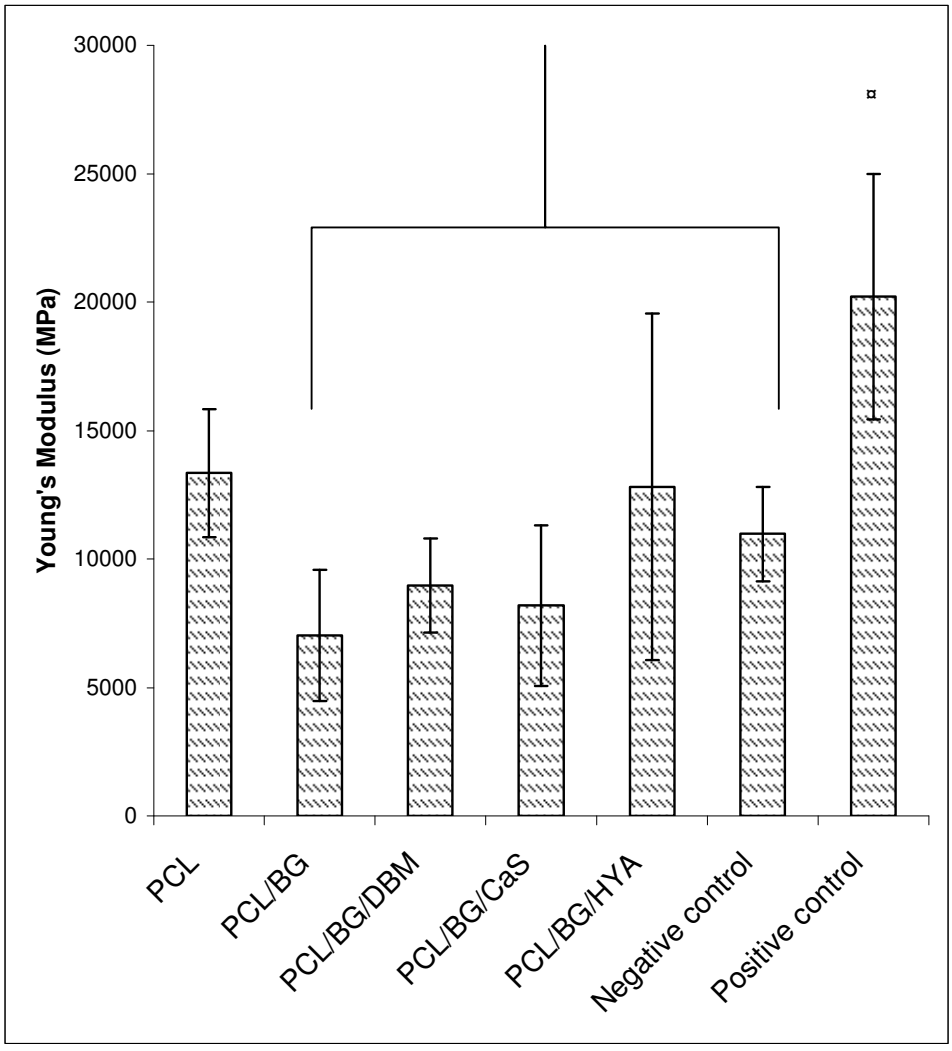

Figure 3.27. Comparison of the Young's moduli for treatment and control groups in three point bending test (¤ indicates the significant difference between positive control and other groups, $p<0.05$)

3.4.2.2 Microhardness Test Results

Microhardness testing is an indentation method that can measure the hardness of a material on a microscopic scale. Hence, to examine the bone-implant interface and implant regions after *in vivo* applications, microhardness testing was applied to evaluate the degree and quality of bone mineralization.

When the hardness values of implant, bone and interface regions were examined, the hardness value was found to increase towards the healthy bone tissue in proportion to the distance from the implant. Therefore, during measurements interface region was examined by considering the two borders: interface I (near to implant) and interface II (near to bone). In literature, it was observed that microhardness measurements of bone-implant interface were similar considering the closeness to the implant or bone sites (Aldini et al., 2002 and Fini et al., 2002). The results of microhardness measurements are given in Figures 3.28-3.30.

When the microhardness values of interface I and II were compared within groups, they were found significantly different from each other for all implant groups, except PCL/BG. These differences in microhardness within groups and also the differences between interfaces and positive control were statistically significant with $p \leq 0.02$. At interface I, only PCL/BG was significantly different than negative control ($p=0.01<0.05$, not shown in the graphs).

When positive control and non-operated parts of the implanted bones were compared (not shown) for their microhardness values they were found as statistically not different from each other.

PCL/BG/HYA group had the lowest microhardness value at the implant site among all groups. This result was an expected outcome as bioactivity and degradation studies also indicated the weakness of this implant for even 15 days after *in situ* incubations.

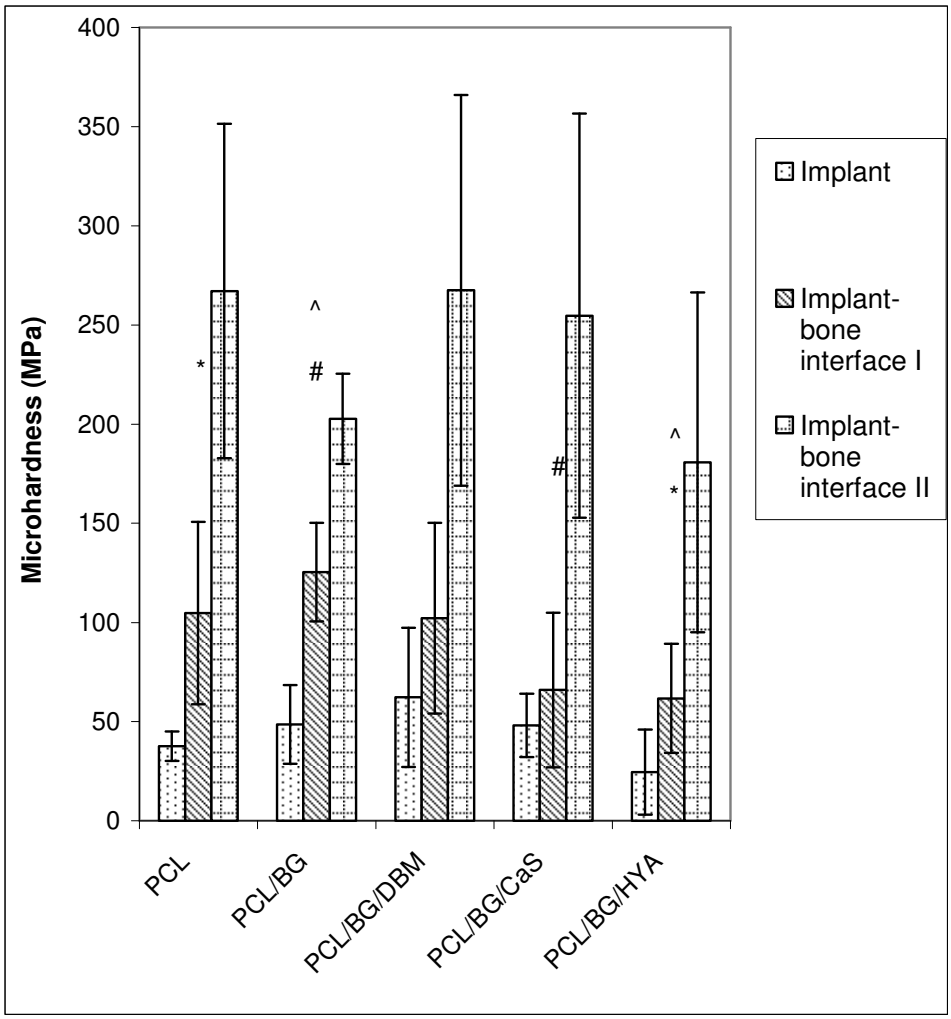

Figure 3.28. The comparison of the microhardness values of implant and bone-implant interfaces after *in vivo* application (Significant differences between groups *, ^, #: $p<0.05$)

The microhardness values of implant regions of all groups were lower than of the negative control. These hardness values belonged to the interior parts of implant. This suggested that the newly formed fibrous or spongy bone tissue had higher microhardness values than the polymer matrix. Only in the case of PCL/BG/DBM implants the microhardness value was closer to the negative

control. This might have resulted from the presence of bone inductive components that enhanced bone ingrowth in this group.

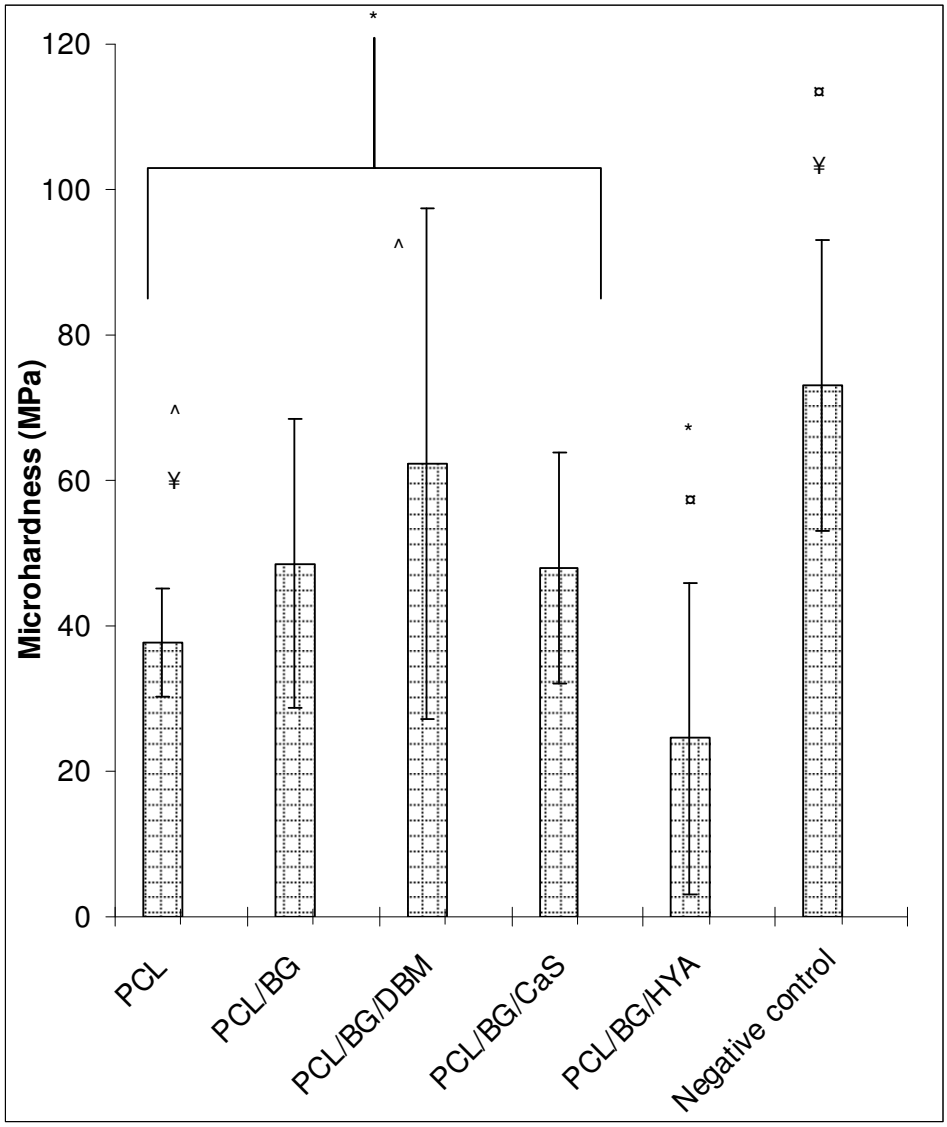

Figure 3.29. The comparison of microhardness values of implant sites after *in vivo* application (Significant differences between groups *, ^, ¥, ¤: $p<0.05$)

When the microhardness values at bone-implant interface II were compared (Figure 3.30), all implant groups were found significantly different from both negative and positive controls. This indicated that the bone healing has begun at the bone site, but not reached to the healthy bone level.

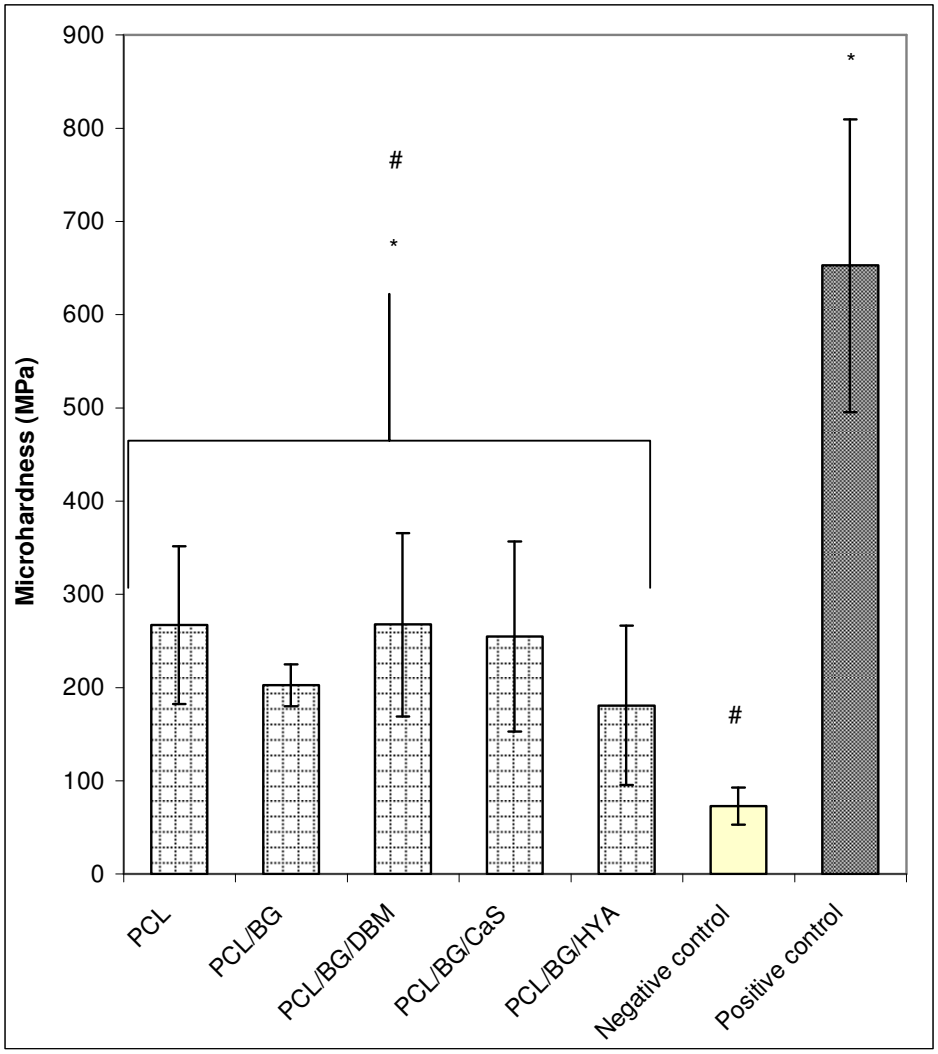

Figure 3.30. The comparison of microhardness values at implant-bone interface II regions after *in vivo* application (Significant differences between groups *, #: $p<0.05$)

Microhardness testing is used in the bone biomechanics studies to investigate the direct structural and functional connection between bone and implants. Giavaresi et al. (2003) examined *in vivo* osseointegration of titanium screws with different surface treatment applications, such as machined (Ti-MA), acid etched (Ti-HF), hydroxyapatite vacuum plasma spray (Ti-HA); and Ca-P anodization followed by a hydrothermal treatment (Ti-AM/HA). After 8 and 12 weeks of implantation in sheep femoral cortical bone, histomorphometric examination, SEM analysis and Vickers microhardness measurements within 200 µm from the interface and inside the thread depth and at the 2000 µm from the top of the screw thread in the host bone were done. With microhardness testing, they compared different surface treated screws by evaluating bone maturation index (BMI) which indicates the percent variation in bone mineralization of the bone tissue and regrowth in the thread inner area at the interface in comparison to preexisting cortical bone. Ti-AM/HA BMI values were nearly constant at two different times. BMI and histological results indicated that the bone growth and mineralization were accelerated for this group. They also observed that bone mineralization and maturation around implants did not reach the healthy bone values (Giavaresi et al., 2003). Aldini et al. (2002) have studied the biocompatibility and osseointegration of RKKP bioglaze® coated or uncoated zirconia in which zirconia cylinders implanted into the distal femoral epiphyses. The Vickers' microhardness testing was applied to two regions of the interface of resin embedded bone samples. They observed higher hardness values for the regions closer to the bone (Aldini et al., 2002).

In another study, PMMA/α-TCP and PMMA were tested for their effect on the biological activities of bone cells and tissue with *in vitro* and *in vivo* studies (Fini et al., 2002). Osteoblast cultures were used for *in vitro* studies. The effects of PMMA/α-TCP and PMMA on cellular viability and activity (i.e. interleukin 6 levels) were determined. For *in vivo* studies, PMMA/α-TCP and PMMA nails were implanted to the femoral condylar trabecular and diaphyseal cortical bone of rabbit models. The rabbits were terminated after 12 weeks and the results were evaluated with histology and microhardness testing. Although PMMA/α-TCP interface showed significantly higher microhardness

values than the PMMA values at both trabecular and cortical implanted groups, they still did not reach the hardness values of pre-existing healthy bone microhardness values. Additionally, there were significant differences between data measured at 200 and 1000 µm distance from the materials, while 200 µm distant regions had smaller hardness values than the farthest region of the interface.

As seen from above studies and the current study, the microhardness value of newly formed bone tissue could not reach to the healthy bone hardness values. However, Guzzardella et al. (2003) observed similar hardness values to the normal healthy bone. In that study, they additionally applied low power laser (LPL) treatment to the hydroxyapatite (HA) implanted femurs of rabbits and compared with the untreated HA implanted femurs. After 3 and 6 weeks, femurs were examined by histomorphometry and microhardness measurements. The stimulus by LPL improved bone implant interface healing as seen from the results of both histology and microhardness data for both time periods. They have also observed that the microhardness values of bone-implant interface were similar to the pre-existing bone at 3 and 6 weeks.

3.4.3. SEM Analysis

After *in vivo* applications, bone-implant interfaces were also examined by SEM and micrographs were taken as seen in Figures 3.31 -3.33.

For negative control group, highly porous spongy bone formation has occurred compared to the dense and smooth appearance of the healthy compact bone (Figure 3.31a and b). Still, there was notable unexpected bone regeneration at the defect region. This might have been caused by the incomplete removal of bone debris at the defect region during the surgical operation. It is well known that any remaining bone particle creates an osteoinductive effect for the regeneration. To avoid such problems, bone debris should be removed by

saline irrigation during defect formation as in similar studies (Nihouannen et al., 2007 and Fellah et al., 2006).

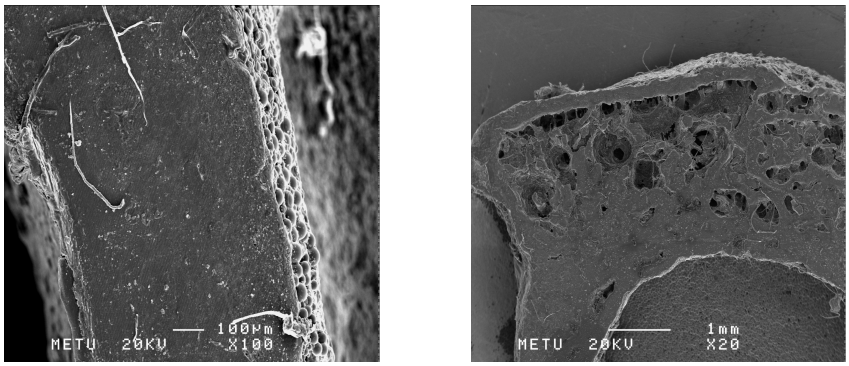

(a) Positive Control (b) Negative Control

Figure 3.31. SEM micrographs of positive and negative control

As seen in Figure 3.32a and Figure 3.33a, there was no apatite crystal formation at bone-PCL implant interface, most probably due to the lack of bioactive components. This result was in accordance with the SEM results after SBF incubations (Figure 3.5) in which no apatite formation was found on the surface of these discs. Despite of the absence of any apatite layer formation and any indication of bonding PCL implants with bone tissue, this implant formed a compatible structure with bone. The PCL implant formed a homogenous and continuous interface with the bone. As seen in previous studies, the *in vivo* degradation of PCL occurs in two stages. During the first stage, collagen filaments containing only occasional giant cells covers the PCL implant. This does not cause a significant weight loss and continues nearly 9 months (non-enzymatic bulk hydrolysis). In the second stage, however, hydrolytic degradation begins resulting in weight loss (Lei et al., 2007). Hence, as stated above the long-degradation time property of pure PCL as well as absence of other soluble components provided a stationary

and smooth surface for the nearby bone tissue for attachment. Besides this, the low glass transition temperature renders pure PCL implant to be in amorphous phase causing high molecular mobility at body temperature (Tay et al., 2007). This property might have provided that PCL became more shapeable by the growing bone tissue and fill the defect region in a better way. Hence, PCL group showed a good integration with the bone appearance as seen in SEM results (Figure 3.32a) which also explains its biomechanical results given in the previous sections despite its lack of any bioactive or osteoinductive material.

For PCL/BG group, apatite crystal formation was observed more at the implant bone-implant interface as shown in Figures 3.32b and 3.33b. When X-ray elemental analysis was done to these structures, they were found to contain calcium and phosphorus elements that are mainly found in apatite molecule (Figure 3.34). Despite the accumulation of crystals at certain regions, the overall bone interfaces of these implants were found as less dense and looser than that with PCL implants. This was thought to be due to the higher reactivity and mobility of the surface in the former group. Hence bioglass molecules might have caused a dynamic media which prevented the formation of an immobile, stable interface. The high percentage of BG in this composite (28 % by weight) might have also caused formation of a less integrated interface with bone than expected for this group. As seen from the study of Lu and her co-workers (2005), the osteoblast response to the composite surface was dependent on the weight percentage of bioglass content and 10 % PLAGA/BG composite showed higher osteoblast growth compared to the 50 % PLAGA/BG composite (Lu et al., 2005).

PCL/BG/DBM group showed a physically quite indistinguishable interface with bone tissue as given in Figure 3.32d and Figure 3.33d. This interface was more similar to bone than other groups' interfaces. When an elemental analysis was done to the interface, calcium, phosphate, carbon and oxygen peaks were observed (Figure 3.35). Calcium and phosphate peaks indicated the existence of apatite or HCA crystal formation while carbon and oxygen peaks are thought to come from the DBM or newly formed cellular structures.

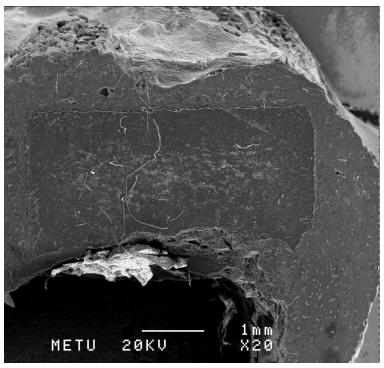

(a) PCL implanted bone

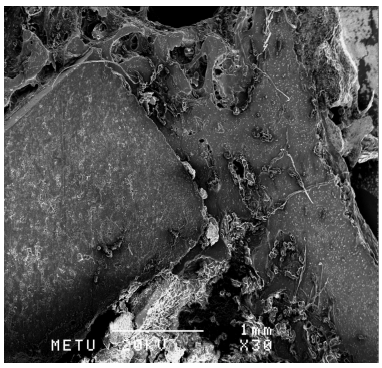

(b) PCL/BG implanted bone

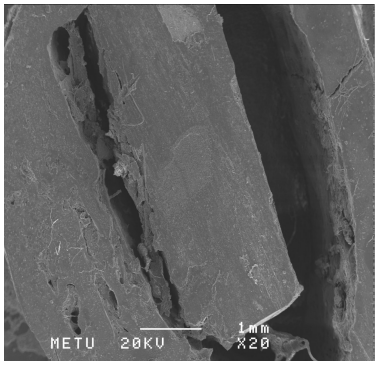

(c) PCL/BG/CaS implanted bone

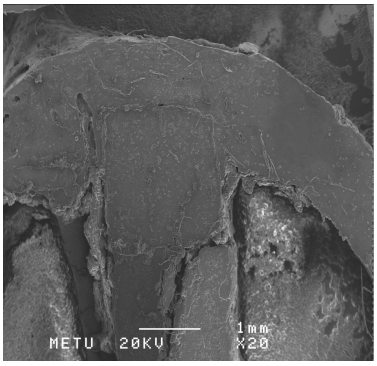

d) PCL/BG/DBM implanted bone

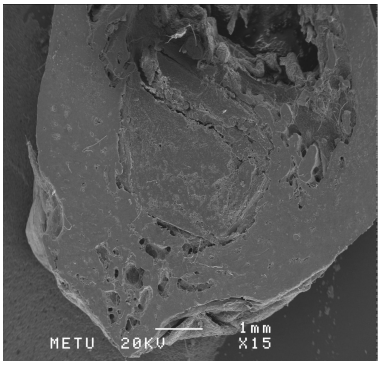

e) PCL/BG/HYA implanted bone

Figure 3.32. General SEM micrographs of the cross-sections of rabbit humeri 52 days after implantation

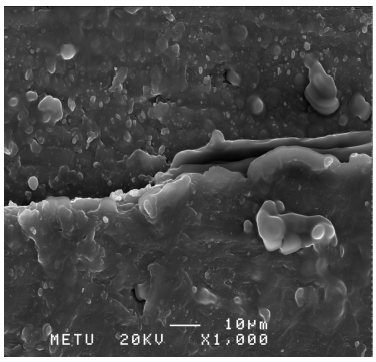

(a) PCL-bone interface

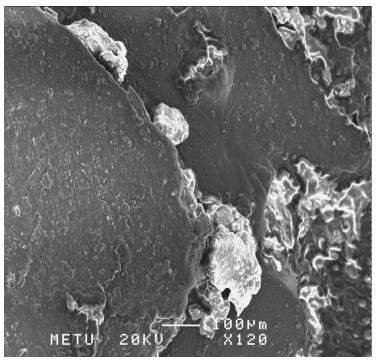

(b) PCL/BG-bone interface

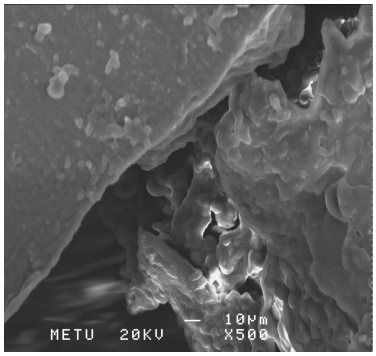

(c) PCL/BG/CaS-bone interface

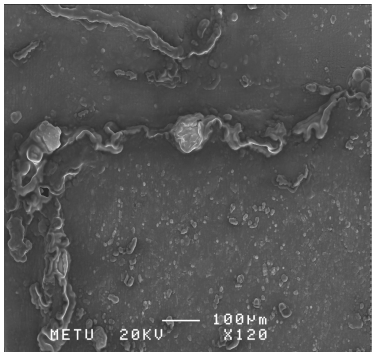

(d) PCL/BG/DBM-bone interface

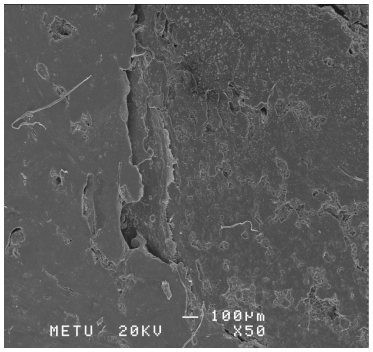

(e) PCL/BG/HYA-bone interface

Figure 3.33. SEM micrographs of implant-bone interfaces after *in vivo* application

Although a well integrated appearance was observed between PCL/BG/CaS and bone after cross-sectioning of the bone, a separation of two phases was seen during SEM analysis (Figure 3.32c and Figure 3.33c). This was thought to be due to the preparation steps at which specimens are rested under high vacuum to remove any dust or chopping particles and then coated with gold. Yet, not having any such disintegration for the other groups suggested that the linkage between this group and the bone tissue was the weakest either due to continuous release of CaS or its being degraded too fast before bone interaction was formed. However, at the defect region, the general appearance was closer to the healthy bone than the negative control most probably owing to stabilization of CaS molecules via interactions with bioglass molecules inside the polymer matrix. In some other studies the fast degradation of CaS was also observed and suggested to prevent the improvement of the ingrowth of new bone tissue (Friedlaender, 2006 and Stubb et al., 2004). The degradation of CaS had a chemical dissolution character rather than cell-mediated resorption/phagocytosis (Hing et al., 2007). This affected bone regeneration negatively as shown in the previous studies (Huan and Chang, 2007). These studies also suggested that CaS, by continuous release and degradation profile creates a highly unstable surface for bone attachment and ingrowth.

Because of the hydrophilic nature of HYA, PCL/BG/HYA group created a deformed bone structure by swelling with imbibed water (Figure 3.32e and Figure 3.33e). The negatively charged (Zhu and Granick, 2003), hydrophilic nature of HYA was thought to cause a spongy bone formation near the implant site. As seen from other studies, bone and other cells adhesions were inhibited by anionic surfaces and the hydrophilic nature of HYA causes limited cell adhesion (Granja et al., 2006, Varghese and Elisseeff, 2006).

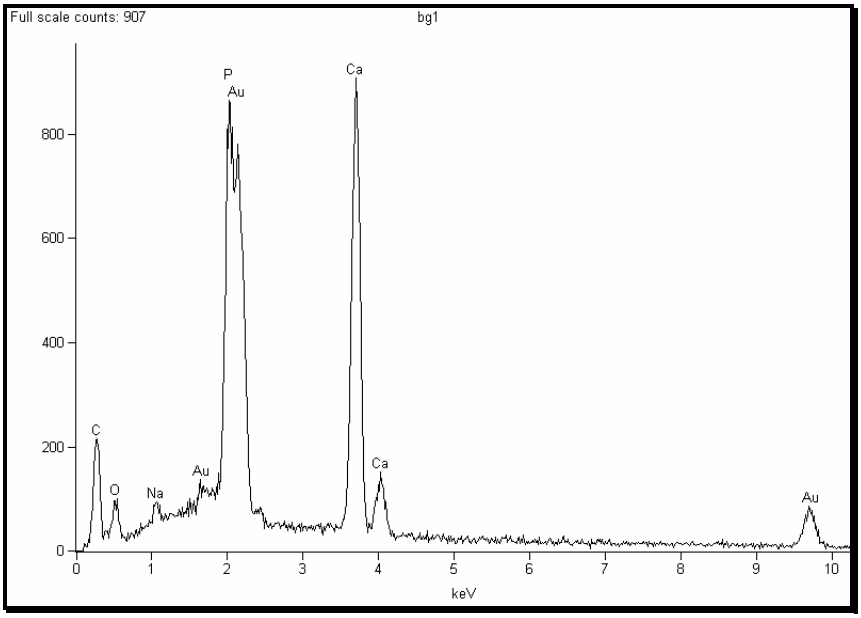

Figure 3.34. The elemental analysis of apatite crystals formed on PCL/BG disc and at bone interface

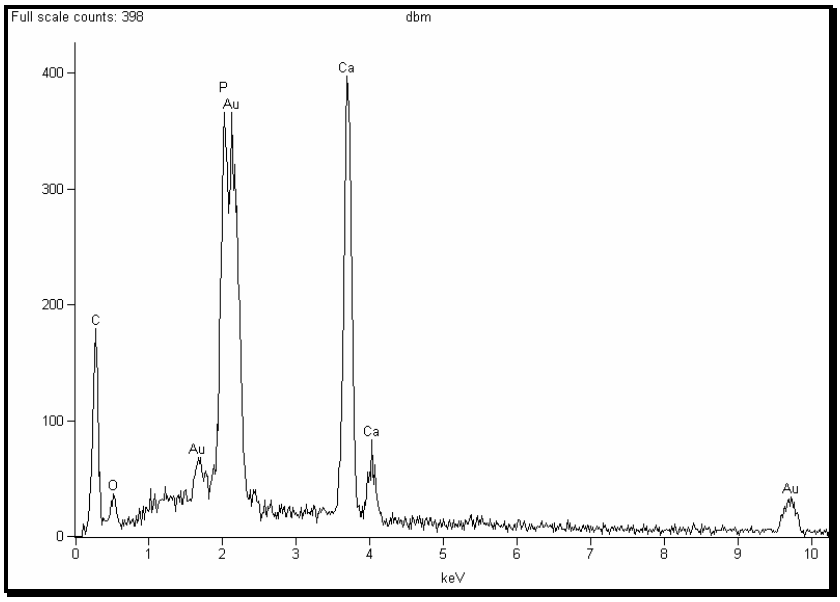

Figure 3.35. The elemental analysis of apatite crystals at the PCL/BG/DBM disc and bone interface

CHAPTER 4

CONCLUSIONS

Bone is a difficult tissue to heal as it requires a support that will provide both the mechanical support and space to the newly formed tissue in time. The mechanical properties of the bone graft materials are besides their biocompatibility, osteoconductivity, and osteoinductivity characteristics are of utmost importance. Considering these requirements, in this study, poly(ε-caprolactone) based composites of different compositions; PCL/BG, PCL/BG/DBM, PCL/BG/CaS, and PCL/BG/HYA or single phase (PCL) implants were prepared and characterized.

The bioactivity and degradation properties of implants were found to be enhanced by both the presence and the amount of BG in the composites as apatite layer increased and water uptake decreased accordingly. However, addition of highly water soluble component (HYA; CaS, or DBM) was found to overcome the effect of BG on the degradation property by increasing the water uptake that finally results in material leaching and void formation in the structure. In correlation with these observations, presence of BG in the discs was found to have protective effect on mechanical properties upon in situ incubations. However, the soluble components that gave high initial strength to the discs by being more compressible during preparation were found to be ineffective in the conservation of the structure during in situ incubations.

In vitro studies showed that all discs except HYA involving group were biocompatible. This unexpected outcome for HYA, was suggested to be related with its high initial concentration within the extraction medium.

After *in vivo* analysis, the QCT results of bones showed that bone-implant interface formation has started in all implant groups. However, the bone mineral densities for all implant interfaces were yet below that of the healthy bone tissue. Only for PCL/BG group, there was a significant density increase from implant region to interface region mostly owing to BG component. The three point bending test results of discs indicated significantly lower elastic moduli compared to healthy bones except for PCL group. This was concluded to be the result of PCL's stable structure that created a more hostile environment for the growing bone tissue. The micro-scale biomechanical properties of composites tested with microhardness have demonstrated that the bone formation has begun at the bone-implant site for all implanted groups with a gradual decrease in microhardness values from the healthy bone towards the implant region. Finally, SEM and EDS analyses of harvested bones illustrated the same effect of BG with in situ incubations for apatite crystal formation around the implants. However, despite no apatite layer formation, PCL implants confirmed a compatible structure with bone owing to its homogenous and continuous interface. PCL/BG/DBM group showed a physically quite indistinguishable interface with bone tissue indicating a better bone integration by this implant. The HYA and calcium sulfate involving discs have created either deformed bone structure or unstable interface due to the high water absorption and leaching by the soluble components.

Suggestions for Future Studies:

As the first suggestion it was thought that the amount of BG component should be optimized considering the ratio of the three components to obtain better apatite formation on disc surfaces and higher osteoblast growth on the implant. Secondly, we suggest that the *in vivo* application period should be increased as the different aspects of regeneration would be more significant through increasing the healing time. Thirdly, development of a more specific macro level mechanical testing technique is suggested that would directly concentrate on the overall defect region instead of covering the whole bone as

applied by the three point bending test in the current study. Finally, use of HYA was thought to give more successful results as a bone graft material if applied via a crosslinking technique.

REFERENCES

Abjornson, C., Lane, J.M., "Demineralized bone matrix and synthetic bone graft substitutes", 2006, Bone Grafts and Bone Graft Substitutes, Friedlaender, G.E., Mankin, H.J., Goldberg, V.M., Ed.s, First Edition, American Academy of Orthopaedic Surgeons, Rosemont, Chap. 2.

Akkas, N., Yeni, Y.N., Turan, B., Delilbası, E., Gunel, U., 1997, "Effect of medication on biomechanical properties of rabbit bones: heparin induced osteoporosis", Clinical Rheumatology, 16, 6, 585-595.

Aldini, N.N., Fini, M., Giavaresi, G., Torricelli, P., Martini, L., Giardino, R., Ravaglioli, A., Krajewski, A., Mazzocchi, M., Dubini, B., Ponzi-Bossi, M. G., Rustichelli, F., Stanic, V., 2002, "Improvement in zirconia osseointegration by means of a biological glass coating: an in vitro and in vivo investigation", J Biomed Mater Res, 61, 282–289.

Ang, K.C., Leong, K.F., Chua, C.K., Chandrasekaran, M., 2007, "Compressive properties and degradability of poly(e-caprolatone)/hydroxyapatite composites under accelerated hydrolytic degradation", J Biomed Mater Res, 80A, 655–660.

Artico, M., Ferrante, L., Pastore, F.S., Ramundo, E.O., Cantarelli, D., Scopelliti, D., Iannetti, G., 2003, "Bone Autografting of the Calvaria and Craniofacial Skeleton: Historical Background, Surgical Results in a Series of 15 Patients, and Review of the Literature", Surg Neurol, 60, 71–9.

Aslan, M., Şimşek, G., Dayı, E., 2006, "The effect of hyaluronic acid-supplemented bone graft in bone healing: experimental study in rabbits", J Biomater Appl; 20; 209.

ASTM D 695M, "Standard test method for compressive properties of rigid plastics: Metric", 1992.

Azevedo, M.C., Reis, R.L., Claase, M.B., Grijpma, D.W., Feijen, J., 2003, "Development and properties of polycaprolactone/hydroxyapatite composite biomaterials", J Mater Sci Mater Med, 14, 103-107.

Balçık, C., Tokdemir, T., Şenköylü, A., Koç, N., Timuçin, M., Akın, S., Korkusuz, P., Korkusuz F., 2007, "Early weight bearing of porous HA/TCP (60/40) ceramics in vivo: a longitudinal study in a segmental bone defect model of rabbit", Acta Biomater, In Press, doi:10.1016/j.actbio.2007.04.004.

Barrabés, M., Sevilla, P., Planell, J.A., 2007, "Mechanical properties of nickel–titanium foams for reconstructive orthopaedics", Mater Sci Eng, In Press, doi:10.1016/j.msec.2007.02.001.

Burg, K.J.L., Porter, S., Kellam, J.F, 2000, "Biomaterial developments for bone tissue engineering", Biomaterials, 21, 2347-2359.

Carson, J.S., Bostrom, M.P.G, 2007, "Synthetic bone scaffolds and fracture repair", Injury, Int. J. Care Injured, 38S1, S33-S37.

Chan, C., Thompson, I., Robinson, P., Wilson, J., Hench, L., 2002, "Evaluation of Bioglass/dextran composite as a bone graft substitute", Int. J. Oral Maxillofac. Surg., 31, 73-77.

Chakkalakal, D.A., Strates, B.S., Mashoof, A.A., Garvin, K.L., Novak, J.R., Fritz, E.D., Mollner, T.J., McGuire, M.H., 1999, "Repair of segmental bone defects in the rat: an experimental model of human fracture healing", Bone, 25, 321-332.

Chambers, B., St. Clair, S.F., Froimson, M.I., 2007, "Hydroxyapatite-coated tapered cementless femoral components in total hip arthroplasty", The Journal of Arthroplasty, 22, 4, 71-74.

Chen, B., Sun, K., 2005, "Poly (ε-caprolactone)/hydroxyapatite composites: effects of particle size, molecular weight distribution and irradiation on interfacial interaction and properties", Polymer Testing, 24, 64-70.

Chesmel, K.D., Branger, J., Wertheim, H., Scarborough, N., 1998, "Healing response to various forms of human demineralized bone matrix in athymic rat cranial defects", J Oral Maxillofac Surg, 56, 857-863.

Cheung, S., Westerheide, K., Ziran, B., 2003, "Efficacy of contained metaphyseal and periarticular defects treated with two different demineralized bone matrix allografts", Int. Orthopaedics (SICOT), 27, 56-59.

Chistolini, P., Ruspantini, I., Bianco, P., Corsi, A., Cancedda, R., Quarto, R., 1999, “Biomechanical evaluation of cell-loaded and cell-free hydroxyapatite implants for the reconstruction of segmental bone defects”, J Mater Sci Mater Med, 10, 739-42.

Cho, B.C., Chung, H.Y., Lee, D.G., Yang, J.D., Park, J.W., Roh, K.H., Kim, G.U., Lee, D.S., Kwon, I.,C., Bae, E.,H., Kwang, H.J., Park, R.W., Kim, I.S., 2005, “The effect of chitosan bead encapsulating calcium sulfate as an injectable bone substitute on consolidation in the mandibular distraction osteogenesis of a dog model”, J Oral Maxillofac Surg, 63, 1753-1764.

Cho, Y.S., Lee, J.W., Lee, J.S., Lee, J.H:, Yoon, T.R:, Kuroyanagi, Y., Park, M.H:, Kim, H.J:, 2002, “Hyaluronic acid and silver sulfadiazine-impregnated polyurethane foams for wound dressing application”, J Mater Sci Mater Med, 13, 9, 861-865.

Chouzouri, G., Xanthos, M., 2007, “In vitro bioactivity and degradation of polycaprolactone composites containing silicate fillers”, Acta Biomater, doi:10.1016/j.actbio.2007.01.005.

Ciapetti, G., Ambrosio, L., Savarino, L., Granchi, D., Cenni, E., Baldini, N., Pagani, S., Guizzardi, S., Causa, F., Giunti, A., 2003, “Osteoblast growth and function in porous poly e-caprolactone matrices for bone repair: a preliminarystudy”, Biomaterials, 24, 3815–3824.

Cook, S.D., Salkeld, S.L., Patron, L.P., Barrack, R.L., 2002, ”The effect of demineralized bone matrix gel on bone ingrowth and fixation of porous implants”, Journal of Arthroplasty, 17, 402-408.

Coombes, A.G.A., Rizzi, S.C., Williamson, M., Barralet, J.E., Downes, S., Wallace, W.A., 2004, “Precipitation casting of polycaprolactone for applications in tissue engineering and drug delivery”, Biomaterials, 25, 315–325.

Cowin, S.C., 1989, Bone Mechanics, CRC Press, Boca Raton.

Cull, P., Ed., 1989, The Sourcebook of Medical Illustration, Park Ridge, NJ: Parthenon.

Currey, J.D., 2002, “Bones: structure and mechanics”, Princeton University Press, USA.

Dalgarno, K.W., Goodridge, R.D., 2004, “Compression testing of layer manufactured metal parts: the RAPTIA compression benchmark”, Rapid Prototyping Journal, 10, 261-264.

Dee, K.C., Puleo, D.A., Bizios, R., 2002, “An introduction to tissue biomaterial interactions”, Wiley-liss, USA, Chap.1.

Doblaré, M., García, J.M., Gómez, M.J., 2004, “Modelling bone tissue fracture and healing: a review”, Engineering Fracture Mechanics, 71, 1809-1840.

Edwards, R.C., Kiely, K. D., Eppley, B.L., 2001, “The Fate of Resorbable Poly-L-Lactic/Polyglycolic Acid (LactoSorb) Bone Fixation Devices in Orthognathic Surgery”, J Oral Maxillofac Surg, 59, 19-25.

Emami, M.J., Oryan, A., Saeidinasab,H., Parizi, A.M., 2002, “The effect of bone marrow graft on bone healing: a radiological and biomechanical study”, Iran J Med Sci; 27, 2, 63-66.

Fellah, B.H., Weiss, P., Gauthier, O., Rouillon, T., Pilet, P., Daculsi, G., Layrolle, P., 2006, “Bone repair using a new injectable self-crosslinkable bone substitute”, J Orthop Res, 24, 628–635.

Fini, M., Giavaresi, G., Aldini, N.N., Torricelli, P., Botter, R., Beruto, D., Giardino, R., 2002, “A bone substitute composed of polymethylmethacrylate and a-tricalcium phosphate: results in terms of osteoblast function and bone tissue formation”, Biomaterials, 23, 4523–4531.

Fratzl, P., Gupta, H.S., Paschalis, E.P., Roschger, P., 2004, “Structure and mechanical quality of the collagen-mineral nano-composite in bone”, J Mater Chem, 14, 2115-2123.

Giavaresi, G., Fini, M., Cigada, A., Chiesa, R., Rondelli, G., Rimondini, L., Aldini, N.N., Martini, L., Giardino, R., 2003, “Histomorphometric and microhardness assessments of sheep cortical bone surrounding titanium implants with different surface treatments”, J Biomed Mater Res, 67A, 112–120.

Glowacki, J:, “Tissue response to bone-derived implants”, 1992, Bone Grafts & Bone Substitutes, Habal, M.B., Reddi, A.H., W.B. Saunders Company, USA, Chap.8.

Goldberg, V.M., Akhavan, S., “Biology of bone grafts”, 2006, Bone Grafts and Bone Graft Substitutes, Friedlaender, G.E., Mankin, H.J., Goldberg, V.M., Ed., First Edition, American Academy of Orthopaedic Surgeons, Rosemont, Chap.1.

Granja, P.L., Jéso, B.D., Bareille, R., Rouais, F., Baquey, C., Barbosa, M.A., 2006, “Cellulose phosphates as biomaterials: In vitro biocompatibility studies”, Reactive & Functional Polymers, 66, 728–739.

Gugala, Z., Davis, A.R., Fouletier-Dilling, C.M., Gannon, F.H., Lindsey, R.W., Olmsted-Davis, E.A., 2007, “Adenovirus BMP2-induced osteogenesis in combination with collagen carriers”, Biomaterials, In Press, doi: 10.1016/j.biomaterials.2007.07.007.

Guo, H.B., Miao, X., Chen, Y., Cheang, P., Khor, K.A., 2004, “Characterization of hydroxyapatite– and bioglass–316L fibre composites prepared by spark plasma sintering”, Materials Letters, 58, 304-307.

Han, B., Yang, Z., Nimni, M., 2005, “Effects of moisture and temperature on the osteoinductivity of demineralized bone matrix”, Journal of Orthopaedic Research, 23, 855-861.

Guzzardella, G.A., Torricelli, P., Aldini, N.N., Giardino, R., 2003, “Osseointegration of endosseous ceramic implants after postoperative low-power laser stimulation: an in vivo comparative study”, Clin. Oral Impl. Res, 14, 226–232.

Hao, J., Yuan, M., Deng, X., 2002, “Biodegradable and biocompatible nanocomposites of poly(ε-caprolactone) with hydroxyapatite nanocrystals: thermal and mechanical properties”, J Appl Polym Sci, 86, 676–683.

Hattar, S., Asselin, A., Greenspan, D., Oboeuf, M., Berdal, A., Sautier, J.M., 2005, “Potential of biomimetic surfaces to promote in vitro osteoblast-like cell differentiation”, Biomaterials, 26, 839-848.

Heatley, F., Scott, J.E., 1988, “A water molecule participates in the secondary structure of hyaluronan”, Biochem. J., 254, 489-493.

Heiserman, D.L., 2004, SweetHaven Publishing Services, http://64.78.42.182/sweethaven/MedTech/Anatomy/coursemain.asp?whichMod=module0406, Last accessed date: September 2007.

Hench, L.L:, “Bioactive bone substitutes”, 1992, Bone Grafts & Bone Substitutes, Habal, M.B., Reddi, A.H., W.B. Saunders Company, USA, Chap.25.

Hench, L.L., Best, S., “Ceramics, Glasses, and Glass-Ceramics”, 2004, Biomaterials Science : An Introduction to Materials in Medicine, Ratner, B.D., Hoffman, A.S., Schoen, F.J., Lemons, J.E., Ed.s, Second Edition, Elsevier Academic Press, Amsterdam , Boston, Section 2.6.

Hernandez, C.J., Keaveny, T.M., 2006, “A biomechanical perspective on bone quality”, Bone, 39,1173–1181.

Hing, K.A., Wilson, L.F., Buckland, T., 2007, “Comparative performance of three ceramic bone graft substitutes”, The Spine Journal, 7, 475–490.

Hsu, W.K., Sugiyama, O., Park, S.H., Conduah, A., Feeley, B.T., Liu, N.Q., Krenek, L., Virk, M.S., An, D.S., Chen, I.S., Lieberman, J.R., 2007, “Lentiviral-mediated BMP-2 gene transfer enhances healing of segmental femoral defects in rats”, Bone, 40, 931–938.

Huan, Z., Chang, J., 2007, “Self-setting properties and in vitro bioactivity of calcium sulfate hemihydrate–tricalcium silicate composite bone cements”, Acta Biomater, In Press, doi:10.1016/j.actbio.2007.05.003.

Intini, G., Andreana, S., Intini, F.E., Buhite, R.J., Bobek, L.A., 2007, “Calcium sulfate and platelet-rich plasma make a novel osteoinductive biomaterial for bone regeneration”, Journal of Translational Medicine, 5, 13.

ISO 10993-5, “Biological evaluation of medical devices” Test for cytotoxicity: In vitro methods, 1992.

Ito, H., Minami, A., Tanino, H., Matsuno, T., 2002, “Fixation with poly-L-lactic acid screws in hip osteotomy: 68 hips followed for 18–46 months”, Acta Orthop Scand, 73, 1, 60–64.

Jee, W.S.S., “Integrated bone tissue physiology: anatomy and physiology”, 2001, Bone Mechanics Handbook, Cowin, S.C., Ed., Second Edition, CRC Press, Boca Raton, Florida, Chap.1.

Jenis, L.G., Erulkar, J., 2006, “Synthetic bone grafts in orthopaedic surgery”, US Musculoskeletal Review, Biomaterials, 48-49.

Juhasz, J.A., Best, S.M., Brooks, R., Kawashita, M., Miyata, N., Kokubo, T., Nakamura, T., Bonfield, W., 2004, “Mechanical properties of glass-ceramic A–W-polyethylene composites: effect of filler content andparticle size”, Biomaterials, 25, 949–955.

Kasten, P., Vogel, J., Luginbühl, R., Niemeyer, P., Tonak, M., Lorenz, H., Helbig, L., Weiss, S., Fellenberg, J., Leo, A., Simank, H.G., Richter, W., 2005, “Ectopic bone formation associated with mesenchymal stem cells in a resorbable calcium deficient hydroxyapatite carrier”, Biomaterials, 26, 5879–5889.

Katti, K.S., 2004, “Biomaterials in total joint replacement”, Colloids and Surfaces B. Biointerfaces, 39, 133-142.

Kim, J., Kim, I.S., Cho, T.H., Lee, K.B, Hwang, S.J., Tae, G., Noh, I., Lee, S.H., Park, Y., Sun, K., 2007, “Bone regeneration using hyaluronic acid-based hydrogel with bone morphogenic protein-2 and human mesenchymal stem cells” Biomaterials, 28, 1830-1837.

Kitamura, M., Ohtsuki, C., Iwasaki, H., Ogata, S., Tanihara, M., 2004, “The controlled resorption of porous α-tricalcium phosphate using a hydroxypropylcellulose coating”, J Mater Sci Mater Med, 15, 1153-1158.

Komaki, H., Tanaka, T., Chazono, M., Kikuchi, T., 2006, “Repair of segmental bone defects in rabbit tibiae using a complex of β-tricalcium phosphate, type I collagen, and fibroblast growth factor-2”, Biomaterials, 27, 5118–5126.

Kong, L., Gao, Y., Lu, G., Gong, Y., Zhao, N., Zhang, X., 2006, “A study on the bioactivity of chitosan/nano-hydroxyapatite composite scaffolds for bone tissue engineering”, European Polymer Journal, Macromolecular Nanotechnology, 42, 3171–3179.

Kwon, B., Jenis, L.G., 2005, “Carrier materials for spinal fusion”, The Spine Journal, 5, 224S–230S.

Lamerigts, N.M.P., Buma, P., Huiskes, R., Schreurs, W., Gardeniers, J., Sloo, T.J.J.H., 2000, “Incorporation of morsellized bone graft under controlled loading conditions. A new animal model in the goat”, Biomaterials, 21, 741-747.

Leach, J.B., Bivens, K.A., Patrick, Jr., C.W., Schmidt, C.E., 2003, "Photocrosslinked hyaluronic acid hydrogels: natural, biodegradable tissue engineering scaffolds", Biotechnol Bioeng, 82, 578–589.

Lee, J.Y., Choo, J.E., Choi, Y.S., Park, J.B., Min, D.S., Lee, S.J., Rhyu, H.K., Jo, I.H., Chung, C.P., Park, Y.J, 2007, "Assembly of collagen-binding peptide with collagen as a bioactive scaffold for osteogenesis in vitro and in vivo", Biomaterials, In Press, doi:10.1016/j.biomaterials.2007.05.040.

Lee, K.J.H., Roper, J.G., Wang, J.C., 2005, "Demineralized bone matrix and spinal arthrodesis", The Spine Journal, 5, 217S-223S.

Lee, S.H., Shin, H., 2007, "Matrices and scaffolds for delivery of bioactive molecules in bone and cartilage tissue engineering", Advanced Drug Delivery Reviews, 59, 339-359.

Lei, Y., Rai, B., Ho, K.H., Teoh, S.H:, 2007, "In vitro degradation of novel bioactive polycaprolactone—20% tricalcium phosphate composite scaffolds for bone engineering", Materials Science and Engineering: C, 27, 293-298.

Li, Z., Ramay, H.R., Hauch, K.D., Xiao, D., Zhang, M., 2005, "Chitosan–alginate hybrid scaffolds for bone tissue engineering", Biomaterials, 26, 3919-3928.

Liberman, J.R., Gamradt, S., "Novel bone repair options in the 21st century", 2006, Bone Grafts and Bone Graft Substitutes, Friedlaender, G.E., Mankin, H.J., Goldberg, V.M., Ed., First Edition, American Academy of Orthopaedic Surgeons, Rosemont, Chap.8.

Lisignoli, G., Fini, M., Giavaresi, G., Aldini, N.N., Toneguzzi, S., Facchini, A., 2002, "Osteogenesis of large segmental radius defects enhanced by basic fibroblast growth factor activated bone marrow stromal cells grown on non-woven hyaluronic acid-based polymer scaffold", Biomaterials, 23, 1043–1051.

Lowry, K.J., Hamson, K.R., Bear, L., Peng, Y.B., Calaluce, R., Evans, M.L., Anglen, J.O., Allen, W.C., 1997, "Polycaprolactone/glass bioabsorbable implant in a rabbit humerus fracture model", J Biomed Mater Res, 36, 536–541.

Lu, H.H., Tang, A., Oh, S.C., Spalazzi, J.P., Dionisio, K., 2005, "Compositional effects on the formation of a calcium phosphate layer and the response of

osteoblast-like cells on polymer-bioactive glass composites", Biomaterials, 26, 6323–6334.

Maeda, H., Maquet, V., Chen, Q.Z., Kasuga, T., Jawad, H., Boccaccini, A.R., 2007, "Bioactive coatings by vaterite deposition on polymer substrates of different composition and morphology", Materials Science and Engineering C, 27, 741–745.

Mano, J.F., Sousa, R.A.,.Boesel, L.F., Neves, N.M., Reis, R.L., 2004, "Bioinert, biodegradable and injectable polymeric matrix composites for hard tissue replacement: state of the art and recent developments", Composites Science and Technology, 64, 789–817.

Marsh, J.L., 2006, "Principles of bone grafting: non-union, delayed union", Surgery, 24, 207-210.

Martin, D.E., Severns, A.E., Kabo, J.M., 2004, "Determination of mechanical stiffness of bone by pQCT measurements: correlation with non-destructive mechanical four-point bending test data", Journal of Biomechanics, Short communication, 37, 1289–1293.

Martinez, V., Corsini, E., Mitjans, M., Pinazo, A., Vinardell, M.P., 2006, "Evaluation of eye and skin irritation of arginine-derivative surfactants using different in vitro endpoints as alternatives to the in vivo assays", Toxicology Letters, 164, 259–267.

Moore, W.R., Graves, S.E., Bain, G.I., 2001, "Synthetic bone graft substitutes", ANZ J. Surg, 71, 354-361.

Mosmann, T., 1983, "Rapid colorimetric assay for cellular growth and survival: Application to proliferation and cytotoxicity assays", J Immunol Methods, 65, 55-63.

Murugan, R., Ramakrishna, S., 2005, "Development of nanocomposites for bone grafting", Composites Science and Technology, 65, 2385-2406.

Müller, L., Müller, F.A., 2006, "Preparation of SBF with different HCO_3^- content and its influence on the composition of biomimetic apatites", Acta Biomaterialia, 2, 181-189.

Nigg, B.M., Herzog, W., 2007, “Biomechanics of the musculo-skeletal systems”, Third Edition, John Wiley & Sons, England, Chap. 2.

Nihouannen, D.L., Saffarzadeh, A. Aguado, E., Goyenvalle, E., Gauthier, O., Moreau, F., Pilet, P., Spaethe, R., Daculsi, G., Layrolle, P., 2007, “Osteogenic properties of calcium phosphate ceramics and fibrin glue based composites”, Journal of Materials Science, 18, 2, 225-235.

Nyman, J.S., Reyes, M., Wang, X., 2005, “Effect of ultrastructural changes on the toughness of bone”, Micron, 36, 566-582.

Oh, S.H., Park, I.K., Kim, J.M., Lee, J.H., 2007, “In vitro and in vivo characteristics of PCL scaffolds with pore size gradient fabricated by a centrifugation method”, Biomaterials, 28, 1664–1671.

Oliva, A., Salerno, A., Locardi, B., Riccio, V., Della Ragione, F., Iardino, P., Zappia, V., 1998, “ Behaviour of human osteoblasts cultured on bioactive glass coatings”, Biomaterials, 19, 1019-1025.

Ono, I., Gunji, H., Kaneko, F., Saito, T., Kuboki, Y., 1995, “Efficacy of hydroxyapatite ceramic as a carrier for recombinant human bone morphogenetic protein”, J Craniofac Surg, 6, 238–44.

Park, S.N., Kim, J.K., Suh, H., 2004, “Evaluation of antibiotic-loaded collagen-hyaluronic acid matrix as a skin substitute”, Biomaterials, 25, 3689–3698.

Patel, V.V., Zhao, L.; Wong, P., Pradhan, B., Bae, H.W., Kanim, L., Delamarter, R.B., 2006, “ An in vitro and in vivo analysis of fibrin glue use to control bone morphogenetic protein diffusion and bone morphogenetic protein–stimulated bone growth”, The Spine Journal, 6, 397-404.

Pecora, G., Andreana, S., Margarone III, J.E., Covani, U., Sottosanti, J.S., 1997, “Bone regeneration with a calcium sulfate barrier”, Oral Surgery Oral Medicine Oral Pathology, 84, 424-9.

Peltier, L.F.,Speer, D.P:, “Calcium sulfate”, 1992, Bone Grafts & Bone Substitutes, Habal, M.B., Reddi, A.H., W.B. Saunders Company, USA, Chap.22.

Peng, Y., Peiyi, W., Siesler, H.W., 2003, “Two-dimensional/ATR infrared correlation spectroscopic study o water diffusion in a poly(ε-caprolactıne) matrix”, Biomacromolecules, 4, 4, 1041-44.

Phillips, J.E., Gersbach, C.A., García, A.J., 2007, “Virus-based gene theraphy strategies for bone regeneration”, Biomaterials, 28, 211-229.

Pietrzak, W.S., Perns, S.V., Keyes, J., Woodell-May, J., McDonald, N.M., 2005, “Demineralized bone matrix graft: a scientific and clinical case study assessment”, The Journal of Foot & Ankle Surgery, 44, 345-353.

Pitt, C., “Poly(ε-caprolactone) and its copolymers” 1990, Biodegradable polymers as drug delivery systems, Chasin, M., Langer, R., Ed.s, Marcel-dekker, New York:; p. 71–120.

Prabhakar, R.L., Brocchini, S., Knowles, J.C., 2005, “Effect of glass composition on the degradation properties and ion release characteristics of phosphate glass-polycaprolactone composites”, Biomaterials, 26, 2209-2218.

Rai, B., Teoh, S.H., Ho, K.H., Hutmacher, D.W., Cao, T., Chen, F., Yacob, K., 2004, “The effect of rhBMP-2 on canine osteoblasts seeded onto 3D bioactive polycaprolactone scaffolds”, Biomaterials, 25, 5499–5506.

Ramakrishna, S., Huang, Z.M., 2007, “Biocomposites”, Comprehensive Structural Integrity, Chapter 9.06, Pages 215-296.

Rammelt, S., Illert, T., Bierbaum, S., Scharnweber, D., Zwipp, H., Schneiders, W., 2006, “Coating of titanium implants with collagen, RGD peptide and chondroitin sulfates”, Biomaterials, 27, 5561-5571.

Ravaglioli, A., Krajewski, A., 1992, “Bioceramics”, Chapman & Hall, Bungay, Suffolk, Chap.7.

Reiner, D., Bellato, P., Bellini, D., Pavesio, A., Pressato, D., Borrione, A., 2005, “Pharmacokinetic behaviour of ACP gel, an autocrosslinked hyaluronan derivative, after intraperitoneal administration”, Biomaterials, 26, 5368-5374.

Rhee, S.H., 2004, “Bone-like apatite-forming ability and mechanical properties of poly(ε-caprolactone)/silica hybrid as a function of poly(e-caprolactone) content”, Biomaterials, 25, 1167–1175.

Rho, J.Y., Kuhn-Spearing, L., Zioupos, P., 1998, “Mechanical properties and the hierarchical structure of bone”, Medical Engineering & Physics, 20, 92-102.

Rooney, J., 2007, Farrier & Hoofcare Resource Center, www.horseshoes.com/farrierssites/sites/rooney/fracturesoflongbones/fracturesoflongbones.htm, Last accessed date: September 2007.

Rundle, C.H., Miyakoshi, N., Kasukawa, Y., Chen, S.T., Sheng, M.H.C., Wergedal, J.E., Lau, K.H.W., Baylink, D.J., 2003, “In vivo bone formation in fracture repair induced by direct retroviralbased gene therapy with bone morphogenetic protein-4”, Bone, 32, 591–601.

Sevilla, P., Aparicio, C., Planell, J.A., Gil, F.J., 2007, “Comparison of the mechanical properties between tantalum and nickel–titanium foams implant materials for bone ingrowth applications”, Journal of Alloys and Compounds, 439, 67–73.

Shao, X.X., Hutmacher, D.W., Ho, S.T., Goh, J.C.H., Lee, E.H., 2006, “Evaluation of a hybrid scaffold/cell construct in repair of high-load-bearing osteochondral defects in rabbits”, Biomaterials, 27, 1071–1080.

Shapoff, C.A., Alexander, D.C., Clark, A.E., 1997, “Clinical use of a bioactive glass particulate in the treatment of human osseous defects”, Compendium, 18, 4, 352-363.

Shen, H.C., Peng, H., Usas, A., Gearhart, B., Cummins, J., Fu, F.H., Huard, J., 2004, “Ex vivo gene therapy-induced endochondral bone formation: comparison of muscle-derived stem cells and different subpopulations of primary muscle-derived cells”, Bone, 34, 982– 992.

Shinzato, S., Nakamura, T., Kokubo, T., Kitamura, Y., 2001, “Bioactive bone cement: effect of filler size on mechanical properties and osteoconductivity”, J Biomed Mater Res, 56, 452–458.

Silver, I.A., Deas, J., Erecińska, M., 2001, “Interactions of bioactive glasses with osteoblasts in vitro: effects of 45S5 Bioglass®, and 58S and 77S bioactive glasses on metabolism, intracellular ion concentrations and cell viability”, Biomaterials, 22, 175-185.

Sopyan, I., Mel, M., Ramesh, S., Khali, K.A., 2007, “Porous hydroxyapatite for artificial bone applications”, Science and Technology of Advanced Materials, 8, 116-123.

Spoerke, E.D., Murray, N.G., Li, H., Brinson, L.C., Dunand, D.C., Stupp, S.I., 2005, “A bioactive titanium foam scaffold for bone repair”, Acta Biomaterialia, 1, 523–533.

Stubbs, D., Deakin, M., Chapman-Sheath, P., Bruce, W., Debes, J., Gillies, R.M., Walsh, W.R., 2004, “In vivo evaluation of resorbable bone graft substitutes in a rabbit tibial defect model”, Biomaterials, 25, 5037–5044.

Su-Gwan, K., Hak-Kyun, K., Sung-Chul, L., 2001, “Combined implantation of particulate dentine, plaster of Paris, and a bone xenograft (Bio-Oss1) for bone regeneration in rats”, Journal of Cranio-Maxillofacial Surgery, 29, 282-288.

Summitt, M.C., Reisinger, K.D., 2003, “Characterization of the mechanical properties of demineralized bone”, J Biomed Mater Res, 67A, 742–750.

Taddei, P., Tinti, A., Reggiani, M., Fagnano, C., 2005, “In vitro mineralization of bioresorbable poly(3-caprolactone)/apatite composites for bone tissue engineering: a vibrational and thermal investigation”, Journal of Molecular Structure, 744–747, 135–143.

Takikawa, S., Bauer, T.W., Kambic, H., Togawa, D., 2003, “Comparative evaluation of the osteoinductivity of two formulations of human demineralized bone matrix”, J Biomed Mater Res, 65A, 37-42.

Tay, B.Y., Zhang, S.X., Myint, M.H., Ng, F.L., Chandrasekaran, M., Tan, L.K.A., 2007, “Processing of polycaprolactone porous structure for scaffold development”, Journal of Materials Processing Technology, 182, 117–121.

Temenoff, J.S., Mikos, A.G., 2000, “Injectable biodegradable materials for orthopedic tissue engineering”, Biomaterials, 21, 2405-2412.

Thamaraiselvi, T.V., Rajeswari, S., 2004, “Biological evaluation of bioceramic materials: a review”, Trends Biomater Artif. Organs, 18(1), 9-17.

Trojani, C., Weiss, P., Michiels, J.F., Vinatier, C., Guicheux, J., Daculsi, G., Gaudray, P., Carle, G.F., Rochet, N., 2005, “Three-dimensional culture and differentiation of human osteogenic cells in an injectable hydroxylpropyl-methylcellulose hydrogel”, Biomaterials, 26, 5509–5517.

Tsukeoka, T., Suzuki, M., Ohtsuki, C., Sugino, A., Tsuneizumi, Y., Miyagi, J., Kuramoto, K., Moriya, H., 2006, “Mechanical and histological evaluation of a

PMMA-based bone cement modified with g-methacryloxypropyltrimethoxy-silane and calcium acetate", Biomaterials, 27, 3897–3903.

Turner, C.H., Burr, D.B., "Experimental techniques for bone mechanics", 2001, Bone Mechanics Handbook, Cowin, S.C., Ed., Second Edition, CRC Press, Boca Raton, Florida, Chap.7.

Turner, C.H., Burr, D.B., 1993, "Basic biomechanical measurements of bone: a tutorial", Bone, 14, 595-606.

Varghese, S., Elisseeff, J.H., 2006, "Hydrogels for musculosketal tissue engineering", Adv Polym Sci, 203, 95-144.

Vogel, M., Voight, C., Gross, U.M., Müller-Mai, C., 2001, "In vivo comparison of bioactive glass particles in rabbits", Biomaterials, 22, 357-362.

Vogt, D.P., 1999, "Xenografting: a promise or a pending disappointment?", Current Surgery, 56, 228-232.

Walsh, W.R., Svehla, M.J., Russell, J., Saito, M., Nakashima, T., Gillies, R.M., Bruce, W., Hori, R., 2004, "Cemented fixation with PMMA or Bis-GMA resin hydroxyapatite cement: effect of implant surface roughness", Biomaterials, 25, 4929–4934.

Wang, H., Li, Y., Zuo, Y., Li, J., Ma, S., Cheng, L., 2007, "Biocompatibility and osteogenesis of biomimetic nano-hydroxyapatite/polyamide composite scaffolds for bone tissue engineering", Biomaterials, 28, 3338–3348.

Waris, E., Ashammakhi, N., Kaarela, O., Raatikainen, T., Vasenius, J., 2004, "Use of bioabsorbable osteofixation devices in the hand", Journal of Hand Surgery (British and European Volume), 29B, 6, 590–598.

Wu, W., Chen, X., Mao, T., Chen, F., Feng, X., 2006, "Bone marrow-derived osteoblasts seeded into porous beta-tricalcium phosphate to repair segmental defect in canine's mandibula", Turkish Journal of Trauma & Emergency Surgery, 12, 4, 268-276.

Wu, Y.C., Shaw, S.Y., Lin, H.R., Lee, T.M., Yang, C.Y., 2006, "Bone tissue engineering evaluation based on rat calvaria stromal cells cultured on modified PLGA scaffolds", Biomaterials, 27, 896–904.

Xin, R., Leng, Y., Chen, J., Zhang, Q., 2005, “A comparative study of calcium phosphate formation on bioceramics in vitro and in vivo”, Biomaterials, 26, 6477–6486.

Xu, H., Ma, L., Shi, H., Gao, C., Han, C., 2007, “Chitosan-hyaluronic acid hybrid film as a novel wound dressing: in vitro and in vivo studies”, Polym Adv Technol, In Press, doi: 10.1002/pat.906, Last accessed date: September 2007.

Yamamuro, T., Nakamura, T., Iida, H., Kawanabe, K., Matsuda, Y.,Ido, K., Tamura, J., Senaha Y., 1998, “Development of bioactive bone cement and its clinical applications”, Biomaterials, 19, 1479-1482.

Yamashita, J., Furman, B.R., Rawls, H.R., Wang, X., Agrawal, C.M., 2001, “The use of dynamic mechanical analysis to assess the viscoelastic properties of human cortical bone”, Biomed Mater Res (Appl Biomater), 58, 47–53.

Yang, Y., Rossi, F.M.V., Putnins, E.E., 2007, “Ex vivo expansion of rat bone marrow mesenchymal stromal cells on microcarrier beads in spin culture”, Biomaterials, 28, 3110–3120.

Yee, A.J.M., Bae, H.W., Friess, D., Robbin, M., Johnstone, B., Yoo, J.,U., 2003, “Augmentation of rabbit posterolateral spondylodesis using a novel demineralized bone matrix-hyaluronan putty”, Spine, 28, 2435-2440.

Yoneda, M., Terai, H., Imai, Y., Okada, T., Nozaki, K., Inoue, H., Miyamoto, S., Takaoka, K., 2005, “Repair of an intercalated long bone defect with a synthetic biodegradable bone-inducing implant”, Biomaterials, 26, 5145–5152.

Zhang, M., James, S.P., 2005, “Silylation of hyaluronan to improve hydrophobicity and reactivity for improved processing and derivatization”, Polymer, 46, 3639–3648.

Zhang, X.S., Linkhart, T.A., Chen, S.T., Peng, H., Wergedal, J.E., Guttierez, G.G., Sheng, M.H., Lau, K.H., Baylink, D.J., 2004, “Local ex vivo gene therapy with bone marrow stromal cells expressing human BMP4 promotes endosteal bone formation in mice”, J Gene Med, 6, 4–15.

Zhou, Y., Chen, F., Ho, S.T., Woodruff, M.A., Lim, T.M., Hutmacher, D.W., 2007, “Combined marrow stromal cell-sheet techniques and high-strength biodegradable composite scaffolds for engineered functional bone grafts”, Biomaterials, 28, 814–824.

Zhu, Y., Granick, S., 2003, “Biolubrication: hyaluronic acid and the influence on its interfacial viscosity of an antiinflammatory drug”, Macromolecules, 36, 973-976.

Zou, X., Li, H., Chen, L., Baatrup, A., Bünger, C., Lind, M., 2004, “Stimulation of porcine bone marrows stromal cells by hyaluronan dexamethasone and rhBMP-2”, Biomaterials, 25, 5375-5385.

APPENDIX A

CALIBRATION CURVE OF THE MTT ASSAY

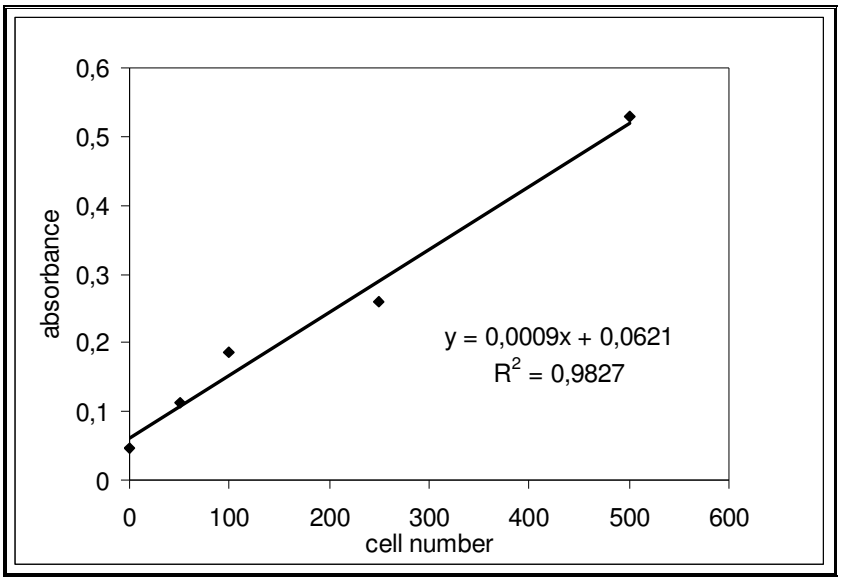

Figure A.1. The calibration curve of Saos-2 cells using MTT analysis

APPENDIX B

CALIBRATION CURVE FOR QCT ANALYSIS

Table B.1. CT numbers of different materials with known densities

Material	Density (g/cc)	CT number
Granite	2.664	2203 ±1236
Teflon	2.162	1032 ±12
Delrin	1.429	392 ±9,2
Ind.Lst	2.241	2168 ±97
Grshale	2.387	2074 ±528
Min.SST	2.444	2031 ±41,6
Water	1.000	0

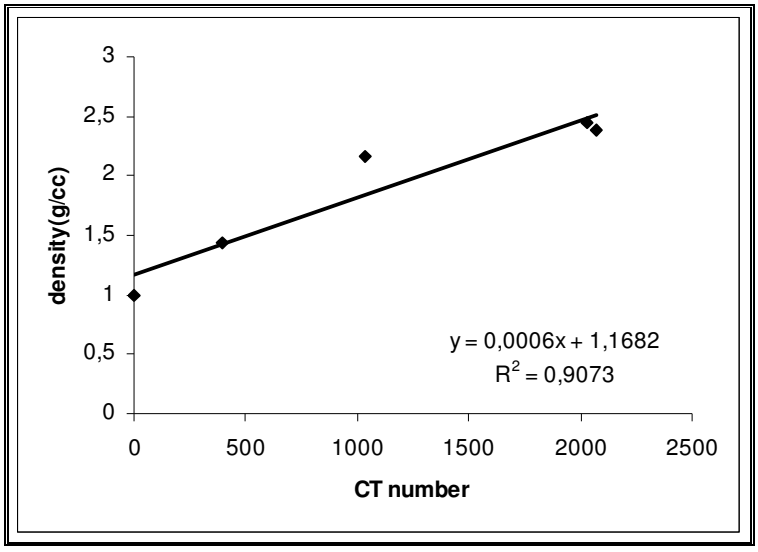

Figure B.1. The calibration curve used in calculations of bone densities

APPENDIX C

THE PARTICLE SIZE DISTRIBUTION TABLES

Table C.1. The particle size distribution table of original commercial bioglass

Size (µm)	Vol Under %	Size (µm)	Vol Under %	Size (µm)	Vol Under %
0.020	0.00	1.002	0.00	50.238	1.11
0.022	0.00	1.125	0.00	56.368	1.19
0.025	0.00	1.262	0.00	63.246	1.28
0.028	0.00	1.416	0.00	70.963	1.40
0.032	0.00	1.589	0.00	79.621	1.54
0.036	0.00	1.783	0.00	89.337	1.75
0.040	0.00	2.000	0.00	100.237	2.04
0.045	0.00	2.244	0.00	112.468	2.44
0.050	0.00	2.518	0.00	126.191	3.01
0.056	0.00	2.825	0.00	141.589	3.79
0.063	0.00	3.170	0.00	158.866	4.89
0.071	0.00	3.557	0.00	178.250	6.39
0.080	0.00	3.991	0.00	200.000	8.42
0.089	0.00	4.477	0.00	224.404	11.12
0.100	0.00	5.024	0.00	251.785	14.62
0.112	0.00	5.637	0.00	282.508	19.05
0.126	0.00	6.325	0.02	316.979	24.50
0.142	0.00	7.096	0.07	355.656	31.01
0.159	0.00	7.962	0.13	399.052	38.47
0.178	0.00	8.934	0.18	447.744	46.74
0.200	0.00	10.024	0.24	502.377	55.53
0.224	0.00	11.247	0.30	563.677	64.47
0.252	0.00	12.619	0.35	632.456	73.12
0.283	0.00	14.159	0.41	709.627	81.06
0.317	0.00	15.887	0.46	796.214	87.88
0.356	0.00	17.825	0.51	893.367	93.28
0.399	0.00	20.000	0.57	1002.374	97.13
0.448	0.00	22.440	0.63	1124.683	99.33
0.502	0.00	25.179	0.69	1261.915	99.99
0.564	0.00	28.251	0.76	1415.892	100.00
0.632	0.00	31.698	0.83	1588.656	100.00
0.710	0.00	35.566	0.90	1782.502	100.00
0.796	0.00	39.905	0.97	2000.000	100.00
0.893	0.00	44.774	1.04		

Table C.2. The particle size distribution table of bioglass after 30 minutes grinding

Size (μm)	Vol Under %	Size (μm)	Vol Under %	Size (μm)	Vol Under %
0.020	0.00	1.002	6.01	50.238	100.00
0.022	0.00	1.125	7.28	56.368	100.00
0.025	0.00	1.262	8.62	63.246	100.00
0.028	0.00	1.416	10.05	70.963	100.00
0.032	0.00	1.589	11.61	79.621	100.00
0.036	0.00	1.783	13.35	89.337	100.00
0.040	0.00	2.000	15.30	100.237	100.00
0.045	0.00	2.244	17.47	112.468	100.00
0.050	0.00	2.518	19.87	126.191	100.00
0.056	0.00	2.825	22.50	141.589	100.00
0.063	0.00	3.170	25.33	158.866	100.00
0.071	0.00	3.557	28.35	178.250	100.00
0.080	0.00	3.991	31.52	200.000	100.00
0.089	0.00	4.477	34.82	224.404	100.00
0.100	0.00	5.024	38.26	251.785	100.00
0.112	0.00	5.637	41.83	282.508	100.00
0.126	0.00	6.325	45.54	316.979	100.00
0.142	0.00	7.096	49.40	355.656	100.00
0.159	0.00	7.962	53.43	399.052	100.00
0.178	0.00	8.934	57.65	447.744	100.00
0.200	0.00	10.024	62.04	502.377	100.00
0.224	0.00	11.247	66.57	563.677	100.00
0.252	0.00	12.619	71.19	632.456	100.00
0.283	0.00	14.159	75.81	709.627	100.00
0.317	0.00	15.887	80.30	796.214	100.00
0.356	0.00	17.825	84.55	893.367	100.00
0.399	0.01	20.000	88.40	1002.374	100.00
0.448	0.11	22.440	91.76	1124.683	100.00
0.502	0.45	25.179	94.52	1261.915	100.00
0.564	0.98	28.251	96.67	1415.892	100.00
0.632	1.72	31.698	98.20	1588.656	100.00
0.710	2.62	35.566	99.18	1782.502	100.00
0.796	3.66	39.905	99.73	2000.000	100.00
0.893	4.80	44.774	99.97		

Table C.3. The particle size distribution table of bioglass after 2 hours-dry grinding

Size (μm)	Vol Under %	Size (μm)	Vol Under %	Size (μm)	Vol Under %
0.020	0.00	1.002	5.95	50.238	99.96
0.022	0.00	1.125	7.40	56.368	100.00
0.025	0.00	1.262	8.96	63.246	100.00
0.028	0.00	1.416	10.66	70.963	100.00
0.032	0.00	1.589	12.50	79.621	100.00
0.036	0.00	1.783	14.51	89.337	100.00
0.040	0.00	2.000	16.69	100.237	100.00
0.045	0.00	2.244	19.05	112.468	100.00
0.050	0.00	2.518	21.57	126.191	100.00
0.056	0.00	2.825	24.26	141.589	100.00
0.063	0.00	3.170	27.10	158.866	100.00
0.071	0.00	3.557	30.09	178.250	100.00
0.080	0.00	3.991	33.25	200.000	100.00
0.089	0.00	4.477	36.56	224.404	100.00
0.100	0.00	5.024	40.04	251.785	100.00
0.112	0.00	5.637	43.71	282.508	100.00
0.126	0.00	6.325	47.58	316.979	100.00
0.142	0.00	7.096	51.63	355.656	100.00
0.159	0.00	7.962	55.88	399.052	100.00
0.178	0.00	8.934	60.29	447.744	100.00
0.200	0.00	10.024	64.81	502.377	100.00
0.224	0.00	11.247	69.39	563.677	100.00
0.252	0.00	12.619	73.93	632.456	100.00
0.283	0.00	14.159	78.34	709.627	100.00
0.317	0.00	15.887	82.50	796.214	100.00
0.356	0.00	17.825	86.31	893.367	100.00
0.399	0.00	20.000	89.68	1002.374	100.00
0.448	0.07	22.440	92.56	1124.683	100.00
0.502	0.28	25.179	94.90	1261.915	100.00
0.564	0.76	28.251	96.73	1415.892	100.00
0.632	1.46	31.698	98.06	1588.656	100.00
0.710	2.35	35.566	98.96	1782.502	100.00
0.796	3.42	39.905	99.52	2000.000	100.00
0.893	4.62	44.774	99.83		

Table C.4. The particle size distribution table of bioglass after 2 hours- wet grinding

Size (μm)	Vol Under %	Size (μm)	Vol Under %	Size (μm)	Vol Under %
0.020	0.00	1.002	6.49	50.238	100.00
0.022	0.00	1.125	7.86	56.368	100.00
0.025	0.00	1.262	9.40	63.246	100.00
0.028	0.00	1.416	11.11	70.963	100.00
0.032	0.00	1.589	12.99	79.621	100.00
0.036	0.00	1.783	15.04	89.337	100.00
0.040	0.00	2.000	17.26	100.237	100.00
0.045	0.00	2.244	19.62	112.468	100.00
0.050	0.00	2.518	22.14	126.191	100.00
0.056	0.00	2.825	24.84	141.589	100.00
0.063	0.00	3.170	27.73	158.866	100.00
0.071	0.00	3.557	30.86	178.250	100.00
0.080	0.00	3.991	34.27	200.000	100.00
0.089	0.00	4.477	38.00	224.404	100.00
0.100	0.00	5.024	42.07	251.785	100.00
0.112	0.00	5.637	46.49	282.508	100.00
0.126	0.00	6.325	51.24	316.979	100.00
0.142	0.00	7.096	56.27	355.656	100.00
0.159	0.00	7.962	61.47	399.052	100.00
0.178	0.00	8.934	66.74	447.744	100.00
0.200	0.00	10.024	71.92	502.377	100.00
0.224	0.00	11.247	76.92	563.677	100.00
0.252	0.00	12.619	81.55	632.456	100.00
0.283	0.03	14.159	85.73	709.627	100.00
0.317	0.12	15.887	89.36	796.214	100.00
0.356	0.31	17.825	92.41	893.367	100.00
0.399	0.57	20.000	94.85	1002.374	100.00
0.448	0.93	22.440	96.73	1124.683	100.00
0.502	1.38	25.179	98.10	1261.915	100.00
0.564	1.92	28.251	99.03	1415.892	100.00
0.632	2.58	31.698	99.60	1588.656	100.00
0.710	3.35	35.566	99.90	1782.502	100.00
0.796	4.26	39.905	100.00	2000.000	100.00
0.893	5.30	44.774	100.00		